A REGULATORY ELEMENT FOR INTERNEURON PROGENITORS
IN THE DEVELOPING VERTEBRATE CENTRAL NERVOUS SYSTEM

by

EVANGELINE TZATZALOS

A dissertation submitted to the

Graduate School-New Brunswick

Rutgers, the State University of New Jersey

and

The Graduate School of Biomedical Sciences

University of Medicine and Dentistry of New Jersey

In partial fulfillment of the requirements

For the degree of

Doctor of Philosophy

Graduate Program in Biomedical Engineering

Written under the direction of

Li Cai, Ph.D.

Martin Grumet, Ph.D.

And approved by

_____

_____

_____

_____

New Brunswick, New Jersey

May, 2012

ABSTRACT OF THE DISSERTATION

A REGULATORY ELEMENT OF INTERNEURON PROGENITORS

IN THE DEVELOPING VERTEBRATE CENTRAL NERVOUS SYSTEM

by

EVANGELINE TZATZALOS

Dissertation Directors:

Li Cai, Ph.D.

Martin Grumet, Ph.D.

The development of the central nervous system (CNS) is regulated by non-protein coding gene regulatory elements that control the expression of neural stem cell genes via the interaction of protein *trans*-acting factors. As a result of recent progress in neuroscience and biotechnology, valuable insight into neural cell growth has been attained from important components of the neural stem cell protein expression profile. However, the role of *cis*-regulatory elements (non-protein coding genomic DNA on the same molecule) in neural stem cells remains confounded. A *cis*-regulatory element of neural progenitors during vertebrate development has been identified and characterized. This regulatory element is a conserved, non-protein coding region located within the established neural stem cell gene, Notch1.

Notch1 is expressed in radial glia, which are self-renewing, neural stem/progenitor cells with long processes that serve as scaffolds for neuronal migration. A conserved non-coding region in the Notch1 locus (i.e., Notch1CR2) is active

exclusively in the ventral CNS during neurogenic periods. On a cellular level, it is active in asymmetrically dividing cells that give rise to GABAergic interneuron progenitors and interneurons. Notch1CR2 is a novel regulatory element for interneuron progenitors.

In this thesis, four studies of Notch1CR2 are presented. In the first study, CNS-specific regulatory activity of Notch1CR2 is revealed during chick embryonic development using *in ovo* electroporation. Second, the temporal-spatial profile of Notch1CR2 activity is determined to be present in cells with an interneuron progenitor phenotype using a transgenic mouse model. Third, the molecular mechanism of Notch1CR2 is investigated, and potential binding *trans*-acting factors of Notch1CR2 are identified. Finally, Notch1CR2 reveals a change in the interneuron progenitor population in the *reeler* mutant mouse compared to the wildtype. *Reeler* is a mutant mouse with deficiencies in neuronal migration and lamination. The discovery and characterization of Notch1CR2 contributes to the current knowledge of gene regulatory elements involved in the neural stem cell decision-making process. Notch1CR2 has the potential to serve as a tool for studying interneurons in other neurodegenerative models or as a platform for engineering cells for transplantation in patients with interneuron deficiencies.

Acknowledgements

iv

in molecular biology techniques, Jennifer Kim for sharing with me her expertise with *in ovo* injections, and Hailing Hao, Ph.D., Sung Tae Doh, Ph.D., Mohammad Islam, and Ying Li for all of the intriguing scientific discussions. I would like to thank Julia Colvin and Sonia Guzman-Ramos for their support and open hearts. Finally, I would like to thank the undergraduates I had the opportunity of mentoring, Tapan Patel and Alson Wu, for all they taught me. I am truly grateful for having the privilege to work with so many dedicated scientists and good-hearted people.

Table of Contents

List of Figures

List of Tables

Abbreviations

βGFP	beta globin promoter
μg	microgram
μl	microliter
BLBP	brain lipid binding protein
bp	base pair
BSA	bovine serum albumin
CAG	chicken β-actin promoter with CMV enhancer
ChIP	chromatin immunoprecipitation
c-LV	caudal lateral ventricle
cm	centimeter
CNS	central nervous system
CP	cortical plate
cPCR	colony polymerase chain reaction
CPu	caudate putamen
CR2	conserved region 2
DCX	doublecortin
DNA	deoxyribonucleic acid
DTT	dithiothreitol
EDTA	ethylenediaminetetraacetic acid
EMSA	electrophoretic mobility shift assay
Exx	embryonic day (e.g. E15.5 is embryonic day E15.5)

GABA	γ-aminobutyric acid
GAD65/67	glutamic acid decarboxylase
GFP	green fluorescent protein
GtIgG	goat immunoglobulin G
hr	hours
IP	interneuron progenitor/precursors
IVZ	intermediate ventricular zone
kbp	kilo base pair
LB	Lucia Broth (media for bacterial cultures)
LGE	lateral ganglionic eminence
ml	milliliter
MGE	medial ganglionic eminence
mIgG	mouse immunoglobulin G
min	minutes
mM	millimolar
ms	milliseconds
MZ	marginal zone
n	sample size
NEB	New England Biolabs
NDS	normal donkey serum
nmol	nanomole
NuMa	nuclear mitotic apparatus
OB	olfactory bulb

p	probability
PBS	phosphate buffered saline
PCR	polymerase chain reaction
pH3	phosphorylated Histone 3
Px	postnatal day (e.g. P0 is postnatal day 0)
RbIgG	rabbit immunoglobulin G
RMS	rostral migratory stream
RNA	ribonucleic acid
r-LV	rostral lateral ventricle
sec	second
SVZ	subventricular zone
TFBS	transcription factor binding site
v/v	volume/volume
V	volts
VZ	ventricular zone
w/v	weight/volume

1 Introduction

Recent advances in stem cell biology have influenced science far beyond the field of developmental biology. Biomedical engineers utilize the fundamentals of stem cell biology to develop cell therapies or tissue scaffolds for potential applications in treating injured or diseased tissue. The ultimate goal of a tissue engineer is to repair or build fully-functional organs on a cell-by-cell basis. To achieve such high aspirations, bioengineers must understand the molecular machinery that regulates the cell decision-making process.

Although the concept of building 'an organ in a dish' seems like science fiction, scientific progress has been made towards the goal of cell and even organ replacement. The field has taken strides with many advances including blood transfusions [1], artificial skin transplants [2], and electrically-active heart 'band-aids' [3]. The first human embryonic stem cell transplant for spinal cord injury was launched by Geron Corporation (Menlo Park, CA) [4]. In the past few years, exciting results from the development of induced pluripotent stem cells illustrate that cell identity can be controlled via engineering of the appropriate genetic factors [5]. This proof-of-concept has the potential of revolutionizing personalized medicine.

The greatest challenges that tissue engineers face are with non-regenerative tissues, such as the central nervous system (CNS). One potential solution is to re-establish radial glial migratory scaffolds to facilitate neuronal delivery to brain regions suffering from neurodegeneration [6]. Bioengineers will only be able to reprogram cells for transplant if they understand the biology of stem cells. How do neural stem cells proliferate? How do

they commit to a path of differentiation? What genes are expressed during this process and how are these genes regulated? The complex regulatory gene networks in stem cells may provide some answers.

Non-protein coding regions that regulate stem cells are a relatively unexplored area of research. Investigators are only beginning to discover the complex network of regulatory regions that play an important role during development. In this thesis, a novel non-coding region has been identified as a regulator of stem cell differentiation, and in particular, is present in interneuron progenitors. Interneuron progenitors are important cells of the nervous system. They give rise to locally-projecting interneurons, which are essential for regulating the activities of neighboring neurons via excitatory and inhibitory cues.

Chapter 2 provides a background review of regulatory elements and the role of neural stem cells in CNS development. **Chapter 3** outlines the experimental methods used in this thesis. The remaining chapters explore the role of a newly identified regulatory element for interneuron progenitors herein referred to as Notch1 Conserved Region 2 (Notch1CR2).

Chapter 4 describes the discovery of Notch1CR2 and its CNS-specific activity *in ovo*. The chick was selected as an initial model for studying the developing embryo due to its affordability and its ease of accessibility for visualizing the embryo.

Chapter 5 describes a complete spatial and temporal characterization of Notch1CR2 in a transgenic mouse model. A transgenic model is important because it addresses the limitations of transient expression *in ovo*. Conservation of Notch1CR2 activity is confirmed in the mouse, which is a more relevant species to human compared to chick.

In addition, the characterization in transgenic mouse reveals a specific profile of Notch1CR2 in interneuron progenitors.

Chapter 6 explores a potential mechanism for Notch1CR2 regulation through the binding of *trans*-acting factors. Since Notch1CR2 is active in interneuron progenitors, then it is expected that interneuron progenitor factors bind to Notch1CR2. From this work, several potential transcription factors have been identified that highlight the importance of Notch1CR2 in interneuron progenitors.

Finally, in **Chapter 7**, Notch1CR2 is used as a tool for identifying interneuron progenitors by following green fluorescent protein (GFP) reporter expression in mice with neural deficiencies. The mutant model used in this study is the *reeler* mouse, which has abnormal neuronal migration and brain lamination. It was expected that this experiment would support scientific literature that claims a normal stem cell/progenitor phenotype in *reeler*. However, this work demonstrates that there is a change in Notch1CR2-GFP expression, suggesting for the first time altered activity of interneuron progenitors in *reeler*.

This thesis contributes to current knowledge of the stem cell genetic network. Notch1CR2 and its *trans*-acting factors can be used to engineer cells with an interneuronal phenotype. Deficiencies in inhibitory interneurons include many psychiatric manifestations such as tuberous sclerosis, epilepsy, and autism [7]. Future work might address these disorders by transplanting cells that have been bioengineered to maintain an interneuron profile.

-PAGE LEFT BLANK INTENTIONALLY-

2   Background

2.1   An appreciation of the history of 'the neuron'

For the interested reader, a brief history of the study of neurons is presented. History provides an appreciation for the difficulties triumphed in the past and perspective for the challenges we face today.

A 'cell' is the simplest individual unit of an organism, as established by Schleiden's and Schwann's Cell Doctrine in 1839. Constitution of this concept formed the basis of modern biology where cells are individual entities that contribute to a compartmental organization. However, it was not until 65 years later that the concept of the 'neuron' as an individual cell was accepted for the nervous system.

The Neuron Doctrine of 1906 marked the beginning of the modern view of neuron as an individual functional unit. Recognition for this work was awarded to Santiago Ramon y Cajal with the 1906 Nobel Prize [8]. He shared this prize with Camillo Golgi, who was rewarded for developing the silver stain, the first method to visualize individual neurons [9]. The concept of the neuron as an individual functional cell opened the field to other revolutionizing discoveries. The Nobel Prize for Physiology was award to Sir Charles Sherrington (1932) for the discovery of the synapse and to Otto Loewi (1936) and John Eccles (1963) for the first insight into the electrical and chemical functions of the neuron.

By the middle of the 20th century, scientists were intrigued by the origin of neurons and neural regeneration. Where do neurons come from? They imagined that there must be a neural precursor or stem cell that gives rise to new neurons during development. Invertebrates were observed to undergo postnatal neurogenesis, where injured neurons

were replaced by new ones. Graziadei and DeHan reported the regeneration of olfactory sensory neurons from frog stem cells at the base of the olfactory neuroepithelium after transection [10, 11]. Invertebrates were considered to have a postnatal source of neural precursor cells that play a role in nerve regeneration. They wondered, do postnatal vertebrates also have a similar (but maybe less active) source for new neurons?

Many leading neuroscientists such as JB Angevine, RL Sidman, J Altman, R Das, MS Kaplan, and JW Hinds pondered the questions of vertebrate neurogenesis. Once formed, where do neurons go and how do they interact with the existing surrounding cells? Angevine and Sidman were the first to show that dividing cells migrate in the developing brain. Dividing chromosomal DNA of mitotic cells can be labeled using tritiated thymidine and visualized using autoradiographic techniques. These techniques were first developed by Hughes, Leblond, and Taylor in 1958 and were used to label dividing cells in forebrain structures. An autoradiographic study of the mouse cerebral cortex showed that dividing cells were migrating outwards [12].

Since scientists were interested in the phenomena of neural regeneration, they questioned whether neurogenesis also occurred in the adult. Although neurogenesis was considered to be restricted to early stages of embryogenesis, there was some evidence of postnatal neurogenesis. Evidence of neural stem cells in the postnatal rat brain was published by Joseph Altman and Gopal Das in 1962 [13]. Neurogenesis was measured by the presence of mitotic figures in the brain using tritiated thymidine. Altman and Das reported neurogenesis in the cerebellum, hippocampus, and olfactory bulb. Postnatally formed neurons were also found in the caudate nucleus after birth. The highest number of labeled neurons was found on the first day after birth, and none were found by the

sixth day. Intensity of labeling was due to the number of mitotic divisions that the precursors experienced before reaching the terminal neuronal state. Intensely labeled neurons were formed earlier and lightly labeled neurons were formed later, which was evidence for neurogenesis [14]. Altman's findings were not taken into consideration until about 30 years later. Other findings of neurogenesis included Kaplan and Hinds, who reported neurogenesis in the dentate gyrus of the hippocampus of three-month old rats [15, 16].

The next area of study that intrigued scientists was the organizational structure of brain tissue. The leading scientist in this field, Pasko Rakic, studied the relationship between neurons and glia and the migration of new neurons along Bergmann glial fibers. In 1971, Rakic reported, for the first time, the migration of young granule cells along densely-packed, highly-oriented Bergmann fibers. Rakic found that granule cells travel for longer distances through the later developmental stages of the cerebellum. The invention of the electron microscope allowed for the visualization of these growing radial glial fibers [17].

Neuroscientists then turned their attention to correlating neurogenesis and neuronal migration to function. In 1983, Fernando Notteböhm published studies on neuronal production, migration, and differentiation in the adult female canary brain during song learning. Autoradiography of canary brains injected with tritium thymidine showed that neurogenesis occurs in the ventricular zone of the vocal control nucleus during periods of song-learning. For the first time, the effect of neurogenesis and neural migration was studied as a function of neural activity [18].

The true appreciation of the neuron as an individual entity took place when neural stem cells were isolated for *in vitro* examination. In fact, the first *in vitro* experimentation, performed by Ross Harrison in 1907, was able to observe the end of live growing fibers (i.e., the growth cone) [19] and successfully confirm the Neuron Doctrine. The first *in vitro* examination of glia-neuronal interactions was performed by Hatten in the early 1980s, who showed that radial glia guide the 'inside-out' migration of postmitotic neurons. At the end of neuronal migration, radial glia release their contacts and transform into astrocytes [20]. The first scientists to culture neurospheres from adult rats were Reynolds and Weiss [21, 22]. Their findings were significant because they revealed a population of stem cells that existed in the adult brain but only proliferated *in vitro*, perhaps due to the inhibitory environment of the brain. This finding brought attention to the concept of both extrinsic and intrinsic factors of the cell decision-making process.

Today, research is focused on elucidating both extrinsic and intrinsic factors that dictate neural stem cell biology. Although the complex genetic network involved in regulating the neural stem cell state remains unexplained, progress has been made in understanding the mechanisms of proliferation and differentiation. For example, Notch1 has been identified as one of the key genes regulating the stem cell state [6, 23]. Research on proliferation and the cell cycle explains the roles of proteins such as Ki67 and pH3 in mitosis [24-26] and the role of nuclear mitotic apparatus (NuMa) in asymmetric division [27, 28]. In conjunction with these intrinsic factors, extrinsic factors such as epidermal growth factor (EGF)-treated and basic fibroblast growth factor (bFGF) have been identified as powerful midogens for the proliferation of neural precursors [29].

One of the most recent approaches to understanding neural stem cell biology is through the study of non-coding regions. Promoters, enhancers, and repressor binding elements are critical components of the genetic stem cell network. In fact, the disruption of regulatory elements has been directly implicated in disease. According to the Genome-Wide Association Studies [30], a large number of disease-implicated loci are variations in non-protein coding regions [31], and many of these diseases are cancers and disorders of cell proliferation. Progress has begun in identifying and characterizing enhancers of stem cell genes for addition to the database of gene regulatory elements. Other regulatory elements of stem cell genes, including Msh1 and Sox2, have been identified and are available on the VISTA Enhancer Browser [32]. As this database grows, the regulatory controls of stem cell biology will be better understood.

2.2 The Notch1 gene and its role in neural stem cells

Notch1 is believed to be a focal gene in the genetic network related to neural stem cell identity [6, 33, 34]. Notch1 is a critical gene in stem cell biology. As published for the first time by Poulson in 1940, Notch1 controls cell fate choice between epidermal and neural lineages [33]. The earliest work on Notch1 receptors and ligands was done in Drosophila. The first evidence that Notch1 inhibits neuronal differentiation in vertebrates was performed *in vitro* in an embryonic carcinoma cell line [35]. Subsequently, the first *in vivo* evidence showed that Hes-1 (a downstream effecter of Notch1) is present in radial glia of the ventricular zone (VZ) and subventricular zone (SVZ) [36]. Notch1 was reported in the mouse embryonic telencephalon to promote the radial glial state - it was not solely inhibiting neuronal differentiation [6]. Radial glia are neural stem cells of the CNS capable of self-renewal and differentiation into glia and neurons. They have long

processes that span the neuroepithelium and act as a scaffold for newborn, migrating neurons [17]. Radial glia also regulate neurogenesis and gliogenesis [37, 38].

Notch1 is temporally expressed during neurogenic periods of development. In the mouse, neurogenesis occurs from embryonic day 9.5 (E9.5) to birth [37]. A first set of radial glial proteins, including nestin, RC1 and RC2, are expressed as early at E9.5 [39, 40]. A second set of radial glial markers is expressed around E13 including BLBP and glutamate transporter (GLAST), and Tenascin C [37, 41-43]. By E16.5, the progenitor pool diminishes and the bulk of the VZ cells migrate out to postmitotic areas [44]. The timeline is different in chick development where neurogenesis occurs from E3 to E9 followed by gliogenesis (E5-E13) [45-47]; however, the sequence of events is similar. Interestingly, neurogenesis has also been reported in the adult avian VZ of the telencephalon [48].

Notch1 expression is located in the ventricular zone of the developing neuroepithelium. Certain regions of strong expression include the boundaries between the medial and lateral ganglionic eminences (MGE/LGE) as well as between the LGE and the neocortex [6]. Notch1 in the postnatal brain expresses in the SVZ, the rostromigratory stream (RMS), and the dentate gyrus, which are all regions of continued neurogenesis in the postnatal brain [49].

The downstream signaling pathway of Notch1 has been extensively studied [50, 51]. However, non-coding sequences are also involved in regulating the expression of coding sequences. Recently, more attention has been given to these regulatory elements with the intent of enhancing knowledge of the neural stem cell state and its process of differentiation.

2.3   The role of *cis*-regulatory elements in neurogenesis

The regulation of gene expression is achieved by understanding the network of interactions between DNA, RNA, and proteins [52]. Protein-coding sequences of DNA provide the information for RNA transcription and protein translation. Non-protein coding DNA sequences are equally important because they orchestrate the regulation of gene expression via the binding of the appropriate *trans*-acting factors.

It is believed that highly conserved non-protein coding regions are important for regulating genes associated with development [53, 54]. Why study non-coding regions that are conserved? Strong sequence conservation suggests conserved function. For example, it has been shown that the process of neurogenesis is highly conserved across a wide range of species [55]. Other basic developmental processes are also likely to be regulated by highly conserved sequences [54]. For instance, the morphogens Dorsal and Twist establish a dorsal-ventral polarity in the early embryo by interacting with numerous enhancers [56-59]. The process of examining conservation across species is referred to as phylogenetic footprinting [60].

Cis-regulatory elements are segments of DNA present on the same DNA molecule as the gene they regulate. In contrast, *trans*-regulatory elements are genes that regulate the expression of distant genes by producing proteins that can diffuse and bind to those distant genes [61]. *Cis*-regulatory elements can be enhancers or repressors of gene expression, and they increase or decrease the rate of transcription from a linked promoter independent of orientation or position relative to the transcription site [62-64]. For instance, some of the first identified enhancers were linked to polymerase II [64]. The difference between enhancers and promoters is that enhancers function upstream, within,

or downstream of the genes they regulate whereas promoters are always located at the 5'
end of the gene [64]. Enhancers can act over a considerable distance which can be
greater than 10 kb [64, 65]. Another characteristic of *cis*-regulatory elements is their
ability to regulate expression in a tissue-specific manner [66].

The mechanism of *cis*-regulatory elements involves a looping mechanism [67, 68].
DNA looping is induced and anchored by transcription factors like GATA1 [66, 69].
This looping mechanism can reach out to other chromosomes and can involve the
interaction between paired homologous genes, resulting in a *trans*-regulatory effect [69].
DNA-looping has been visualized by electron microscopy [70, 71]. The first
visualization was the binding of the *lac* repressor to two *lac* operators via the formation
of a loop.

The databases available for *cis*-regulatory elements are not comparable to the
databases available for DNA and protein expression. The KEGG database, for instance,
contains information on the structure and function of about 110,000 genes for 29 species
[72]. There are only a few known regulatory elements for neural stem cell genes. For
instance, Sox10 regulates its own expression via a known enhancer during neural crest
development [73]. Enhancers have also been reported for Sox2, a stem cell gene present
in the developing CNS [32]. To the best of our knowledge, there are no known enhancers
or *cis*-regulatory elements for Notch1.

2.4   Prediction of non-protein coding *cis*-regulatory elements of Notch1

Since current research is aimed at trying to understand the regulatory elements
involved in neural stem cells, a common stem cell gene Notch1 was chosen as the focus
of this dissertation. In order to identify functional Notch1 non-coding regions, the *cis*-

regulatory elements of Notch1 were predicted computationally. The genomic sequences covering Notch1 were obtained from Ensembl [74], and a non-coding sequence retrieval system based on comparative genomics was used to perform a global pair-wise alignment [75]. Four conserved regions were identified based on two criteria: (1) the sequence must have 70% similarity across species and (2) the conserved region must be at least 100 bp in length. In this work, only conserved region 2 of Notch1 (Notch1 CR2) is examined. Notch1CR2 is a 399-base pair region in the second intron of the Notch1 locus (Figure 3.1) with 164 predicted transcription factor binding sites (TFBS), as determined by MatInspector [76].

Notch1CR2 was selected as the non-protein coding region for examination in this thesis because it is a better candidate for studying neural stem cells of the developing CNS. Previous work has shown that Notch1CR2 is active in the retina [77], which is derived from the neural ectoderm and is part of the CNS. In contrast, Notch1CR1 activity displays specificity in the lens, which is derived from the external ectoderm and is not part of the CNS [77]. Notch1CR3 and 4 have not been tested to date and will be characterized by future investigators. The work presented here characterizes Notch1CR2 activity in the brain, retina, and spinal cord.
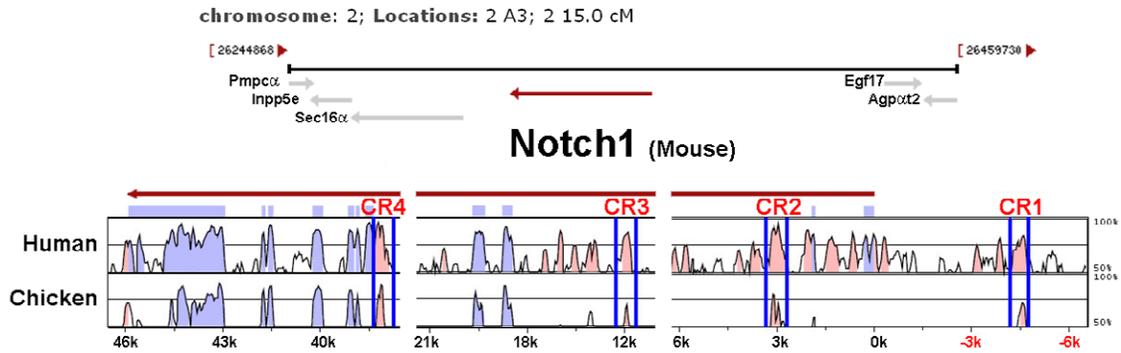
Figure 2.1. Computational prediction of *cis*-regulatory element for the Notch1 gene.
The top panel is a genomic context view of mouse Notch1 gene. The bottom panel is a segmental view of the sequence alignment of homologous Notch1 genes from human, chicken, and mouse. The mouse sequence serves as the baseline for comparative analysis. The comparison identifies four highly evolutionarily conserved regions (CR1-CR4) as Notch1 *cis*-regulatory candidates (marked by blue bars). CR1 (356 bp) is located about 4.5 kbp upstream of the Notch1 transcription start site. CR2 (399 bp) and CR3 (229 bp) are located in the second intron (between exons 2 and 3). CR4 (347 bp) is located in intron 27 (between exons 27 and 28). Pink peaks represent non-coding sequences with >70% identity and a length of at least 100 bp. Blue peaks represent Notch1 coding regions/exons (34 exons in total for Notch1 gene). [77]

2.5 The role of Notch1 and Reelin in neuronal migration and brain lamination

Radial glia are the multipotential stem cells that give rise to neurons and then glia during CNS development. Dividing radial glia possess long bipolar processes and support their own migration [12, 78, 79] as well as the migration of nascent neurons along the glial shaft [17, 80, 81]. Neurons follow guidance cues on the radial glial process as well as extrinsic cues of protein gradients. One influential protein, Reelin, is secreted by Layer I Cajal-Retzius cells and permeates into the deeper layers of the cortex. Neurons climb from their place of birth in the ventricular zone (VZ) up this increasing gradient of Reelin to their final site of differentiation and maturation [17, 80, 81].

The relationship between radial glia and neuronal migration has been studied in the *reeler* mutant mouse. During normal brain development, the pre-plate of the neuroepithelium gives rise to the first two postmitotic neuronal populations - the Cajal-Retzius cells in the marginal zone (MZ) and the sub-plate neurons. Neurons born from the VZ will migrate radially past the sub-plate into the cortical plate (CP). Neurons born from the VZ of the striatum will tangentially migrate into neocortex where they are fated to become interneurons [82-89]. Both radial and tangential migration of neurons is guided by a gradient of Reelin that is produced by the Cajal-Retzius cells [90]. In addition, interneurons demonstrate tangential migration from the striatum to the neocortex. The *reeler* mice lack the ability to produce Reelin and thus display abnormal neuronal migration, disrupted cell positioning, and inverted cortical lamination. This pathology begins with the failure of the pre-plate to split into the MZ and the sub-plate.

The relationship between Reelin and Notch1 exists such that a decrease in Reelin signaling yields a decrease in brain lipid binding protein (BLBP) and the radial glial phenotype [91]. It has been shown that Notch1, BLBP, and Hes5, are downregulated in *reeler* [92] and that a downstream factor of Reelin (Dab1) binds to Notch1 [91]. This thesis examines the direct/indirect effect of Reelin on this Notch1 *cis*-regulatory element (Notch1CR2).

3   Experimental Methods

The results of Chapters 4-6 were obtained using a combination of computational and experimental approaches. The first goal was to determine the regulatory activities of Notch1CR2 during embryonic development. Potential candidates of *cis*-regulatory regions of Notch1 were predicted based on evolutionary conservation (Section 2.4). A traditional way to discover *cis*-regulatory regions was implemented. A sequence predicted to contain regulatory activity was placed in context with a basal promoter to drive expression of a promoter gene. A GFP reporter plasmid was developed in previous work to study Notch1CR2 activity (Section 3.1). Both chick and mouse models were studied because it was important to validate conservation of Notch1CR2 (Section 3.2). Initial insight into the activity of Notch1CR2 was attained using transient transfection models in chick (Section 3.3) and in mouse (Section 3.4). The temporal and spatial profile of Notch1CR2 was analyzed in a transgenic mouse model (Section 3.2). The protocol for processing chick and mouse tissue was optimized, particularly the steps of tissue fixation (Section 3.5). The method for immunohistochemistry was established for a panel of antibodies in both mouse and chick (Section 3.6). Finally, several techniques were used to determine potential transcription factors that bind to Notch1CR2, including electrophoretic mobility shift assay (EMSA) (Section 3.7), mutagenesis (Section 3.8), and chromatin immunoprecipitation (ChIP) (Section 3.9).

3.1   Genomic sequence analysis and reporter plasmid Notch1CR2

The genomic sequences covering Notch1 were obtained from Ensembl. A non-coding sequence retrieval system based on comparative genomics was used to perform a global pair-wise alignment [75].

The Notch1CR2 enhancer vector was designed to identify enhancer activity through GFP reporter expression. The vector consists of the Notch1CR2 conserved region and a GFP reporter gene driven by the βGP (Figure 3.1). The βGP drives basal levels of GFP. When the 399-base pair region is activated by endogenous transcription factors, detectable levels of GFP are expressed. Therefore, a functional non-protein coding region will have the ability to drive cell-type specific reporter expression.
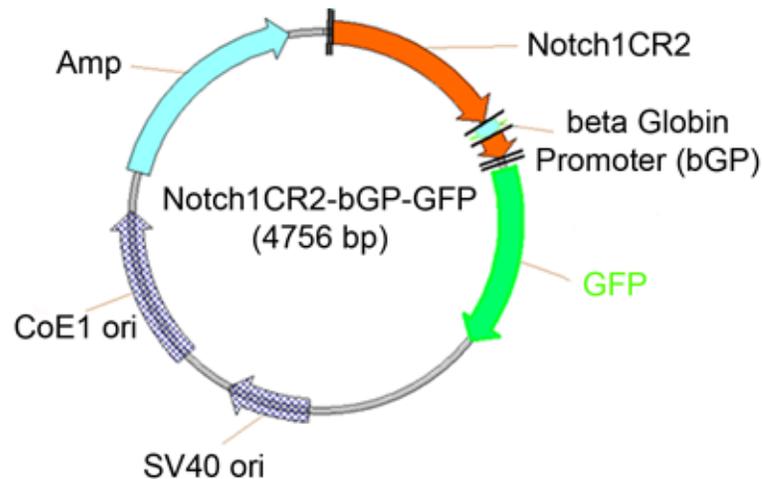
Figure 3.1. Notch1CR2-βGFP-GFP is a GFP reporter construct.
The plasmid contains the 399-bp, non-protein coding region of Notch1CR2 followed by the beta globin promoter (bGP) and green fluorescence reporter protein (GFP).

Positive and negative controls were tested to support Notch1CR2-βGP-GFP expression. A positive control, consisting of a known enhancer (for the Rhodopsin gene), was shown to drive oligodendrocyte-specific expression of the GFP reporter [77]. The transfection control is GFP or DsRed, which is driven by the strong constitutively active chicken actin promoter with CMV enhancer (CAG), which drives expression in all cell types (Figure 4.1). Negative controls, which consist of GFP driven by βGP alone or with a random sequence, do not show the ability to drive GFP expression *in vivo* or *in vitro* [77].

3.2   Chick and Mouse Animal Models

Fertilized eggs were purchased from Sunrise Farms, Inc. and incubated at 37^oC with 60% humidity. The developmental stages of the chicks were determined according to stages established by Hamilton and Hamburger [93].

Transgenic mice of Notch1CR2 were obtained by the Transgenic/Knock-out Mouse Core Facility at the Cancer Institute of New Jersey/University of Medicine and Dentistry of New Jersey (New Brunswick, NJ).

The *reeler* mice were graciously donated by Prof. Gabriella D'Arcangelo from the Department of Cell Biology & Neuroscience at Rutgers University. Heterozygous mutants *reeler*$^{+/-}$ were crossed with Notch1CR2-βGP-GFP$^+$ transgenic mice. The colonies of Notch1CR2$^+$ heterozygote mutants were expanded to the F2 generation by crossing mice of the F1 generation that were Notch1CR2$^+$/*reeler*$^{+/-}$. Mice that were both Notch1CR2$^+$/*reeler*$^{+/-}$ were crossed to obtain embryonic day 15.5 (E15.5) or postnatal day 0 (P0) samples that were Notch1CR2$^+$ *reeler* homozygous mutants (Notch1CR2$^+$/*reeler*$^{-/-}$). Genotyping confirmed the presence of the Notch1CR2 transgene or the homozygous mutant of *reeler* using the primers listed in the table below. The following band sizes are present for each genotype: Notch1CR2$^+$ (800 bp), *reeler*$^{+/+}$ (280 bp), *reeler*$^{+/-}$ (280 & 380 bp), *reeler*$^{-/-}$ (380 bp).

Table 3.1. Primer design for genotyping Notch1CR2 and *reeler*

Primer Name	Primer
GM75	TAA TCT GTC CTC ACT CTG
3R1	TGC ATT AAT GTG CAG TGT TG
3W1	ACA GTT GAC ATA CCT TAA TC
GFP forward	GCA ACG TGC TGG TTA TTG TGC TGT
GFP reverse	GTG GTA TTT GTG AGC CAG GGC ATT

3.3   *In ovo* electroporation and detection of enhancer activity

Chick embryos were transfected at Hamilton Hamburger stage 12 (HH12). After piercing the end of the egg with a syringe and removing 2 ml of albumin, an aperture of 1-cm diameter was created in the side wall of the egg using forceps. A glass heat-pulled needle was used to inject the DNA into the neural tube of the embryo at the telencephalic/diencephalic boundary. The solution of DNA consisted of 6 μg/μl of Notch1CR2, 6 μg/μl CAG/DsRed, and 10% Fast Green for visualization. Gold-plated, L-shaped electrodes (Model 512 Genetrodes^{TM}, Harvard Biosciences Inc.) were placed along the right and left sides of the embryo. An electric pulse at 60 V for 50 ms was applied 4 times at 1-second intervals using an ECM 830 Electro Square Porator (BTX Harvard Apparatus). After the transfection, the aperture was sealed with tape, and the eggs were returned to the incubator. Embryos were harvested at the desired time points (E4, E6, E8) and examined under a fluorescent whole mount microscope (Leica, Model MZ16FA). Transfections were performed until patterns of enhancer activity were highly reproducible (20 embryos at E4, 15 embryos at E6, and 10 at E8).

3.4 *In utero* electroporation

Mouse embryos from Balb/cJ pregnant dams were transfected at E13.5. To anaesthetize the dam, 0.9% Avertine was injected intraperitoneally. When the dam became unresponsive, the limbs were taped down for immobilization and the abdominal skin was sterilized using gauze soaked with 70% ethanol. An incision was made horizontally across the abdomen, and the embryos were gently lifted out of the abdominal cavity. At this stage, the eyes are visible through the uterine lining and were used as a guideline. A glass, heat-pulled needle (from borosilicate glass capillaries) was used to deliver the DNA mixture into the lateral ventricle of the embryo. The electrodes were positioned on lateral sides of the skull. Five 37 V pulses were delivered enduring 50 ms at an interval of 1 sec (World Precision Instruments, Model 1B100F-4.) The DNA was prepared at a concentration of 3 µg/µl in 0.05% Fast Blue.

3.5 Tissue processing

For immunohistochemical analysis, three embryos at each time point were processed. Whole chick embryos were fixed in 4% paraformaldehyde for 4-6 hr and mouse embryos for overnight. Subsequently, the fixed embryos were washed in cold, sterile PBS (three times, 15 min each) and soaked in sterile 30% sucrose (prepared in PBS) overnight until sinking to the bottom. The tissue was mounted in Tissue Tek® OCT Compound, frozen at -80C, and sectioned at 12-15 µm thickness using the Cryotome E (Thermo Electron Corporation). Slide-mounted sections immersed in blocking buffer containing 10% (w/v) donkey serum, 0.1% (v/v) TritonX, and 0.1% (v/v) Tween for 30 min at room temperature.

3.6 Immunohistochemistry

Slide-mounted sections were incubated overnight in primary antibodies against Brn3a, Doublecortin, NeuN, Notch1, Pax6, Tbr1, Tbr2, and Sox2. A co-staining with anti-GFP was used to help visualize Notch1CR2-GFP in transfected chick embryonic tissue or with mouse tissue where indicated. Primary antibodies were diluted in blocking buffer and then washed three times (10 min each) with PBS containing 0.1% (v/v) Tween (PBST). For immunofluorescent staining, tissue sections were incubated with the appropriate secondary antibodies conjugated to various fluorophores (Jackson ImmunoResearch Labs). The secondary antibodies against anti-GFP were either donkey anti-RbIgG or donkey anti-GtIgG Alexxa 488 (Millipore, Inc., 1:300). The secondary antibodies against the other antibodies were either donkey anti-mIgG Alexxa 549, donkey anti-RbIgG Alexxa 549, donkey anti-mIgG Alexxa 647, or donkey anti-RbIgG Alexxa 647 (Jackson Laboratories, Alexxa 549 1:300, Alexxa 647 1:150). Secondary antibodies were also prepared in blocking buffer and were applied at room temperature for one hour, followed by three 10 min washes with PBS and a 5 min rinse in distilled water to remove salt crystals. After air-drying for 5 min, slides were mounted with 40 μl of mounting media with Dapi (Vector Laboratories).

Table 3.2. Antibodies for immunohistochemistry

Antigen	Cell type	Reactivity	Isotype	Company	Cat#	Dilution
BLBP	Radial Glia	M, R	RbIgG	Chemicon	AB9558	1:500
Brn3a	Sensory Neuron	M,R,A	mIgG$_1$	Millipore	MAB1585	1:100
CR50	Reelin	M,R	mIgG			1:1000
Doublecortin	Early Neuron	M,R,H	RbIgG	Cell Signaling	4604	1:250
CD133	Radial Glia	M,H	mIgG$_{2B}$	Abcam	Ab27699	1:100
Ki67	Mitotic cell	M,H	mIgG	BD Biosciences	550609	1:50
GABA	Neuron	M,R	RbIgG	Sigma	A2052	1:5,000
GAD65/67	Interneuron Precursor	M,R	RbIgG	Chemicon	AB1511	1:200
GFP	N/A	WT/Rec	RbIgG	Mllipore	AB10145	1:1000
GFP	N/A	WT/Rec	GtIgG	Abcama	AB6673	1:300
Nestin	Radial Glia	M, R, C	mIgG$_1$	DSHB	Rat-401	1:10
NeuN	Mature Neuron	M,R,C	mIgG$_1$	Chemicon	MAB377	1:1,000
Notch1	Radial Glia	M,R	RbIgG	Cell Signaling	3608	1:500
NuMa	Mitotic Spindle	M,R	RbIgG	Abcam	Ab5675	1:250
Pax6	Radial Glia	M,R,C	mIgG$_1$	DSHB	Pax6	1:10
PH3	Mitotis	M,R	RbIgG	Cell Signaling	3377	1:300
Sox2	Stem Cell	M,R	mIgG$_2$	Millipore	MAB4423	1:300
Tbr1	Layer I Neuron	M,R	RbIgG	Santa Cruz	SC-48816	1:250
Tbr2	Intermediate Progenitor	M,R,H	RbIgG	Abcam	AB23345	1:300
VGAT	GABAergic neuron	M,R	mIgG$_3$	Synaptic Systems	131 011	1:200

(M)ouse, (R)at, (C)hicken, (A)vian, (H)uman, (Rec)combinant, (W)ildtype

3.7 Electrophoretic mobility shift assay

Nuclear protein extracts for the binding reactions were collected from chick embryo brain at E4, E8, E12, and E16. The dissected brains were mechanically dissociated in chilled culture media (MEM, GIBCO) using 16 ½, 18 ½ and 21 ½ gauge syringe needles. After two washes in chilled sterile PBS, the tissue pulp was resuspended in Buffer A (10mM Hepes, 10mM KCl, 0.1mM ethylene diamine tetra-acetic acid (EDTA), protease inhibitor, 1mM dithiothreitol (DTT), 0.4% TritonX100 for ten min to allow for lysis of the cell bodies. The sample was centrifuged and the pellet of cellular nuclei was resuspended in Buffer B (20mM Hepes, 0.4mM NaCl, 1.0mM EDTA, 10% glycerol, protease inhibitor, 1mM DTT) for 2 hr at 4°C to allow for the release of nuclear protein extract from the ruptured nuclei. The supernatant of the centrifuged sample was

aliquoted and stored at -80°C. Active probes were prepared from single stranded oligomers (obtained from Integrated DNA Technology, Inc.) via biotinylation. The 3'ends were labeled with biotin in a room temperature reaction of 1μM unlabeled oligo with 5μM biotin-11-dUTP and 2U/μl of Terminal Deoxynucleotidyl Transferase (TdT). The base solution consisted of TdT reaction buffer and ultrapure water. Complimentary biotinylated single-stranded oligomers were annealed at equimolar concentrations at room temperature for one hour. Complimentary unlabeled single stranded oligomers were annealed as a competition control. Evidence of binding disappeared when unlabeled probe was added to the binding reaction with labeled probe if binding was specific.

The polyacrylamide non-denaturing gels were prepared at 4%-12% polyacrylamide depending on probe size. The respective percentage of AccuGel acrylamide was prepared in Tris-Borate-EDTA (TBE), 5% glycerol, 0.1% APS, and 0.1% TEMED for the initiation of polymerization. After annealing the labeled and unlabeled probes and casting the gels, the actual binding reaction was prepared. The nuclear extract (1 μg) was mixed with binding buffer and 50 ng of poly D(I-C) and ultrapure water for 10 min at room temperature. The final volume of each sample was brought up to 20 μl using water. Poly D(I-C) will inhibit non-specific protein binding. Then biotin labeled probe (100 fmol) was added for 15 min at room temperature. For the competition control, 1 nmol of unlabeled probe was added to the binding reaction and incubated at room temperature for 15 min before adding the biotinylated probe.

3.8   Mutagenesis

Mutations were generated by deleting one or four base pairs of the core-binding sequences. Primers were designed based on the 399 bp sequence of Notch1CR2 with deletions at position 76-79 and 235-239 as a control. Position 235-239 contains no known core-binding sequence and thus serves at the positive control. Polymerase chain reaction (PCR) was performed using high fidelity enzyme ExTaq with the following program: initial heat inactivation = 95°C, 5 min; 16 cycles of heat inactivation [95°C, 30 sec]; annealing [T$_m$, 1 min], extension [72°C, 10 min]. The PCR product was transformed into NEB5α competent cells (NEB), colonies were analyzed by colony PCR (cPCR), and their sequences were confirmed by Genewiz, Inc. (South Plainfield, NJ). Confirmed sequences were amplified using MidiPrep^{TM} (Invitrogen, Inc.) and expression was tested in chick embryos (Section 3.3).

3.9   Chromatin immunoprecipitation

Chromatin immunoprecipitation (ChIP) was performed using MAGnify^{TM} kit (Millipore, Inc.). Brain tissue was isolated at E6. A single-cell suspension was created in HBSS (Invitrogen, Inc.) via gentle pipetting and filtration through a 40 μm filter (Millipore, Inc). Cells were counted and aliquoted into $1 * 10^6$ cells/tube. Subsequent fixation, cell lysis, and sonication were performed according to the MAGnify^{TM} protocol. Brn3a antibody was used for the immunoprecipitation at 5 μg per reaction (GtIgG, Millipore, Inc.). PCR was used to verify the binding of Brn3a to Notch1CR2 (forward primer: gcctttggcttgaaaggtgtccat; reverse primer: tgggaggcgattaatgctgtgtga).

4   CNS-Specific Gene Regulatory Activities of Notch1CR2 During Embryonic Chick Development

The function of the non-coding regions of Notch1 remains confounded.   These regions may be involved in regulating one of the roles of Notch1: maintaining the stem cell state, regulating neurogenesis, or regulating gliogenesis.   Which non-coding region has the highest potential of regulating the role of Notch1?   Highly conserved regions hold a greater probability of being developmentally significant (refer to Section 2.3).   Based on this theory, a 399-base pair sequence (i.e. Notch1CR2) was identified as a possible *cis*-regulatory element of Notch1 because it is highly conserved across species.

In Chapter 4, it is demonstrated Notch1CR2 is active *in ovo* during neurogenesis.   To test this *cis*-regulatory candidate, the Notch1CR2-βGP-GFP plasmid (Figure 3.1) was electroporated into early chick embryos.   The chick was chosen instead of the mouse to study the transient activity of Notch1CR2 due to the ease of accessibility of the chick's embryonic stages.   Activity was measured by the ability of the conserved region to drive expression of GFP in the presence of a minimal promoter βGFP.   The non-coding region of DNA is "activated" through the binding of specific *trans*-acting factors, which are only present at specific times and in unique regions.   Thus, regulation is time- and tissue/cell-specific.

It was hypothesized that this non-coding region of Notch1 (Notch1CR2) is active in radial glia or Notch1$^+$ cells during the development of the CNS.   The hypothesis was tested using *in ovo* electroporations with the Notch1CR2-βGP-GFP plasmid into the neural tube followed by immunohistochemical analysis of sectioned brains at E4-E8.

The results support the hypothesis by showing that Notch1CR2 is active in stem cells and not differentiated neurons.

4.1 Notch1CR2 directs reporter GFP expression specifically in the CNS of the developing chick

Activity of the Notch1CR2 *cis*-regulatory element was examined by following GFP expression after the electroporation of chick embryos at HH12. The extent of transfection was tracked by co-transfecting Notch1CR2-GFP with a transfection control plasmid of CAG-DsRed at equal concentrations. Notch1CR2 is initially active in the mesencephalic and rhombencephalic regions (Figure 4.1). Further characterization focused on the optic lobes of mesencephalic regions. At E4, 78% of transfected cells (detected by DsRed) displayed Notch1CR2 activity (as marked by GFP) (Figure 4.1). Notch1CR2 activity in transfected cells drops to 38% by E6. By E8, 15% of transfected cells express Notch1CR2-GFP.

Earlier time points were not examined even though Notch1 protein expression is first detected 6-7 hours after incubation (HH2) [94]. The earliest time point analyzed was E4 since neurogenesis occurs from E3 to E9 in chick [45-47]. Note that Notch1CR2 is also expressed at E3 as seen in one sample.
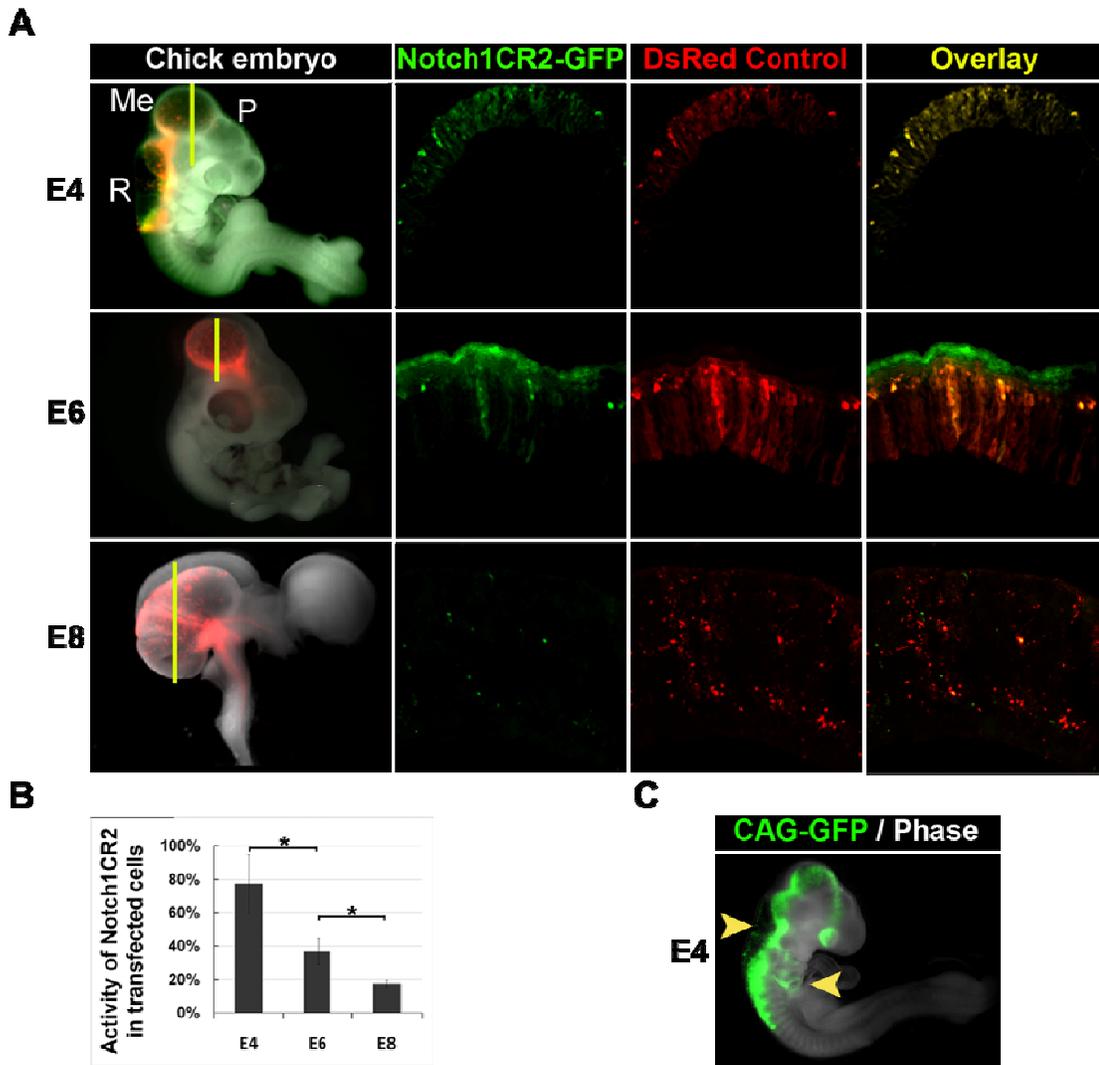
Figure 4.1. Notch1CR2-GFP expression is exclusively expressed in the embryonic chick CNS but is diminished over time.
(A) Chick embryos, harvested at E4, E6, and E8 were co-transfected with equal concentrations of Notch1CR2-GFP and a transfection control at E2. GFP and DsRed are present in the mesencephalon (M), and rhombencephalon (R) at E4 but not the prosencephalon (P). The transfection was limited to the mesencephalon at E6 and E8. The fraction of co-labeled cells in transfected cells (DsRed$^+$) decreases from E4 to E8. **(B)** Percentage of co-localization was quantified using fluorescent images. At E4, Notch1CR2 drives GFP expression in 78% of the transfected cells. Expression decreases to 38% at E6 (p<0.05) and 15% at E8 (p<0.05). At E8, there are significant decreases to 38% and 15% Notch1CR2 activity in transfected cells. **(C)** Transfection of a CAG-GFP control shows non-neural expression in the skin and limbs.

4.2   Notch1CR2 directs reporter GFP expression in chick neural stem/progenitor cells

To obtain the phenotype of Notch1CR2-GFP$^+$ cells, immunohistochemistry was performed on sections of embryonic chick brain. Immunostaining of E4 sections using Sox2 (a stem marker), Pax6 (a neural progenitor marker), and anti-Notch1 (a radial glial marker) showed that Notch1CR2 is active in neural stem/progenitor cells similar to the control. GFP$^+$ or DsRed$^+$ cells of the dorso-lateral optic lobe were counted. As shown in Figure 4.2, 90% of Notch1CR2-GFP$^+$cells co-localize with Sox2, and 93% of Notch1CR2-GFP$^+$ cells co-localize with Pax6. In addition, 47% of Notch1CR2-GFP$^+$ cells co-localize with anti-Notch1. Similarly, 94%, 93%, and 49% of CAG-DsRed$^+$ cells co-localize with Sox2, Pax6, and anti-Notch1, respectively. There is no significant difference of percent co-localization of these markers with Notch1CR2-GFP and the CAG-DsRed transfection control. At least 100 cells were counted for each Notch1CR2-GFP and DsRed in three different samples (chick sample size, n=3).

At E8, prevalence of the neural stem/progenitor phenotype decreases in both the Notch1CR2-GFP$^+$ population and the transfection control. As shown in Figure 4.3, 7% and 15% of the Notch1CR2-GFP$^+$ population co-localize with Sox2 and anti-Notch1, respectively. In comparison, 9% and 16% of the DsRed$^+$ population show co-localization. There is no significant difference between Notch1CR2-GFP and CAG-DsRed populations in either stain. At least 100 cells in three different samples were counted for Notch1CR2-GFP.
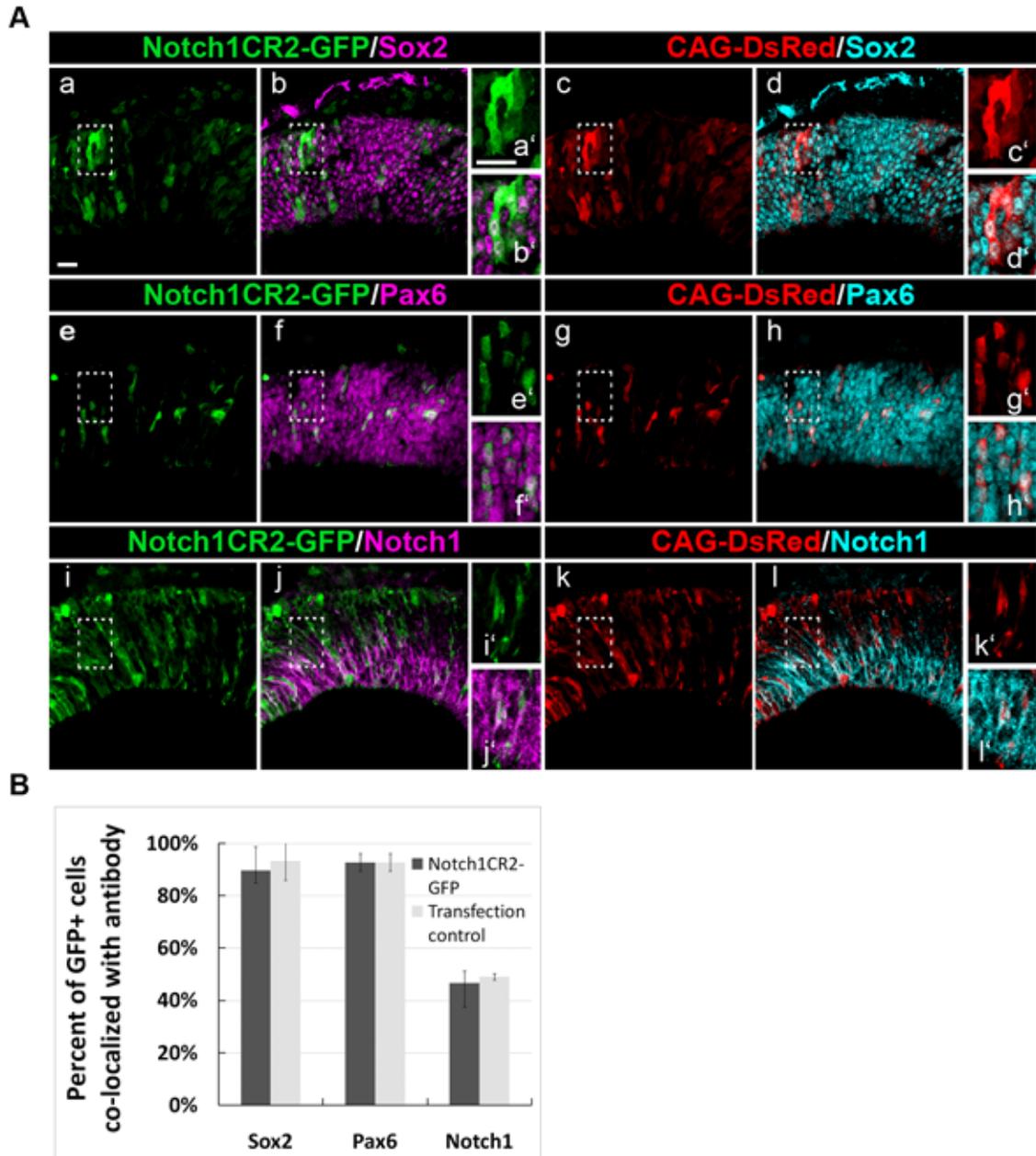
Figure 4.2. Notch1CR2 displays stem cell/progenitor phenotype at E4.
Embryos (HH 12) were co-transfected with **(a,e,i)** Notch1CR2-GFP and **(c,g,k)** CAG-DsRed and were harvested at E4. **(b,d)** The stem cell phenotype, as marked by Sox2, co-stains with 90% of the Notch1CR2 population and 94% of the transfection control (no significant difference). **(f,g)** Neuronal progenitor marker Pax6 co-localizes with 93% of Notch1CR2-GFP cells and 93% of the transfection control. **(j,l)** Anti-Notch1 co-localizes with 47% of Notch1CR2 cells and 49% of the transfection control. Scale bars = 20μm.

4.3 Gene regulatory activity of Notch1CR2 is decreased in neuronal cells

At E8, the neuronal phenotype is less prevalent in Notch1CR2-GFP^{+} cells compared to the DsRed^{+} cells. As seen in Figure 4.3, neuronal marker NeuN stains 52% of DsRed cells but only 17% of Notch1CR2-GFP^{+} cells (p=0.04). Early neuronal marker doublecortin (DCX) stains 46% of DsRed^{+} cells but only 10% of Notch1CR2-GFP^{+} cells (p=0.018). Similarly, Brn3, a neuronal transcription factor, co-localizes with 42% of DsRed^{+} cells but only 15% of Notch1CR2-GFP^{+} cells (p=0.002). At least 100 cells were counted for Notch1CR2-GFP^{+} cells (n=3) and 400 cells counted for DsRed^{+} cells (n=3).

4.4 Discussion

This chapter presents experimental validation of a computationally predicted non-coding region of Notch1, Notch1CR2, during early neural development. It was hypothesized that a region with high conservation across species, that is Notch1CR2, would be active in the developing CNS. If Notch1CR2 is activated through the binding of appropriate transcription factors, it may be involved in regulating or enhancing Notch1 expression.

Indeed, the data supports the hypothesis that Notch1CR2 is active during early neural development. However, is Notch1CR2 relevant to radial glial expression? Could it be an enhancer of Notch1? Yes, it is possible as was determined by the temporal and spatial profile of Notch1CR2 in chick embryos. Notch1CR2 is active during neurogenic periods of chick CNS development [45-47]. It is also present in radial glia during early development but it is diminished in neurons as neurogenesis proceeds.
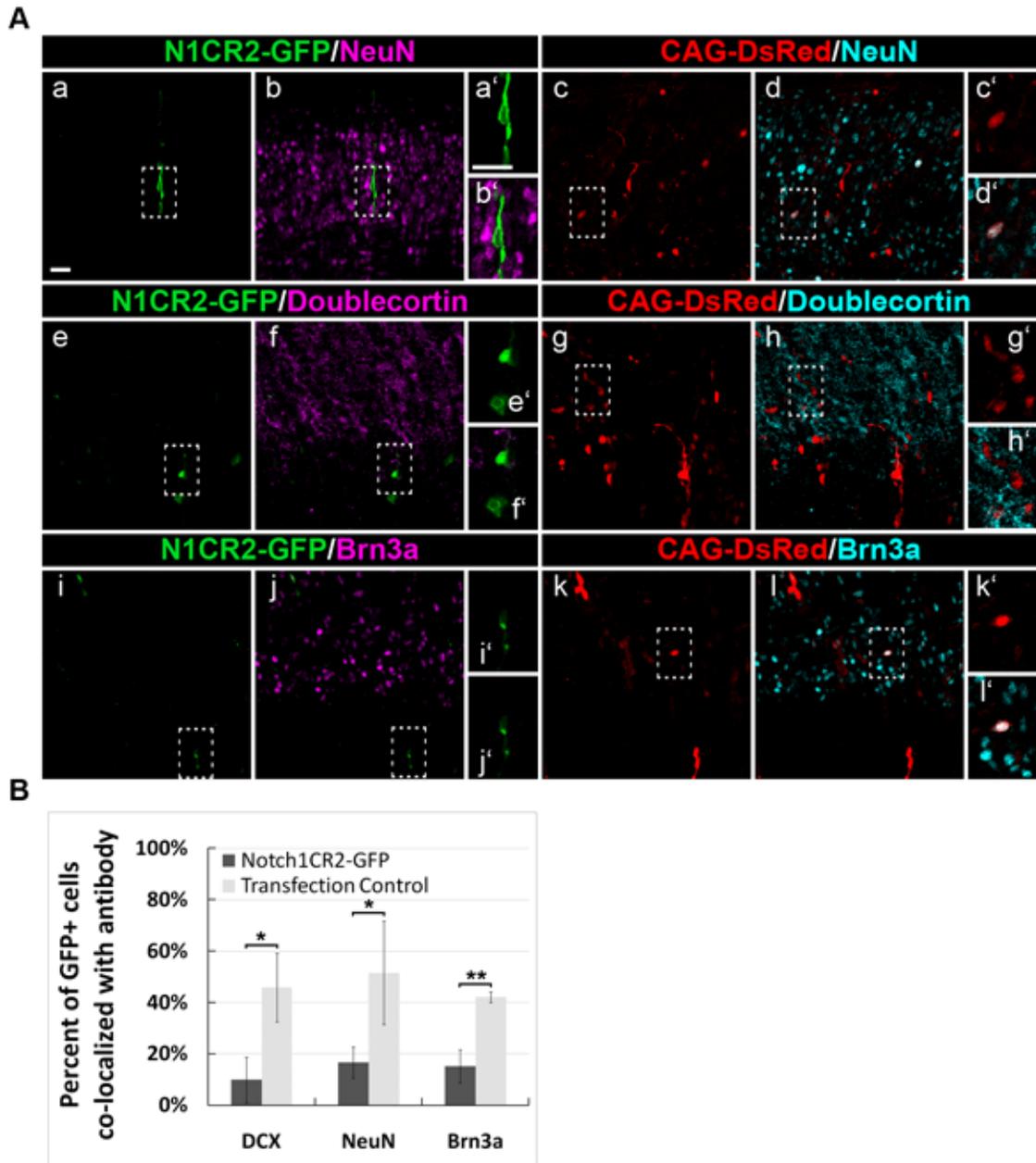
Figure 4.3. Gene regulatory activity of Notch1CR2-GFP is decreased in neurons at E8.

[A] Embryos (HH 12) were co-transfected with **(a,e,i)** Notch1CR2-GFP and **(c,g,k)** CAG-DsRed and were harvested at E8. Sections were stained with neuronal markers **(b,d)** NeuN, **(f,h)** double cortin (DCX), and **(j,l)** Brn3a.

[B] The neuronal phenotype, as marked by NeuN, is present in 16% of Notch1CR2-GFP^{+} cells (a,b,c) and with 52% of the transfection control (p=0.07). The newborn neuronal phenotype, as marked by doublecortin, is present in 10% of Notch1CR2-GFP^{+} cells, while 56% of the transfection control are doublecortin-positive (p=0.017). Brn3a, a neuronal marker, co-localizes with 24% of Notch1CR2-GFP^{+} cells and with 31% of the transfection control (p=0.06). *Scale bars = 20 μm.*

The next chapter provides data that challenges this hypothesis. The analysis of Notch1CR2 was extended into a transgenic mouse model to address the limitations of transient transfection and thus obtain a more thorough understanding of its temporal and spatial profile. The results from the transgenic mouse reveal that the profile of Notch1CR2 is not strictly a radial glial regulatory element as determined by the *in ovo* model. By the end of Chapter 5, the data supports a more refined hypothesis: Notch1CR2 is active in asymmetrically dividing progenitors that give rise to interneurons.

5   Gene Regulatory Activities of Notch1CR2 in Interneuron Progenitors of Transgenic Mouse

In this chapter, a complete temporal and spatial distribution of Notch1CR2 is described using a transgenic mouse model of Notch1CR2. Resources were invested into the development of a transgenic mouse because it would allow the precise examination of the regions of Notch1CR2 activity. This extent of analysis is limited in the transient chick model due to inconsistency in regions of transfection. Despite their limitations, *in ovo* transient transfections provided insight into two important phenomena: (1) Notch1CR2 is conserved across murine and avian species since the mouse sequence of Notch1CR2 drives GFP expression in chick and (2) Notch1CR2 is active in cells with a radial glial/non-neuronal phenotype.

Chapter 5 discusses various characteristics of Notch1CR2 activity in mouse and introduces a role of Notch1CR2 in interneuron progenitors. First, a pilot experiment confirmed the activity of Notch1CR2 in mouse via *in utero* transfections (Section 5.1). These experiments were done in collaboration with Dr. Mladen-Roko Rasin from the Department of Neuroscience and Cell Biology, University of Medicine and Dentistry of New Jersey. Sections 5.3-5.5 present the characterization of Notch1CR2 in the brain of the transgenic mouse at embryonic and postnatal time points including E12.5 (Section 5.3), E15.5 (Section 5.4), and P0 (Section 5.5). When Notch1CR2 activity subsides or ceases, Notch1CR2$^+$ cells are fated to become interneurons as suggested by the results of GFP recovery experiments (Section 5.6). Section 5.7 describes the presence of Notch1CR2-GFP in neural progenitors of the retina and spinal cord supporting that Notch1CR2 is active in the entire CNS.

5.1 Notch1CR2 is active in radial glia of mouse embryos as demonstrated by *in utero* electroporation

It was first confirmed that Notch1CR2-GFP is expressed in the brain of mouse embryos by performing transfection of embryos *in utero*. This experiment served as a pilot test before commissioning the development of the transgenic mouse. Notch1CR2-GFP was injected and electroporated into mouse embryos *in utero* at age E13.5, and samples were harvested at E14.5 (n=1), E17.5 (n=1), and P7 (n=1). Samples collected at E17.5 and P7 were co-transfected with equal concentrations of CAG-DsRed (1µg/µl Notch1CR2-GFP + 1µg/µl CAG-DsRed). In contrast, samples harvested at E14.5 were not co-transfected; instead, CAG-GFP was transfected into separate embryos because a red fluorescent transfection control was not available at the time. The single transfection at E14.5 also showed that GFP fluorescence was due to Notch1CR2-GFP and not bleed-through from a co-transfected construct.

As shown in Figure 5.1a-d, Notch1CR2-GFP expression is visible at E14.5 and E17.5 in the dorsal left hemispheres. The Notch1CR2-GFP expression pattern of the E17.5 whole brain is similar to the control. The dispersed GFP$^+$ fluorescence in the Notch1CR2-GFP$^+$ brain at P7 is most likely autofluorescence from arteries and not migrating GFP$^+$ neurons due to the large size of those green marks. However, coronal sections show differences in morphology and cellular phenotype. At this point, it is confirmed that Notch1CR2 is active during neurogenesis of the mouse. A more thorough analysis of the spatial distribution of Notch1CR2 in the mouse was performed in the transgenic mouse (Sections 5.2-5.7).
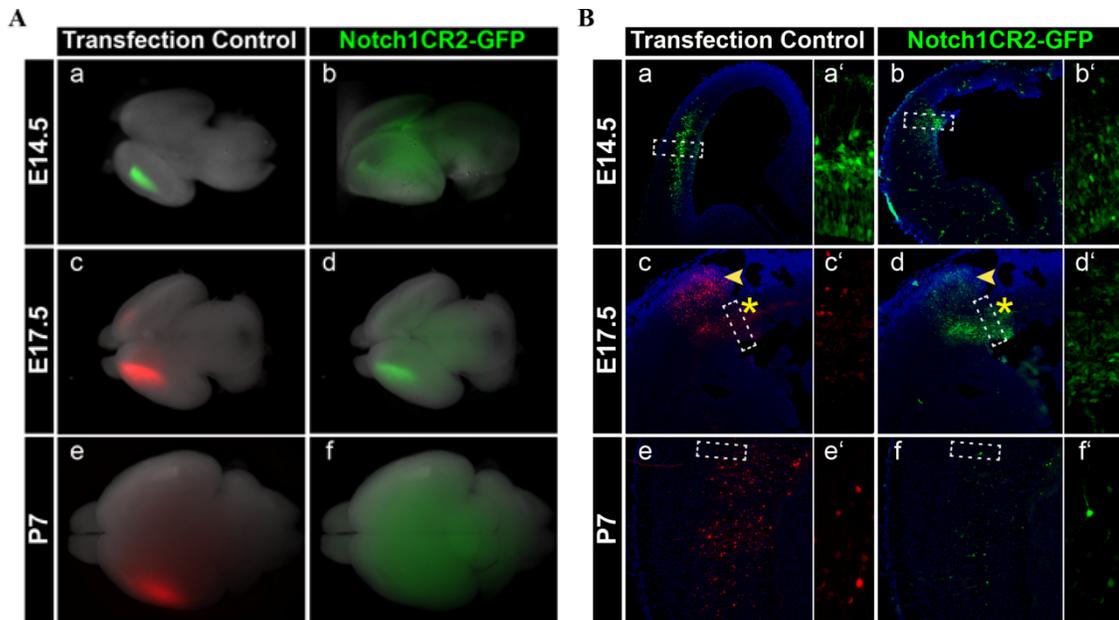
Figure 5.1. Notch1CR2-GFP is expressed in embryonic and postnatal brains of mouse embryos after *in utero* transfection.
[A] Embryos were consistently injected and electroporated at E13.5 by Dr. Mladen-Roko Rasin, and subsequently, harvested at E14.5, E17.5, and P7. **(a)** The transfection control CAG-GFP is strongly expressed in the left hemisphere at E14.5. **(b)** Notch1CR2-GFP is weakly visible at E14.5 in the left hemisphere. Ambiguous signal is present at the lateral commissure. **(c-d)** E17.5 samples were co-transfected with equal concentrations of the transfection control CAG-DsRed and Notch1CR2-GFP (1µg/µl each). Both CAG-DsRed and Notch1CR2-GFP are expressed strongly in the left hemisphere. **(e-f)** P7 mouse brains, which were similarly co-transfected, only display fluorescence from CAG-DsRed and not Notch1CR2. DNA plasmids were transfected at 3µg/µl at an approximate volume of 1 µl. (Note: Magnifications are not similar.)
[B] Coronal sections of the left hemisphere at each stage reveal differences between the transfection control and Notch1CR2. **(a-b)** At E14.5, CAG-GFP illuminates the VZ, SVZ, and IVZ while Notch1CR2 is only present in the VZ/SVZ. **(c-d)** By E17.5, cells expressing CAG-DsRed have migrated into the cortical plate. However, the highest density of Notch1CR2-GFP^{+} cells remain in the VZ/SVZ. **(e-f)** By P7, there is decreased Notch1CR2-GFP expression compared to the co-transfected CAG-DsRed. Since E17.5 embryos and P7 pups were co-transfected, c&d as well as e&f are identical regions. The eppendyma is on the right side of the image. All sections were stained with anti-GFP and imaged using the Zeiss fluorescent microscope. *(VZ = ventricular zone, SVZ = subventricular zone, IVZ = intermediate ventricular zone.)*

On a cellular level, Notch1CR2 maintains a mitotically-active, non-neuronal, early progenitor phenotype. This experiment provided the first piece of evidence that Notch1CR2 in mouse is active in the same type of cells as in chick. At E14.5

Notch1CR2 co-localizes with vimentin, a neural stem cell marker, as indicated by the yellow regions (Figure 5.2a-f). Because vimentin labels the cytoskeleton in the cytoplasm of the cell body and processes, it is sometimes unclear whether co-localization of Notch1CR2 and vimentin is from the same cell. It is possible that the process of a vimentin$^+$ cell is wrapped around a Notch1CR2-GFP$^+$ cell. Therefore, vimentin was not used for further analysis in the transgenic mouse.

Another antibody used in this analysis was Pax6, which is a neural progenitor transcription factor that is localized in the nucleus and thus serves as a clear indicator of the neural progenitor/neural stem cell state (Figure 5.2g-l). Pax6 clearly co-stains the CAG-GFP$^+$ radial cells of the ventricular zone (VZ) and sub-ventricular zone (SVZ) but not the cells in the intermediate ventricular zone (IVZ). In contrast, most Notch1CR2-GFP$^+$ cells are located in the VZ and SVZ and thus co-localize with Pax6. An additional antibody found in progenitors is Ki67, a mitotic marker of dividing cells in regions of the VZ, SVZ, and IVZ (Figure 5.2m-r). Similar to Pax6, Ki67 stains most Notch1CR2-GFP$^+$ cells. Interestingly, it also stains most CAG-GFP$^+$ cells in the VZ, SVZ, and IVZ unlike Pax6, which only stained CAG-GFP$^+$ cells of the VZ and SVZ.

Finally, we expected these "progenitor-like" Notch1CR2$^+$ cells to be negative for neuronal markers. As predicted, Notch1CR2-GFP$^+$ cells are NeuN$^-$ while some CAG-GFP$^+$ cells in the cortical plate are NeuN$^+$. The trends just described for Pax6, Ki67, and NeuN were quantified for one sample (n=1) (Figure 5.2B). Since the *in utero* transfections were designed as a pilot test of Notch1CR2 activity in mouse, counts were only performed for n=1. Therefore, significance of differences cannot be determined from the given data. Vimentin was not quantified at all because its non-nuclear staining

pattern is difficult to quantify. For each antibody, at least 300 cells were counted over at least three images.
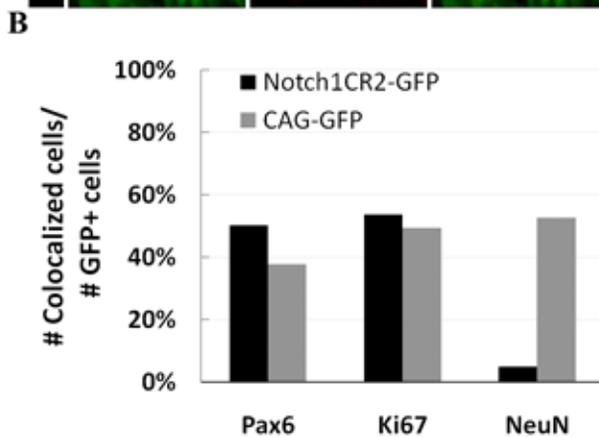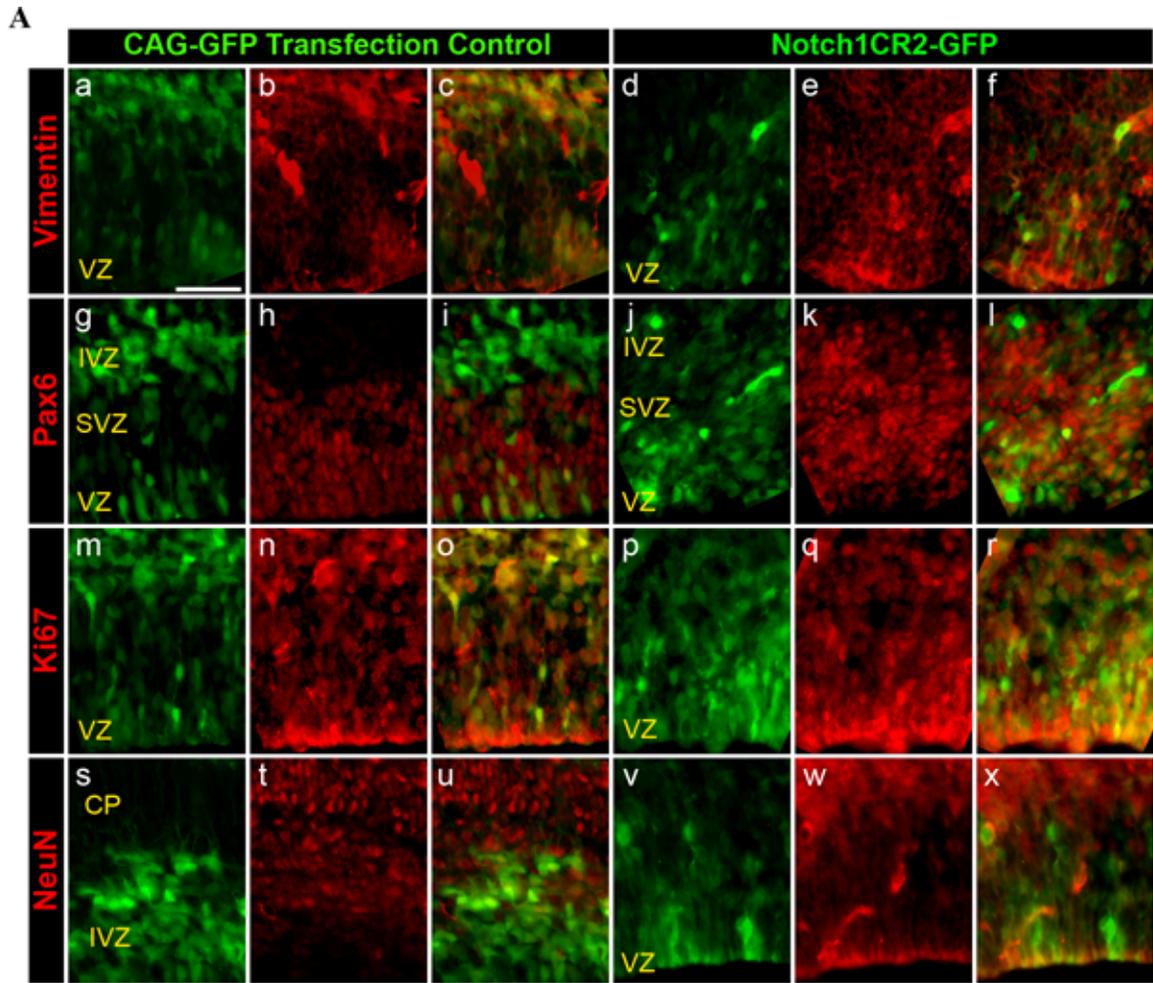
Figure 5.2. Notch1CR2-GFP activity at E14.5 is increased in neural stem cells and decreased in neurons of *in utero* transfected mouse embryos.
[A] Neural stem cell markers stain both **(a-c)** CAG-GFP and **(d-f)** Notch1CR2-GFP. **(g-i)** CAG-GFP is expressed in the VZ, SVZ, and IVZ. Of these cells, only CAG-GFP$^+$ cells in the VZ and IVZ co-localize with Pax6, neural progenitor marker. **(j-l)** However, most of Notch1CR2-GFP$^+$ cells are present mostly in the VZ and IVZ where they co-localize with Pax6. Ki67, which marks mitotic cells, is prevalent in both CAG-GFP$^+$ and Notch1CR2-GFP$^+$ cells. Although, some CAG-GFP co-localizes with NeuN, none of the Notch1CR2-GFP$^+$ cells co-localize with this neuronal marker. Samples were sectioned coronally, and all images are orientated with apical (VZ) at the bottom. Images were taken on the Zeiss fluorescent microscope using the 40x lens. *Scale bar = 20 µm.*
[B] Quantification of results supports the visual observation in (A) and shows less prevalence of the NeuN$^+$ neuronal phenotype in the Notch1CR2-GFP$^+$ population compared to the control. On a similar note, there is a slight prevalence of Pax6 and Ki67 in Notch1CR2 compared to the control. Since this experiment was a pilot test, counts were only done for n=1, and therefore significance of differences cannot be determined from the given data. At least 300 cells were counted for each antibody.

Notch1CR2-GFP expression decreases in embryos harvested at later time points of E17.5 at P7. As seen in Figure 5.3A, CAG-DsRed cells primarily occupy the cortical plate at E17.5. Few CAG-DsRed$^+$ cells extend horizontal red processes from the VZ, suggesting differentiation into neurons. In contrast, there are not as many Notch1CR2-GFP$^+$ cells in the cortical plate. Although there are green cells above the Tbr2$^+$ IVZ, there are no horizontal green processes, suggesting that Notch1CR2-GFP$^+$ cells are not differentiating into neurons like the control (Figure 5.3A).

By P7, there is less Notch1CR2-GFP than CAG-DsRed in the neocortex near the lateral ventricle (Figure 5.3B). Although Notch1CR2-GFP is not visible in the P7 whole mount, GFP was detected in coronal sections that were stained with anti-GFP. NeuN was used to landmark the location of transfected cells because it is present in these transfected regions. Surprisingly, the few GFP$^+$ cells remaining at P7 co-localized with NeuN. One possible explanation is that anti-GFP detects residual GFP that remains in differentiated cells after Notch1CR2 is no longer active. Section 5.6 provides a more detailed
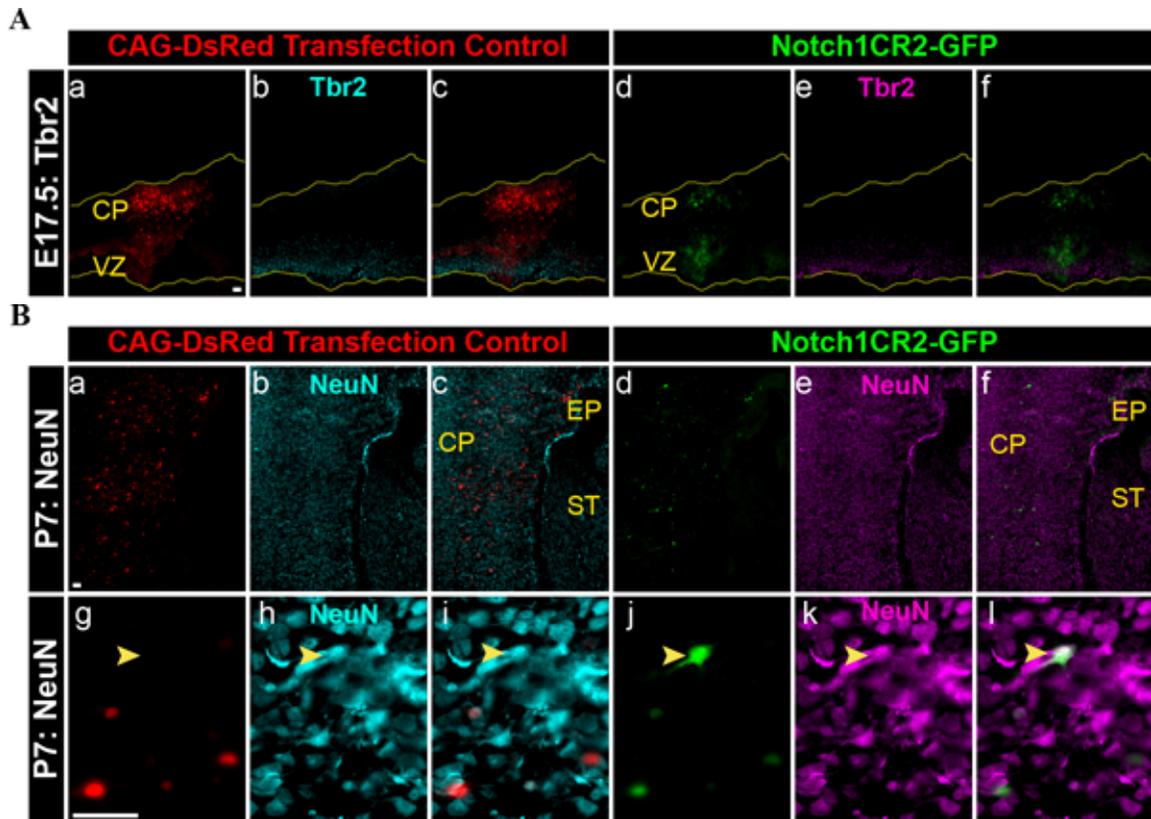
Figure 5.3. Transfected cells migrate above the SVZ/IVZ, as marked by Tbr2 in embryos harvested 4 days (at E17.5) and 14 days (at P7) after transfection,.

[A] Since this sample was co-transfected, the regions in the CAG-DsRed transfection control and Notch1CR2-GFP sample are identical. Tbr2 was used to visualize the IVZ, and it is falsely colored light blue in the transfection control and purple in Notch1CR2-GFP. Anti-GFP was used to aid in the visualization of Notch1CR2-GFP. **(a-c)** There is a high density of CAG-DsRed[+] in the cortical plate. Red horizontal processes lie above the Tbr2^{+} IVZ (light blue). **(d-f)** Notch1CR2-GFP expression is less compared to CAG-DsRed. Notch1CR2-GFP is present in the VZ/SVZ/IVZ as well as the cortical plate. Transfection was done *in utero* at E13.5.

[B] Notch1CR2-GFP is expressed in fewer cells at P7 compared to the transfection control. The sections were also stained with anti-GFP and with NeuN, a neuronal marker, which served as a landmark when mapping out DsRed and GFP expression. **(a-f)** Fewer cells are GFP[+] than DsRed[+]. Both GFP and DsRed are dispersed throughout the CP. **(g-l)** Interestingly, most DsRed^{+} cells and some GFP^{+} cells co-localize with NeuN. The arrow denotes a Notch1CR2-GFP[+] cell that is NeuN[+] but does not have CAG-DsRed. This example denotes that CAG-DsRed does not bleed through into the green channel. (*CP=cortical plate, EP=eppendyma, ST=striatum*)

explanation on the implications of GFP recovery.[1] Quantitative analysis was not performed for E17.5 and P7, but instead was performed in the neocortex of the transgenic mouse.

In summary, the pilot *in utero* experiment provided three pieces of valuable insight: (1) the 399-base pair sequence for Notch1CR2 is conserved across chick and mouse, (2) the duration of Notch1CR2 activity corresponds to periods of neurogenesis as also seen in chick, and (3) the neural stem cell/progenitor phenotype is predominant over the differentiated neuronal phenotype in Notch1CR2^{+} mouse cells. Given this information, the development of the transgenic mouse was commissioned. With this key resource, it was possible to perform a more thorough investigation of the complete temporal and spatial distribution of Notch1CR2. For the remainder of Chapter 5, characterization of the Notch1CR2-βGP-GFP transgenic mouse is presented.

5.2 CNS-specific Notch1CR2-GFP is expressed during neurogenesis as demonstrated in transgenic mouse

The complete temporal and spatial expression profile of Notch1CR2 was examined in a transgenic mouse containing the Notch1CR2-βGP-GFP transgene. As shown in Figure 5.4, GFP expression at embryonic time points ranges from E10.5 to E15.5 (Figure 5.4A). Embryonic immunohistochemical analysis focused on E12.5, when radial glial activity has peaked, and E15.5, when radial glia begin to disappear (refer to Sections 5.3-5.4). Time points between E15.5 and birth have not been examined and will be characterized by future investigators. GFP expression is also present in P0 pups, visible

---

[1] At P7, Pax6 and Ki67 are no longer present in the regions where the transfected cells are present. Tbr2 is also not useful for analysis because it stains the eppendyma and the hippocampus, areas that do not express DsRed and hence were not transfected.

only after sectioning (refer to Section 5.5). However, sections of older pups are GFP negative at P7 and P16. The time points and their sample sizes are E10.5 (n=3), E11.5 (n=2), E12.5 (n=4), E14.5 (n=5), E15.5 (n=10), P0 (n=3), P7 (n=3), and P16 (n=1).

Embryonic Notch1CR2-GFP expression patterns are strongest in the ventral brain, in particular the VZ and SVZ of the ganglionic eminences (Figure 5.4B). The morphology of these GFP$^+$ cells is radial, indicative of radial glia. At P0, Notch1CR2-GFP remains present in the VZ and SVZ of the lateral ventricles but also illuminates the rostral migratory pathway including the olfactory bulb (Figure 5.4C). The next sections present data that describes the cellular phenotype of Notch1CR2$^+$ cells using immunohistochemistry.

Later time points (P7 and P16) were sectioned and stained to determine whether low levels of Notch1CR2-GFP were present at P7 and P16. Although GFP is not visible at P7, GFP is visualized after treatment with anti-GFP. This method of GFP recovery will mark cells with either (1) low levels of Notch1CR2-GFP or (2) residual GFP during its degradation process. By P16, GFP is not detectable even with anti-GFP staining. In other words, low levels of GFP are absent 16 days after it is last naturally observed at P0. Since P0 is the latest time point with visible Notch1CR2-GFP without GFP recovery, it can be concluded that Notch1CR2 activity subsides between P0 and P7. Interestingly, this observation corresponds with the known half-life of GFP which is 26 hr. Based on this information, it can be said that recovered GFP at P7 represents less than 1% residual GFP from P0 [95]. Accordingly, any remaining GFP at P7 should degrade by P16, which corresponds with the GFP negative samples at P16. The utilization of GFP recovery to examine cell fate is described in Section 5.6.

A

Notch1CR2-GFP

E10.5 E12.5 E14.5 E15.5

B

Notch1CR2-GFP⁺

E15.5

C

Notch1CR2-GFP⁺
P0

c-LV

r-LV

RMS

OB

c-LV r-LV

RMS OB
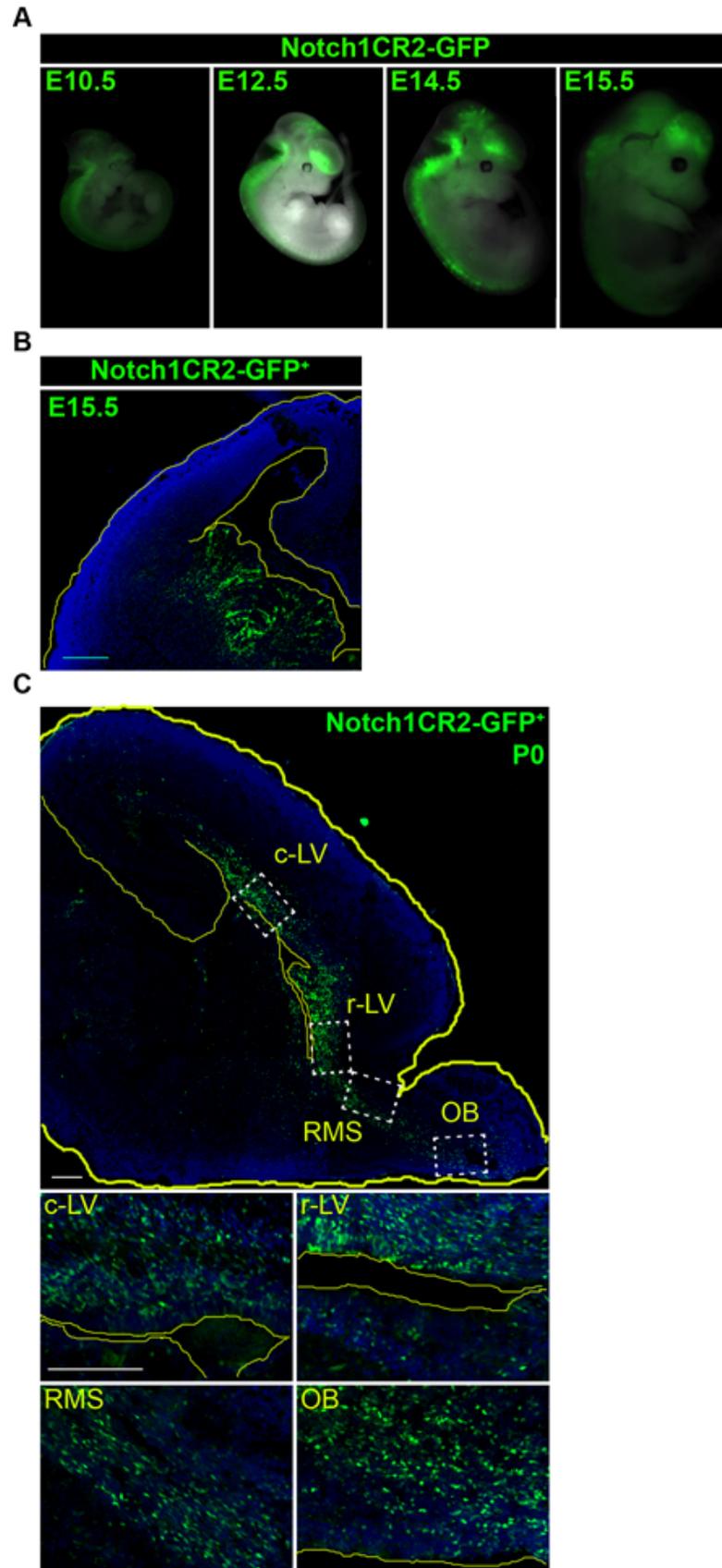
Figure 5.4. CNS-specific Notch1CR2-GFP expression in transgenic mice is exclusive during embryonic development.
(A) Embryos at E10.5, E12.5, E14.5 and E15.5 were collected and imaged using the Leica fluorescent microscope. Notch1CR2-GFP is expressed exclusively in the CNS from the telencephalon to the sacral spinal cord at E10.5, E11.5, E12.5, E14.5, E15.5.
(B) Coronal sections at E15.5 show GFP expression in the GE of Notch1CR2$^+$.
(C) Saggittal sections of P0 wildtype show GFP expression in the olfactory bulb, the rostral migratory stream, and regions surrounding the lateral ventricle. Saggittal sections were stained with nuclear marker Dapi and were imaged using a fluorescent microscope. These images were subsequently organized into a montage. *(Scale bar = 20 μm, GE = ganglionic eminences, c-LV= caudal lateral ventricle, r-LV – rostral lateral ventricle, RMS = rostral migratory stream, VZ = ventricular zone)*

5.3 Notch1CR2-GFP is predominantly expressed in the embryonic ganglionic eminence during early neurogenesis at E12.5

Sections 5.3-5.5 present characterization of Notch1CR2-βGP-GFP transgenic mice via immunohistochemistry. An array of markers was used to stain for radial glia, progenitors, asymmetrically dividing cells, neurons, and glia. Embryos at E12.5 were first selected for immunohistochemical analysis because it is the period of peak radial glial (and thus Notch1) activity. Notch1CR2-GFP$^+$ cells co-localize with radial glial (as marked by anti-Notch1 and BLBP) and with asymmetrically dividing cells (as marked by NuMa). However, Notch1CR2-GFP does not co-localize with post-mitotic neuronal markers such as doublecortin and Tbr1 (Figure 5.5).
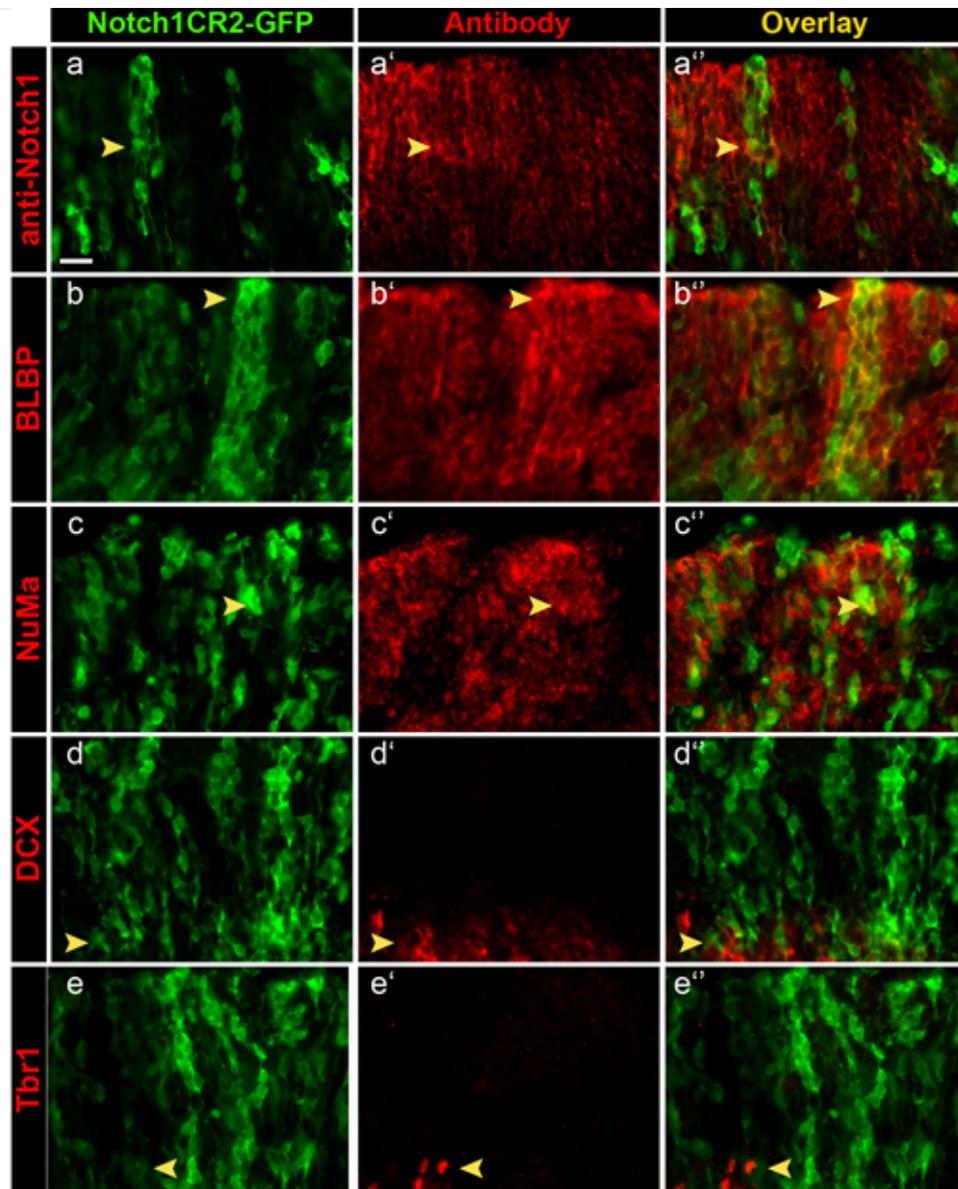
Figure 5.5. Notch1CR2-GFP is expressed in neural progenitors and not neurons during early neurogenesis at E12.5.
The lateral ganglionic eminence in coronal sections was stained with an array of markers. Notch1CR2 co-localizes with **(a)** anti-Notch1, **(b)** radial glial marker BLBP, and **(c)** NuMa, which is a marker for asymmetric division. Notch1CR2 does not co-localize with **(d)** early neuronal marker doublecortin and **(e)** Layer VI neuronal marker Tbr1.

5.4 Notch1CR2-GFP is expressed in asymmetrically dividing progenitors of the GE at E15.5

Similar to E12.5, Notch1CR2-GFP$^+$ cells are asymmetrically dividing. In E15.5 embryos, Notch1 protein is expressed in some Notch1CR2-GFP$^+$ cells as indicated by its co-localization with anti-Notch1 (Figure 5.6a). Radial glial marker BLBP as well as asymmetric mitotic marker NuMa also stained Notch1CR2-GFP$^+$ cells (Figure 5.6c). However, the phenotype of Notch1CR2-GFP is not neuronal, as indicated by the lack of co-localization with DCX, respectively (Figure 5.6).
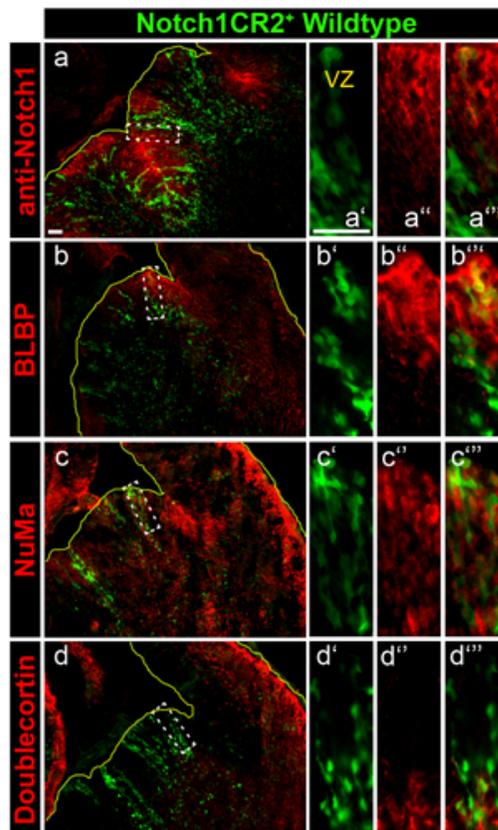
Figure 5.6. Some GFP$^+$ cells in E15.5 Notch1CR2$^+$mice maintain a radial glial phenotype while most are progenitors undergoing asymmetric division.
Notch1CR2$^+$ E15.5 embryos were sectioned coronally and immunostained with radial glial markers (anti-Notch1 and BLBP), mitotic marker (nuclear mitotic apparatus marker, NuMa), or early neuronal marker, (doublecortin, DCX). Some GFP$^+$ cells co-localize with **(a)** anti-Notch1 and **(b)** BLBP. However, more co-localize with **(c)** NuMa. In comparison, GFP$^+$ cells do not co-stain with **(d)** DCX. *(Scale bar = 20 μm)*

5.5 Notch1CR2-GFP+ cells continue as neural progenitors at P0

At P0, Notch1CR2-GFP activity persists and is localized in three areas of the brain: (1) the VZ/SVZ/IVZ of the dorsal lateral ventricle, (2) the rostral migratory stream, and (3) the olfactory bulb (Figure 5.4C and Figure 5.7). In more lateral sections, there is also expression in the caudate putamen (Figure 5.8B). Finally, there are a few dispersed GFP$^+$ cells in the neocortex (Figure 5.9A).

A

B

Notch1CR2/Tbr2/Dapi
P0

C

Notch1CR2/DCX/Dapi
P0
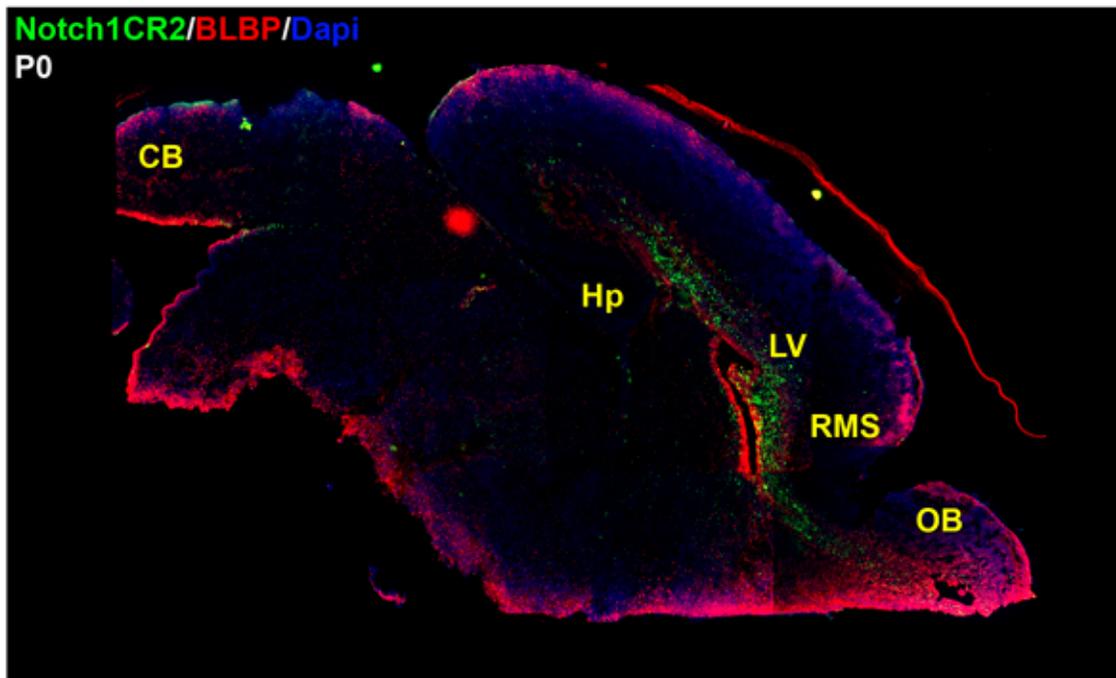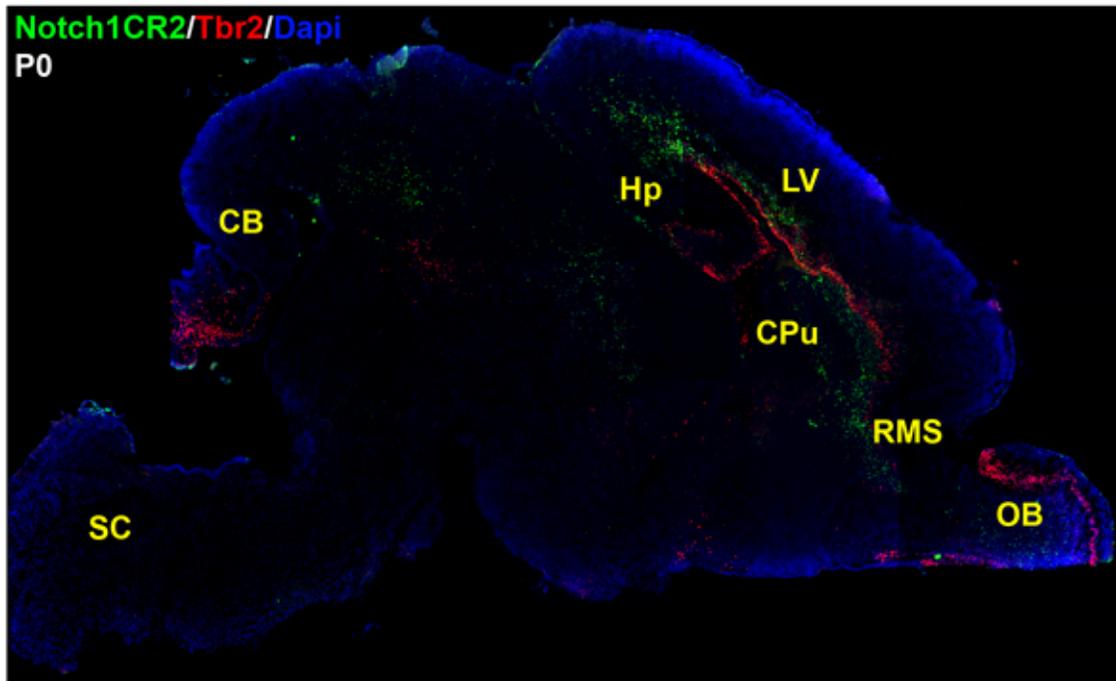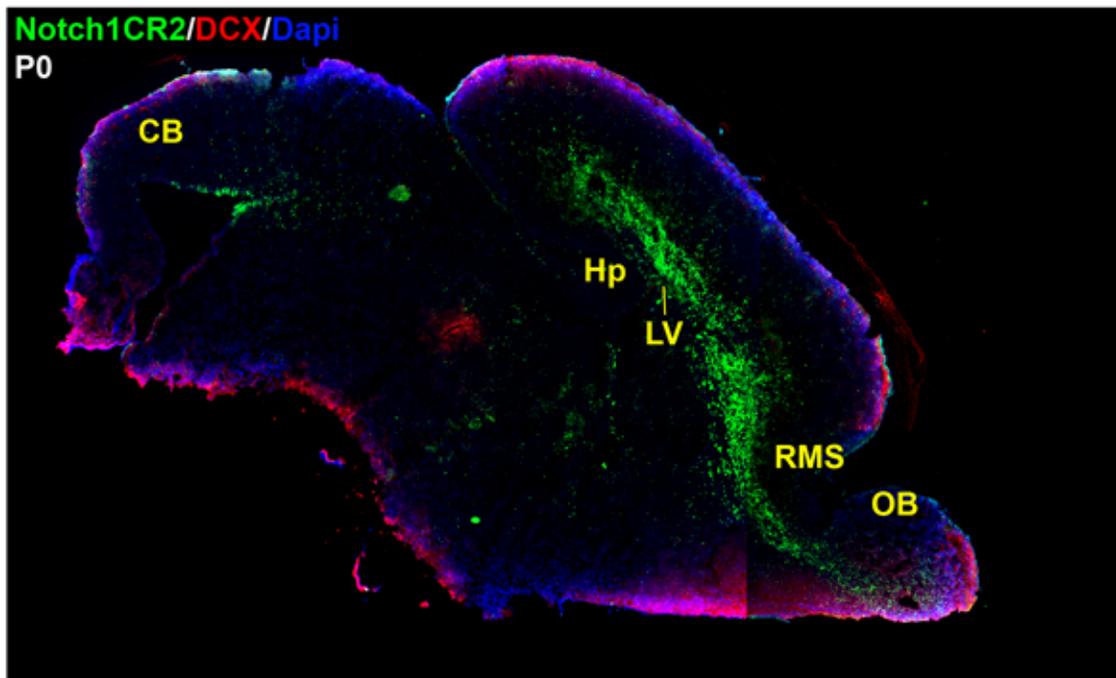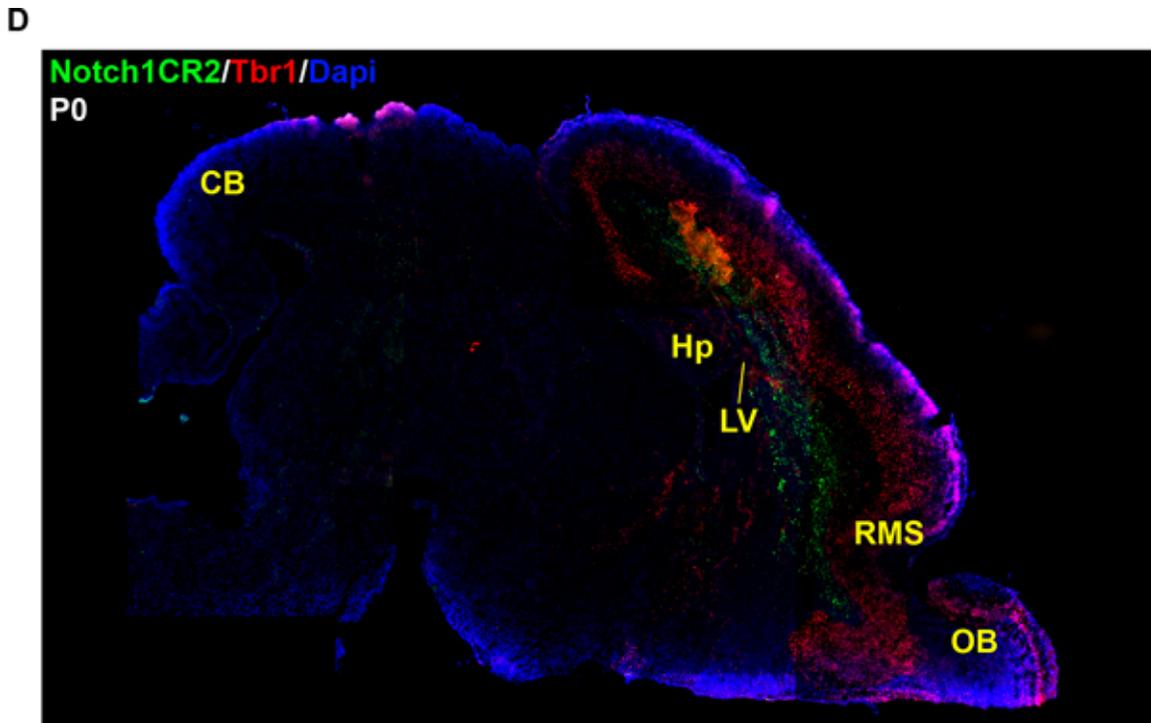
Figure 5.7. Notch1CR2-GFP$^+$ cells are located around the lateral ventricle, rostral migratory stream, and olfactory bulb at P0.
Saggittal sections at P0 were stitched into montages for easy visualization of Notch1CR2-GFP and antibody patterns. As seen in all four montages, Notch1CR2-GFP is expressed in the LV, RMS, and the OB. **(A)** Notch1CR2 of the VZ co-localizes with BLBP. BLBP is expressed in the VZ and in the upper neocortex near the pial surface. **(B)** Notch1CR2-GFP that is expressed in the IVZ co-localizes with Tbr2, an intermediate progenitor marker. **(C-D)** Notch1CR2 does not co-localize with doublecortin, which is an early neuronal marker present in the superficial layers. **(D)** The regions of Notch1CR2-GFP and Tbr1 expression are very distinct, indicating that Notch1CR2 is not active in Layer VI neurons. (*CB = cerebellum, CPu = caudate putamen, Hp = hippocampus, LV=lateral ventricle, OB = olfactory bulb, RMS = rostral migratory stream, SC = spinal cord*)

The pattern of GFP is clearly visualized in the montage of saggittal cross-sections. GFP$^+$ cells in the VZ or IVZ co-localize with BLBP (radial glial marker) and Tbr2 (IVZ marker), respectively. No GFP$^+$ cells stain with doublecortin (early neuron marker) or Tbr1 (Layer VI marker). These results show that the phenotype of Notch1CR2 is of neural progenitors and not neurons. This pattern corresponds with the phenotype determined at E15.5 (see Section 5.4). The sections were characterized further at higher

magnification and with additional antibodies (Figure 5.8). Notch1CR2 activity was examined in several regions of the brain including **the VZ/IVZ/SVZ**, **the upper layers of the neocortex**, **the caudate putamen**, and **the olfactory bulb**.

At P0, GFP positive cells maintain a progenitor phenotype and inhabit the **VZ/SVZ/IVZ**. As shown in Figure 5.8A-B, GFP$^+$ cells in the VZ co-localize with anti-Notch1 and BLBP (the yellow outline marks the boundary of the lateral ventricle). This pattern is consistent with the co-localizations at E15.5 (Figure 5.6). Notch1CR2$^+$ cells of the VZ also co-localize with NuMa (Figure 5.8B-a). Interestingly, Notch1CR2 co-localizes with glutamate decarboxylase (GAD65/67), a marker for γ-aminobutyric acid (GABA) interneurons (Figure 5.8B-b). Some GAD65 neurons have been shown to be dividing cells [96]. Therefore, GAD65/67 marks both interneuron progenitors and interneurons. GFP expression continues into the caudate putamen where it has an interesting staining pattern with NuMa and GAD65/67 (will be discussed in Figure 5.9).

Markers that do not co-localize with Notch1CR2 in the **VZ/SVZ/IVZ** are also important. Notch1CR2-GFP$^+$ cells do not co-localize with early neurons (doublecortin) or by Layer VI neurons (Tbr1) (Figure 5.8C). The boundary between Notch1CR2-GFP and Tbr1 is distinct, suggesting that Notch1CR2 is not active in differentiated cortical neurons. By P0, the peak of neurogenesis is over, neural stem cell activity decreases, and gliogenesis becomes the prominent form of differentiation. At this stage, differentiated astrocytes as well as some radial glia express glial fibrillary acidic protein (GFAP), a glial marker. Notch1CR2 does not co-localize with GFAP, suggesting that Notch1CR2 is not present in astrocytes or gliogenic radial glia.
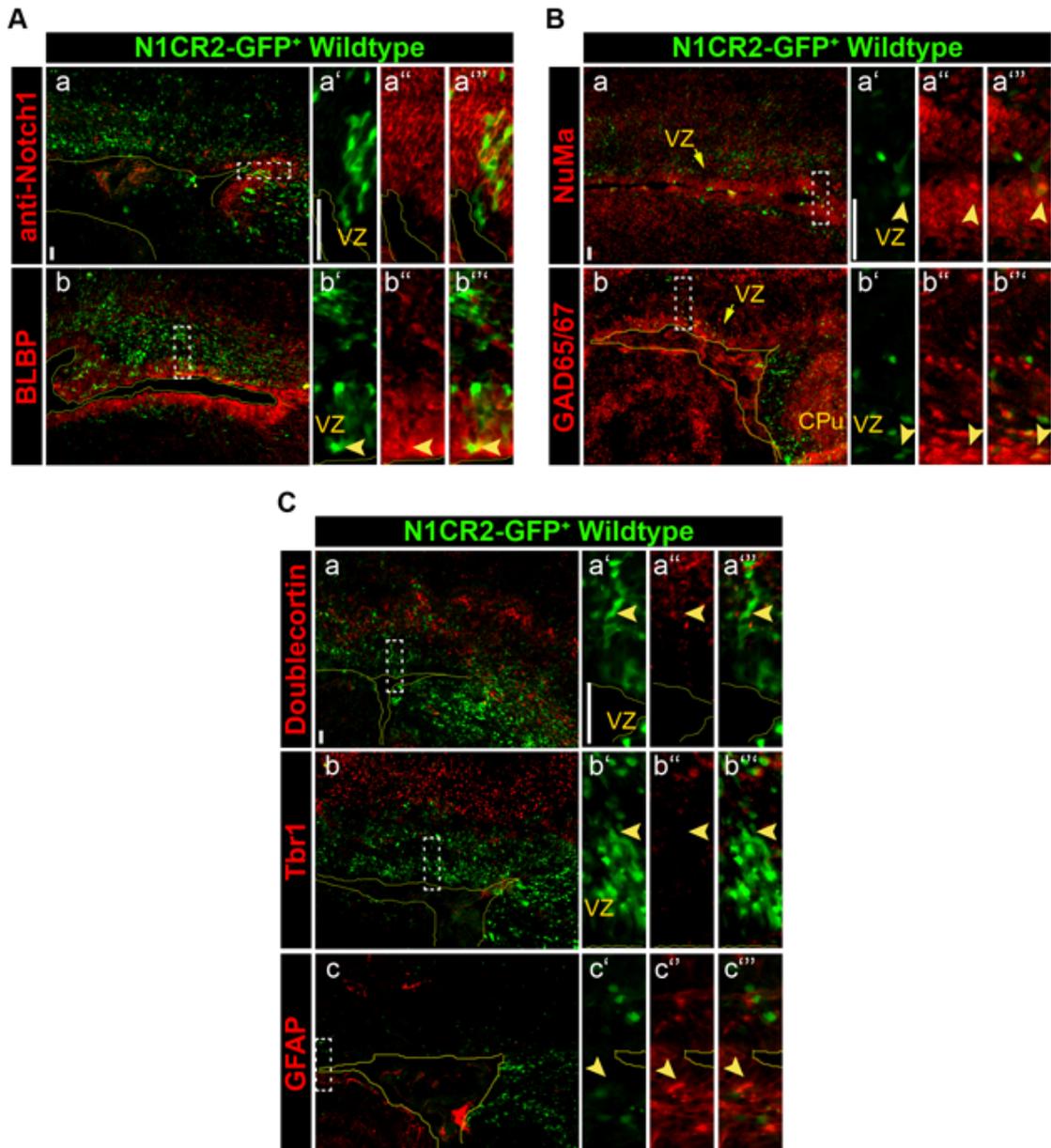
Figure 5.8. Notch1CR2-GFP^{+} cells of the VZ at P0 are asymmetrically dividing cells and interneuron precursors.
[A] Notch1CR2-GFP^{+} cells in the VZ are radial glia. Notch1CR2-GFP^{+} cells co-localize with **(a)** anti-Notch1 and **(b)** BLBP.
[B] Notch1CR2-GFP^{+} cells in the VZ are asymmetrically dividing interneuronal precursors. **(a)** NuMa, a marker for asymmetric division, is expressed in the GFP^{+} cells of the VZ. **(b)** Notch1CR2-GFP^{+} cells of the VZ also co-localize with interneuron precursor marker, GAD65/67.
[C] The neuronal and glial phenotypes are not present in Notch1CR2-GFP^{+} cells. Notch1CR2-GFP does not co-localize with (a) doublecortin^{+} early neurons (b) Tbr1^{+} Layer VI neurons, or (c) GFAP[+] glia. Saggittal sections were immunostained and imaged using the Zeiss fluorescent microscope. *GFAP = glial fibrillary acidic protein*

The **upper layers of the neocortex** are dispersed with Notch1CR2-GFP$^+$ interneuron precursors. GFP is found in both radial and neuronal cells. For example, the arrow in Figure 5.9A-d points to a radial cell while the arrow in Figure 5.9A-c points to a neuronal-like cell, which might even be extending its process in a horizontal fashion. In these upper layers, Notch1CR2-GFP is found in asymmetrically dividing cells (NuMa) and interneuron precursors (GAD65/67). Co-localization with more mature GABAergic interneurons (VGAT, vesicular GABA transporter) is not clear. However, a few feint GFP$^+$ processes were found co-stained with VGAT (Figure 5.9A-b). NeuN is a general neuronal marker and is highly expressed in this region. However, a closer look reveals that Notch1CR2-GFP does not completely co-stain with NeuN, but rather neighbors the NeuN expression (Figure 5.9A-d). The data from this panel of antibodies suggests that Notch1CR2-GFP$^+$ cells are asymmetrically dividing interneuron precursors in the upper layers of the neocortex. As these precursors differentiate, Notch1CR2-GFP activity decreases, and the cells obtain a GABAergic neuronal phenotype.

Notch1CR2-GFP$^+$ cells display a dual pattern in the **caudate putamen** (CPu) as seen in Figure 5.8B-b. In the outer layer of the caudate putamen, Notch1CR2-GFP$^+$ cells are radial, pointing towards the center of the caudate putamen. These cells do not co-localize with NuMa or GAD65/67. In contrast, the inner layer of the caudate putamen displays a more punctuate GFP expression pattern, indicative of neurons. The inner GFP$^+$ cells of the caudate putamen co-localize with NuMa and GAD65/67 (Figure 5.9B). The results suggest that the caudate putamen at P0 contains a population of asymmetrically dividing interneuron precursors with active Notch1CR2.

The **olfactory bulb** is illuminated primarily with neuron-like and not radial Notch1CR2-GFP$^+$ cells. These cells co-localize with NuMa and GAD65/67 suggesting that they are asymmetrically dividing and that they are interneuron precursors. In contrast to the upper layers of the neocortex and to the caudate putamen, the olfactory bulb contains more Notch1CR2-GFP$^+$/NeuN$^+$ cells, indicating a more differentiated neuronal phenotype in Notch1CR2-GFP$^+$ cells. Although VGAT is expressed in the same regions as GFP, it is difficult to discern whether GFP$^+$ processes co-localize with VGAT. A higher resolution confocal image is needed to resolve this question.

In summary, Notch1CR2-GFP is not exclusively expressed in radial glia as initially hypothesized in the chick model described in Chapter 4. Instead, Notch1CR2 is active in a more committed mitotic cell-type which undergoes asymmetric division. The data suggests that these cells are interneuron precursors fated to become GABAergic interneurons. The underlying question is to identify the appropriate *trans*-acting factors than are activating Notch1CR2-βGFP-GFP. Chapter 6 explores potential *trans*-acting factors, in particular transcription factors of interneuron precursors, which could be responsible for activating Notch1CR2-GFP.

A

Pial Surface of Cortex
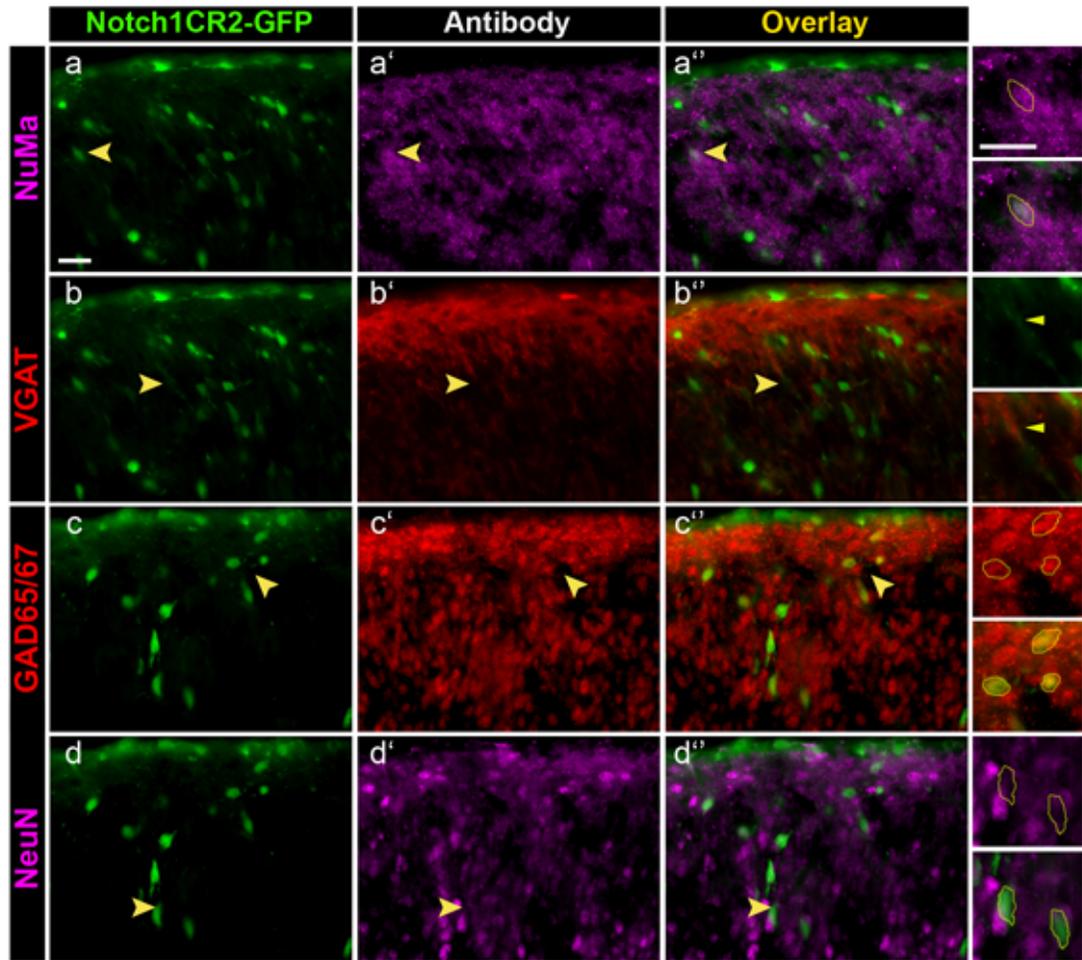
B

Mid-Region of Caudate Putamen
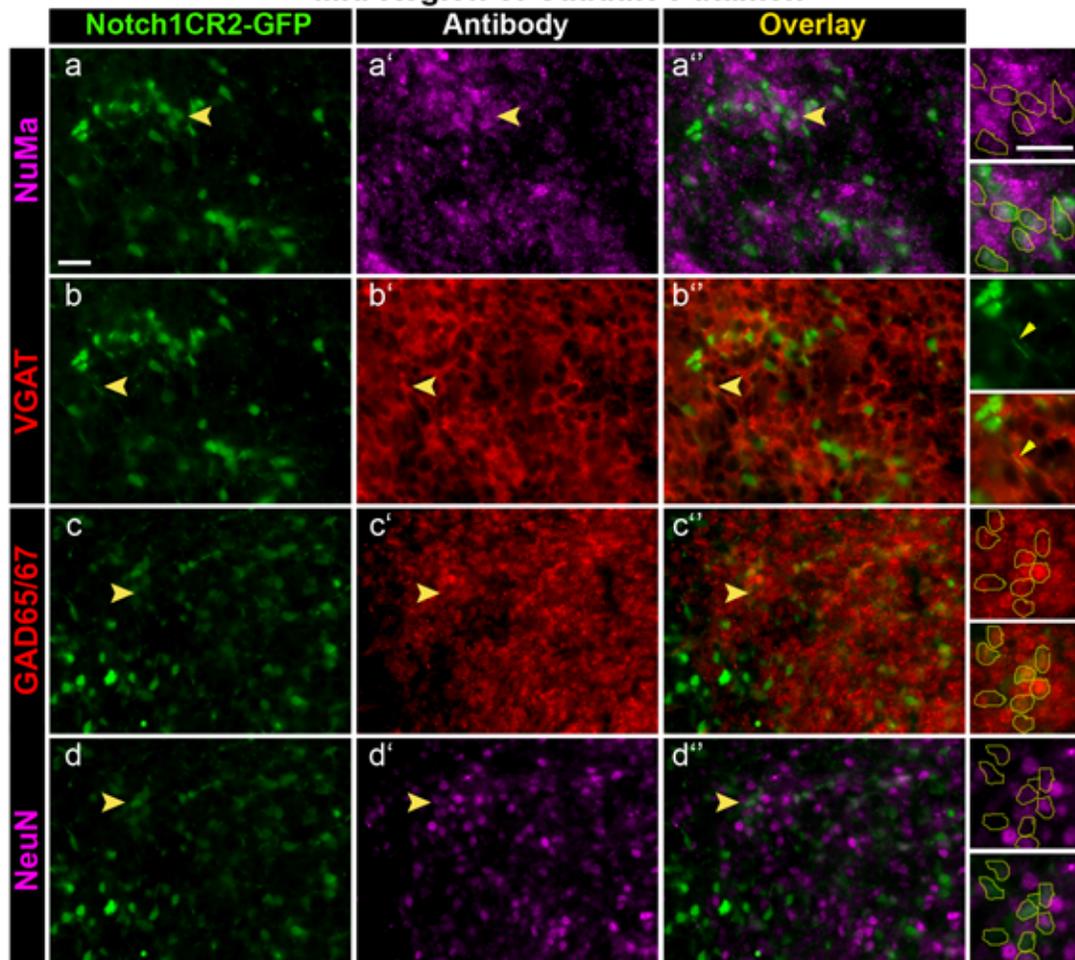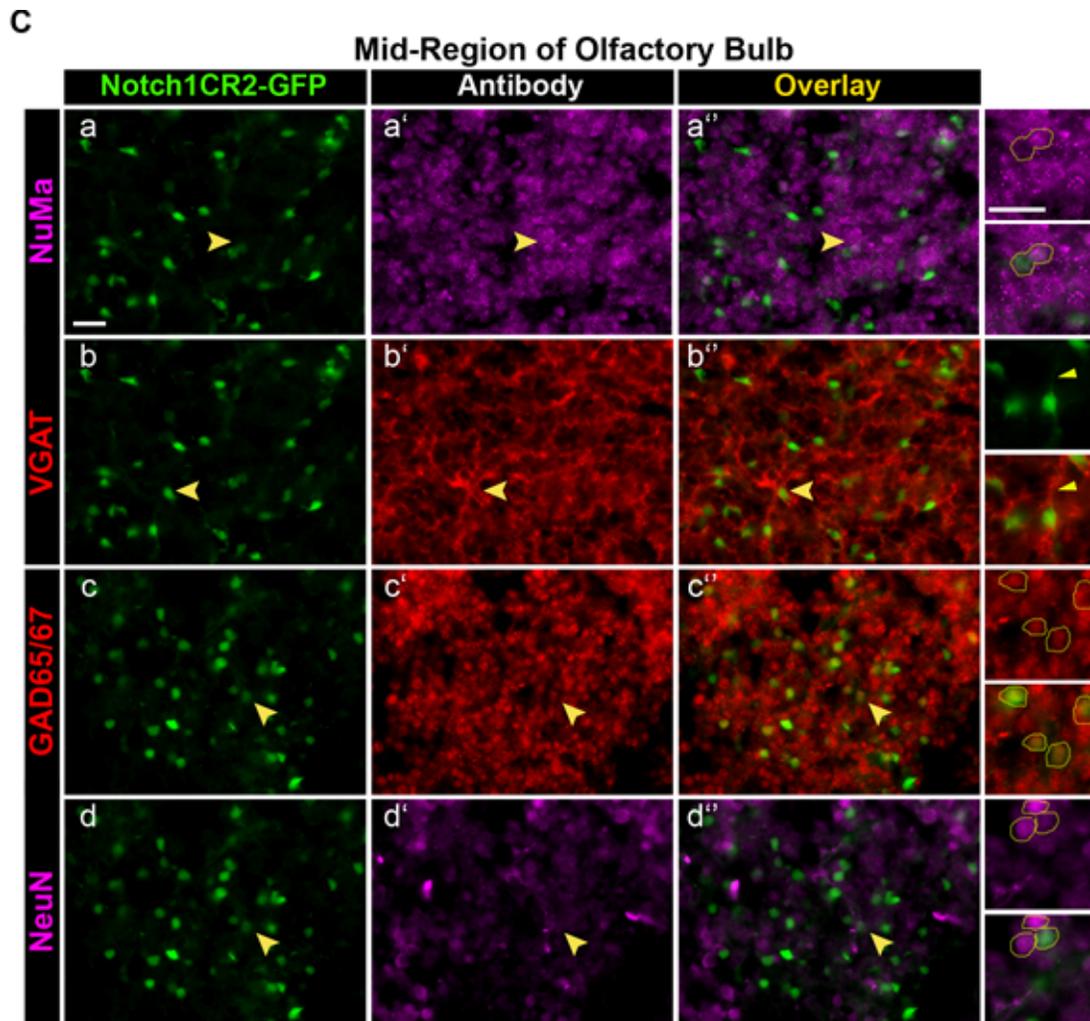
Figure 5.9. Notch1CR2-GFP^{+} cells are asymmetrically dividing interneuron precursors near the pial surface, in the caudate putamen, and in the olfactory bulb.
[A] Pial surface of P0 Notch1CR2 pup. **(a)** Notch1CR2-GFP[+] co-localizes with NuMa, a marker for asymmetric division. **(b)** The processes of some Notch1CR2-GFP^{+} cells co-localize with the process of VGAT[+] interneurons. **(c)** GAD65/67 stains the majority of cells in the upper layers of the neocortex and co-localizes strongly with Notch1CR2-GFP. **(d)** Some but not all Notch1CR2-GFP^{+} cells co-localize with NeuN. In the higher magnification, the two circled green cells are NeuN negative.
[B] Caudate putamen of P0 Notch1CR2 pup. Notch1CR2-GFP[+] strongly co-localizes with **(a)** NuMa and **(b)** GAD65/67. **(c)** Processes of VGAT co-localize with feint GFP. **(d)** NeuN neighbors Notch1CR2-GFP expression.
[C] Olfactory bulb of P0 Notch1CR2 pup. Similar co-localization patterns occur in the olfactory bulb. Notch1CR2-GFP[+] co-localizes with **(a)** NuMa and **(b)** GAD65/67 and neighbors **(d)** NeuN expression. **(c)** Processes of VGAT co-localize with feint GFP. The arrows denote the region that is amplified on the right. Samples were sectioned on the saggittal plane at 15 μm thickness.

5.6 Recovery of residual/low-levels of GFP reveals an interneuronal fate

Since the detection of fluorescence with a fluorescent microscope is often weak, antibodies against fluorescent proteins have been engineered to amplify expression and address this limitation. Protein expression (i.e., GFP) is a dynamic process dictated by rates of protein expression and degradation. For example, the half-life of GFP is 26 hr. Accordingly, it takes 7 days for 99% of the GFP to degrade after initial expression. Therefore, when anti-GFP is used for signal amplification, up to 7-day old GFP is being amplified. Using anti-GFP marks "false-positives" or cells that *had* but do not necessarily currently *have* Notch1CR2 activity. On the other hand, this technique of GFP recovery can be utilized to reveal interesting information about the cell fate of Notch1CR2$^+$ cells. Since GFP remains for 7 days after initial expression, anti-GFP can amplify GFP that was expressed up to 7 days earlier. Therefore, a Notch1CR2$^+$ cell can be "tracked" for approximately 7 days after Notch1CR2-GFP is no longer expressed. *(Note: Anti-GFP does not amplify detectable levels of basal GFP as expressed by βGP-GFP alone.)*

Using GFP retrieval, new populations of GFP$^+$ cells were unveiled at E12.5, E15.5, and P7 (Figure 5.10). Without anti-GFP, only the VZ/SVZ layers of the embryonic ganglionic eminence are inhabited by radial GFP$^+$ cells. When anti-GFP is applied, three new regions are illuminated. Bright GFP$^+$ cells now occupy the ganglionic eminence below the VZ/SVZ and the basal (top) layer of the neortex, while feint radial cells stretch across the neocortex (Figure 5.10A-a to A-d). By P0, only the ventral VZ/SVZ of the lateral ventricle and a few dispersed cells in the cortical plate express GFP without anti-

GFP. The application of anti-GFP illuminates the VZ/SVZ of the entire lateral ventricle and a greater number of cortical plate cells (Figure 5.10A-e to A-f). At P7, no GFP is visible until anti-GFP recovers expression in the eppendyma, cortical plate, hippocampus, and midbrain (Figure 5.10B). The expression in the midbrain is most likely remaining from Notch1CR2$^+$ cells that extend to the spinal cord in the embryo (Figure 5.17). There was no GFP expression at P16, even with anti-GFP treatment. Interestingly, there is a 7 day lag (from P0 to P7) where GFP can only be detected with anti-GFP, and then after 9 more days (P7 to P16), GFP cannot be detected at all. This time line corresponds with the known half-life of GFP, which calculates that is takes approximately 7 days for GFP to disappear.

If GFP can be detected up to 7 days after Notch1CR2-GFP stops expression, what is the cell fate of Notch1CR2 cells? It was hypothesized that Notch1CR2$^+$ cells of the ganglionic eminence differentiate into interneurons that tangentially migrate into the neocortex. The hypothesis was supported by the anti-GFP$^+$ cells in the basal neuroepithelium that co-localize with an early neuronal marker (doublecortin, DCX) but not radial glial markers (anti-Notch1 and BLBP) (See Figure 5.11). Since the antibodies for Notch1, BLBP, and doublecortin are cytoplasmic, their staining patterns are best viewed in low magnification. Anti-Notch1 stains the VZ, and BLBP appears in both apical and basal surfaces because BLBP$^+$ radial glia extend their process from the VZ to the pial surface.

A

	No GFP Retrieval	GFP retrieval
E12.5	a	b
E15.5	c	d
P0	e	f

B

Notch1CR2⁺
anti-GFP
P7
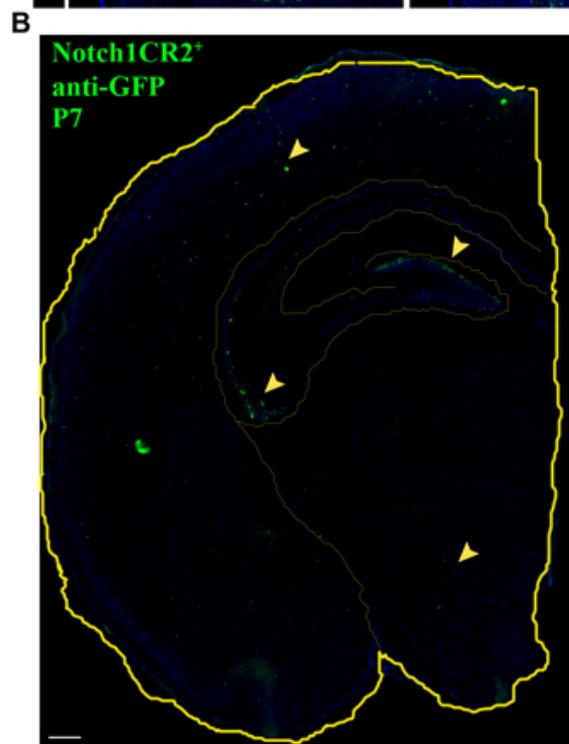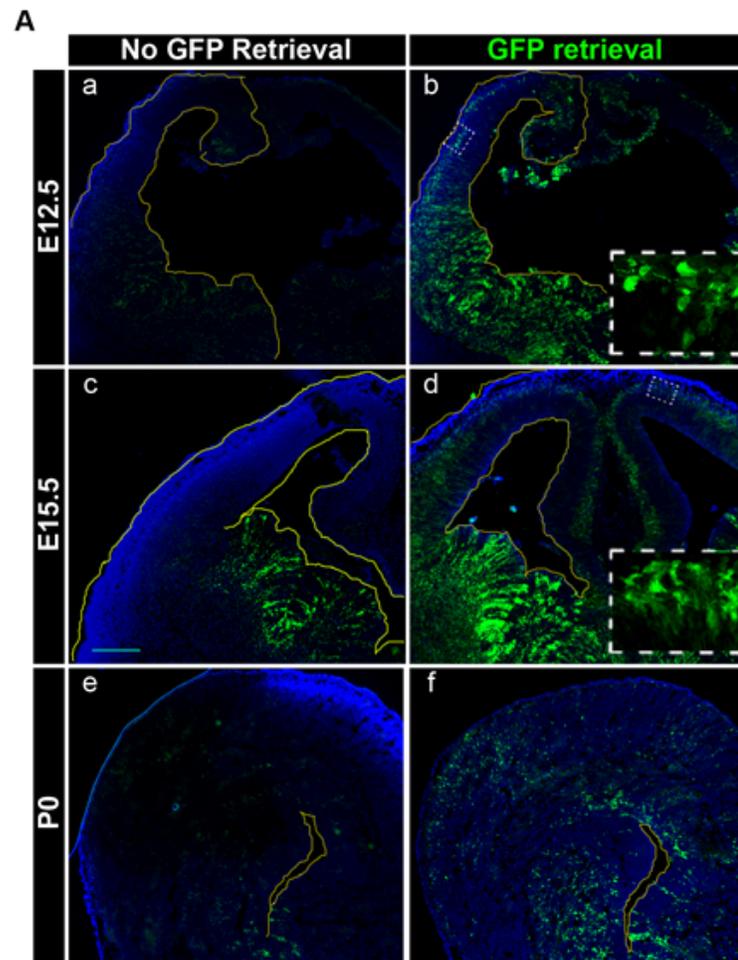
Figure 5.10. GFP can be recovered in the neocortex of Notch1CR2 transgenic samples at E12.5, E15.5, P0, and P7.

[A] Low levels and residual GFP were amplified using anti-GFP. **(a)** Without anti-GFP, the cells in the VZ/SVZ of the GE at E12.5 are GFP$^+$. **(b)** However, anti-GFP reveals three additional populations of GFP$^+$ cells located in the following regions: (1) ventral GE below the VZ/SVZ, (2) the basal (upper) layers of the neocortex, and (3) VZ/SVZ of the neocortex. The third region only consists of feint GFP$^+$ cells. **(c)** Similarly, E15.5 samples show the same GFP recovery patterns as E12.5. **(d)** P0 samples without anti-GFP show radial expression around the lateral ventricle (especially around the ventral region) and dispersed in the cortical plate. In contrast, anti-GFP not only stains the VZ/SVZ of the entire lateral ventricle but also stains many more cells in the cortical plate.

[B] At P7, GFP is only visible when anti-GFP is applied. Anti-GFP stains the eppendyma, the hippocampus, and dispersed cells of the cortical plate and the midbrain (indicated by the arrows). The samples were sectioned coronally. Serial sections were examined with and without anti-GFP at each time point.
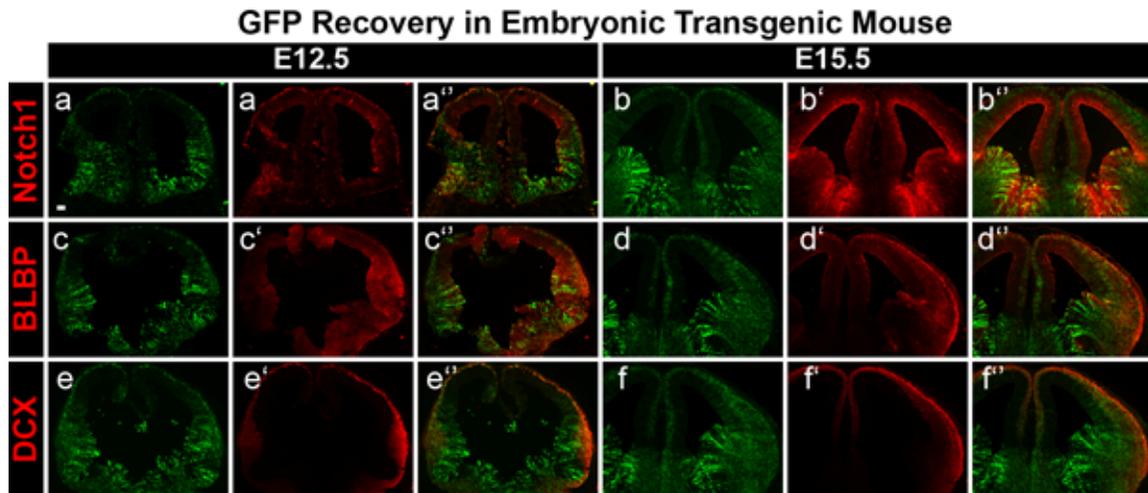
Figure 5.11. The phenotype of cells with recovered GFP shows decreased activity in radial glia and an increased activity in newborn neurons.

(a-b) While anti-Notch1 is expressed in the VZ, anti-GFP$^+$ cells populate regions beyond the VZ into the differentiated region of the GE and even the cortical plate. Most of anti-GFP$^+$ cells do not co-localize with anti-GFP. **(c-d)** BLBP co-localizes with anti-GFP in the basal (top) and apical (bottom) surfaces. **(e-f)** Doublecortin co-localizes with the bright anti-GFP in the basal (top) surface. These patterns are similar at E12.5 and E15.5. Sections are coronal, and Dapi marks the nucleus. Scale bar = 20 μm.

In order to further test the hypothesis that cells with Notch1CR2 are fated to neuronal tangential migration, anti-GFP expression in the neocortex was characterized immunohistochemically at E15.5 and P7 (Figure 5.12). NuMa shows the greatest co-localization with Notch1CR2–GFP at both time points. At E15.5, NuMa labels the feint, radial GFP cells of the neocortex, while at P7, NuMa labels bright GFP cells. In fact, the percentage of GFP$^+$ cells with NuMa/GFP co-staining increases from 20% to 57% at E15.5 to P7, respectively. Early neuronal marker doublecortin is prevalent at E15.5 (44%) but drops (2%) at P7. At P7, the minority of anti-GFP$^+$ cells are Tbr2$^+$ intermediate progenitors while the majority of cells remain as Tbr1 (about 30%) Layer VI neurons. This result contrasts the results without anti-GFP at P0 (Figure 5.7), which show that the Notch1CR2-GFP$^+$ cells occupy a separate, yet neighboring region from Tbr1$^+$ cells.

So far, GFP has been retrieved in the apical layers of embryonic transgenic, but postnatal P7 samples reveal expression in the eppendyma, the neocortex, and the hippocampus as well. At P7, anti-GFP expression in the hippocampus is present in cells with a neuronal morphology as seen in Figure 5.13. These cells co-localize with Tbr1 and NuMa, suggesting that Notch1CR2 is/was active in asymmetrically dividing cells or newborn neurons. They also co-localize with GAD65/67$^+$ interneuron precursors. However, they are not yet differentiated into mature VGAT$^+$ GABAergic interneurons. Anti-GFP$^+$ cells are also not BLBP$^+$ radial glia or Tbr2$^+$ intermediate progenitors. The data suggests that Notch1CR2-GFP regulates neurogenesis and that Notch1CR2-GFP$^+$ cells are fated to become GABAergic interneurons.
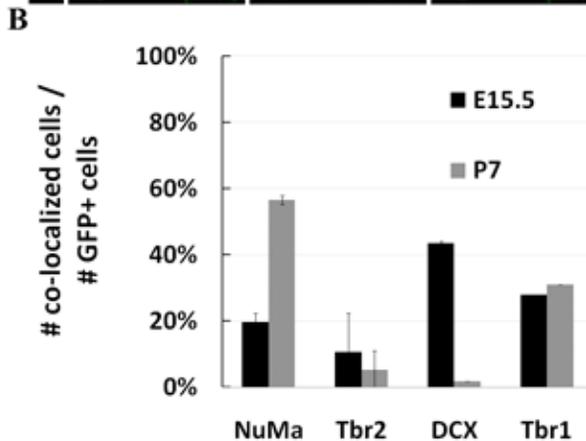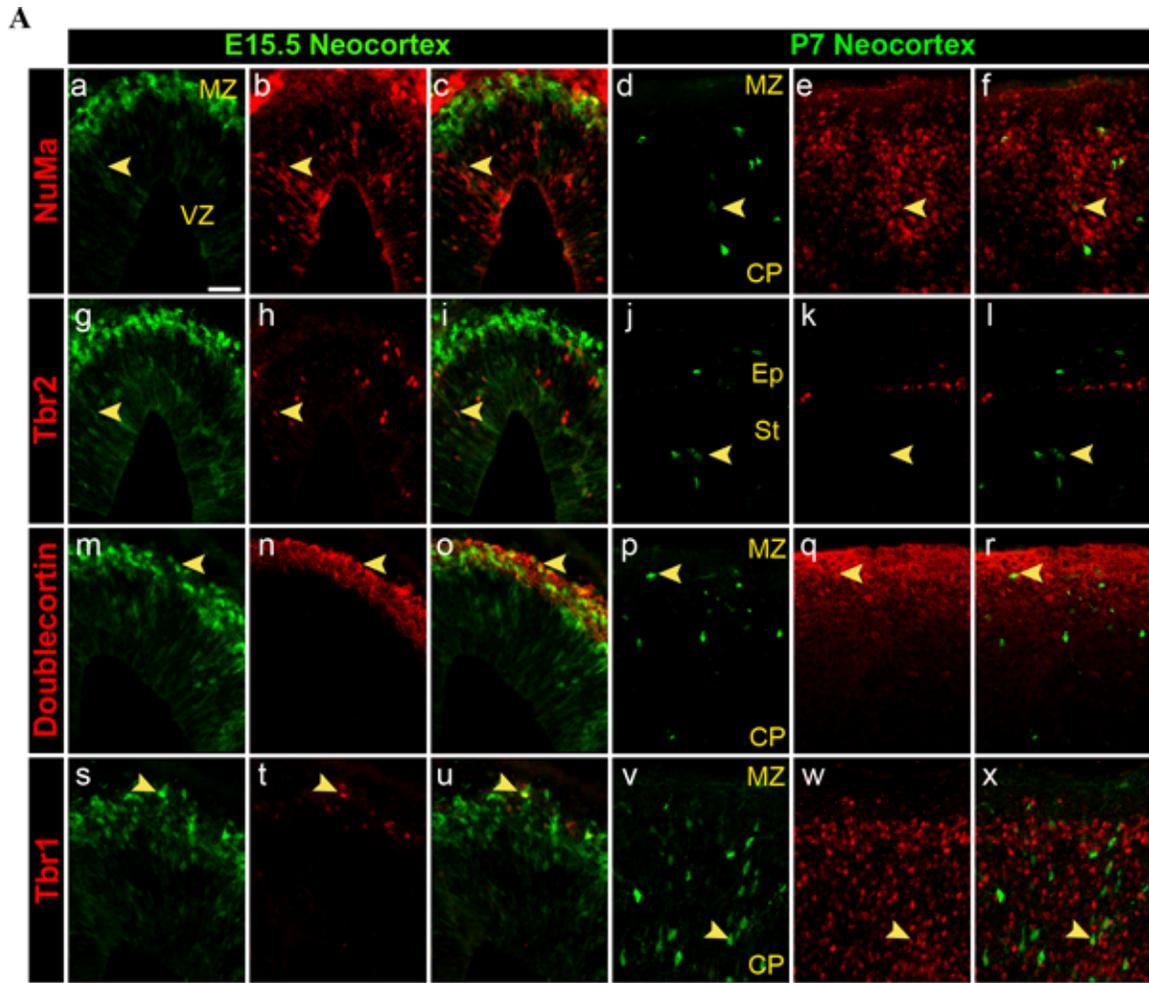
Figure 5.12. Anti-GFP reveals neocortical Notch1CR2-GFP expression at E15.5 and P7.

[A] At E15.5, there is one population of bright Notch1CR2-GFP$^+$ cells in the MZ. Another population is feint and radial and occupies the cortical plate. **(a-c, g-i)** Most feint GFP cells co-localize with NuMa compared to the few cells that co-localize with Tbr2. **(m-o, s-u)** The bright basal cells co-localize with young doublecortin$^+$ neurons and

Tbr1$^+$ Layer VI neurons. By P7, there are only bright GFP$^+$ cells, which co-localize with NuMa (d-f) and Tbr1 (v-x) but not Tbr2 (j-l). Few co-localize with doublecortin.

[B] The number of antibody/GFP co-stained cells was normalized to the number of GFP$^+$ cells. The prevalence of NuMa in the Notch1CR2-GFP$^+$ population increases from 20% to 57% from E15.5 to P7 while the prevalence of DCX decreases from 44% to 2%. Tbr1 and Tbr2 are consistently present in Notch1CR2 at both ages (about 10% and 30%, respectively). However, co-localization with Tbr2 is low. At least 300 cells in each of the three samples were counted for each antibody. The only exception was Tbr1 at E15.5 which had a sample size of n=1.
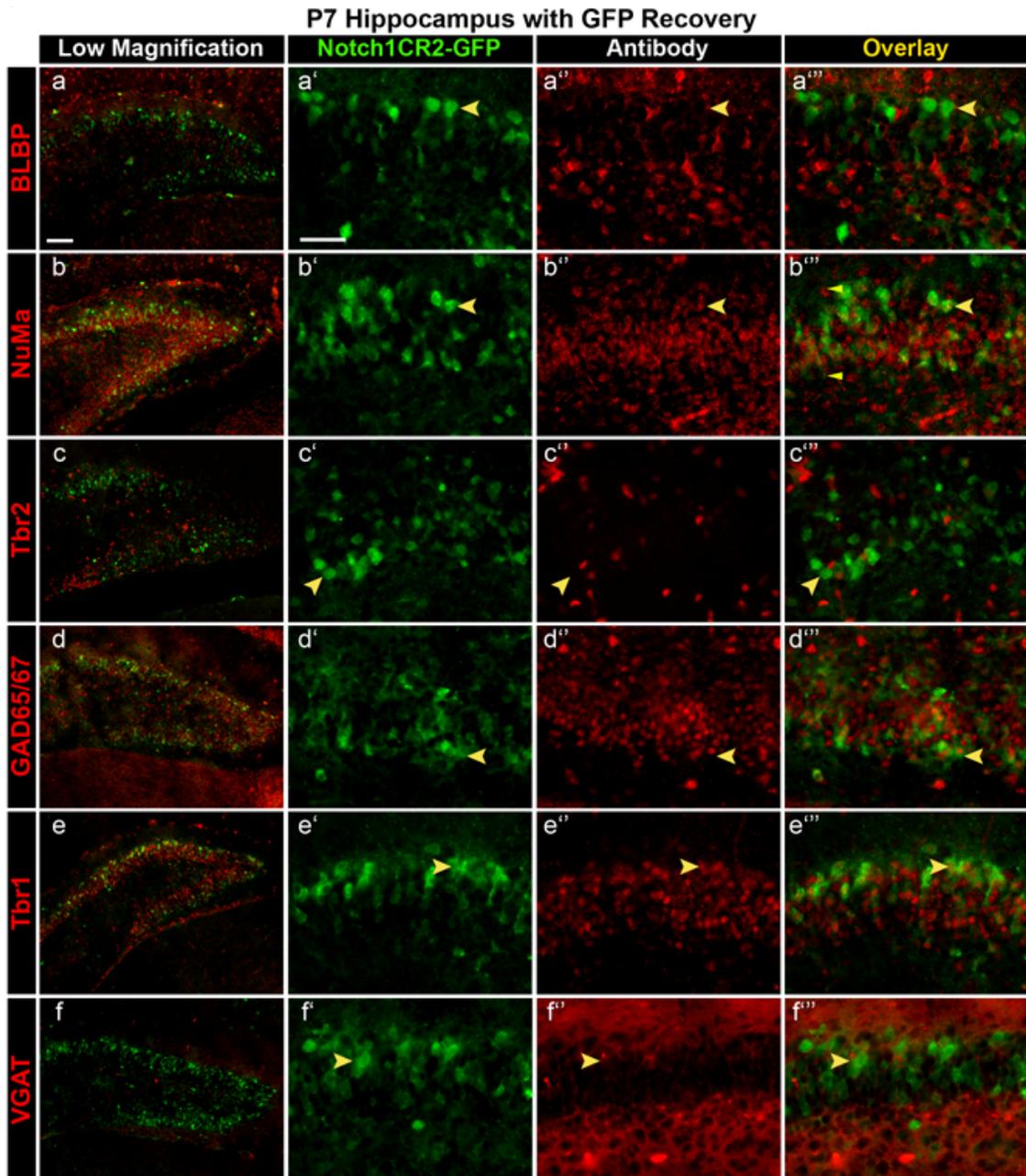
Figure 5.13. GFP is recovered in asymmetrically dividing cells of the hippocampus at P7.

P7 is the first time point in which GFP is detected in the hippocampus, but only with GFP recovery. Anti-GFP does not co-stain with **(a)** BLBP[+] radial glial markers, **(c)** Tbr2^{+} intermediate progenitors, or **(f)** VGAT[+] GABAergic interneurons. However, anti-GFP[+] does co-localize with **(b)** NuMa[+] asymmetrically dividing cells, **(d)** GAD65/67[+] interneuron precursors, and **(e)** Tbr1^{+} neurons. Sections are coronal. *Scale bar = 20 µm.*

5.7 Notch1CR2 is active in the entire developing CNS, including the retina and spinal cord

In addition to the cortex, Notch1CR2-GFP is also expressed in the retina and the spinal cord. In cases of GFP recovery, the phenotype of Notch1CR2-GFP$^+$ cells in retina is similar to the brain in that (1) some GFP$^+$ cells are radial glia, (2) some are neuronal, and (3) the majority are asymmetrically dividing. GFP retrieval allowed for examination of all levels of activity, including low expression.

In the retina, GFP$^+$ cells are radial in morphology and span all the layers. In the retina, the nuclei of radial glia are found in various positions but their endfeet are positioned in the apical and basal layers [97]. Immuhistochemistry was performed at two embryonic time points, E12.5 and E15.5 (n=3 for each). Sections of retina were stained with anti-GFP and a panel of stem/progenitor markers (Figure 5.16) and differentiated neuronal markers (Figure 5.16). The lack of co-localization of GFP$^+$ cells with BLBP does not support a radial glial phenotype. However, GFP$^+$ cells are not entirely excluded from possessing radial glial features as seen by the co-localization of two endfeet with BLBP at E12.5 (Figure 5.15a). More GFP$^+$ cells co-localize with neural progenitors as marked by Pax6 at E12.5. However, this feature of Notch1CR2-GFP decreases by E15.5, also due to the decrease of Pax6 staining at this stage.

Although Notch1CR2-GFP activity is not present in progenitor/stem cells, it is present in a variety of retinal neuronal types. The profile of Notch1CR2-GFP activity includes ganglion cells (Brn3 and Islet1) and amacrine cells (NeuroD). There are four other retinal cell types: photoreceptors, horizontal cells, bipolar cells, and glia [98]. Bipolar cells and glia are born after birth and were therefore not tested. A horizontal cell

marker (Lim1/2) did not express at E12.5. Further analysis at later time points would

capture the entire neurogenic potential of Notch1CR2 in the retina.
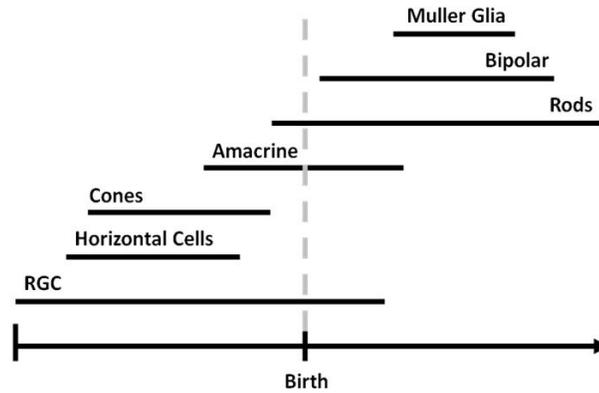
Figure 5.14. Timeline of retinogenesis.
The retina consists of seven cell types, born in the following order: retinal ganglion cells (RGC), horizontal cells, cones, amacrine cells, rods, bipolar cells, and Müller glia. The duration of genesis of each type is shown above.
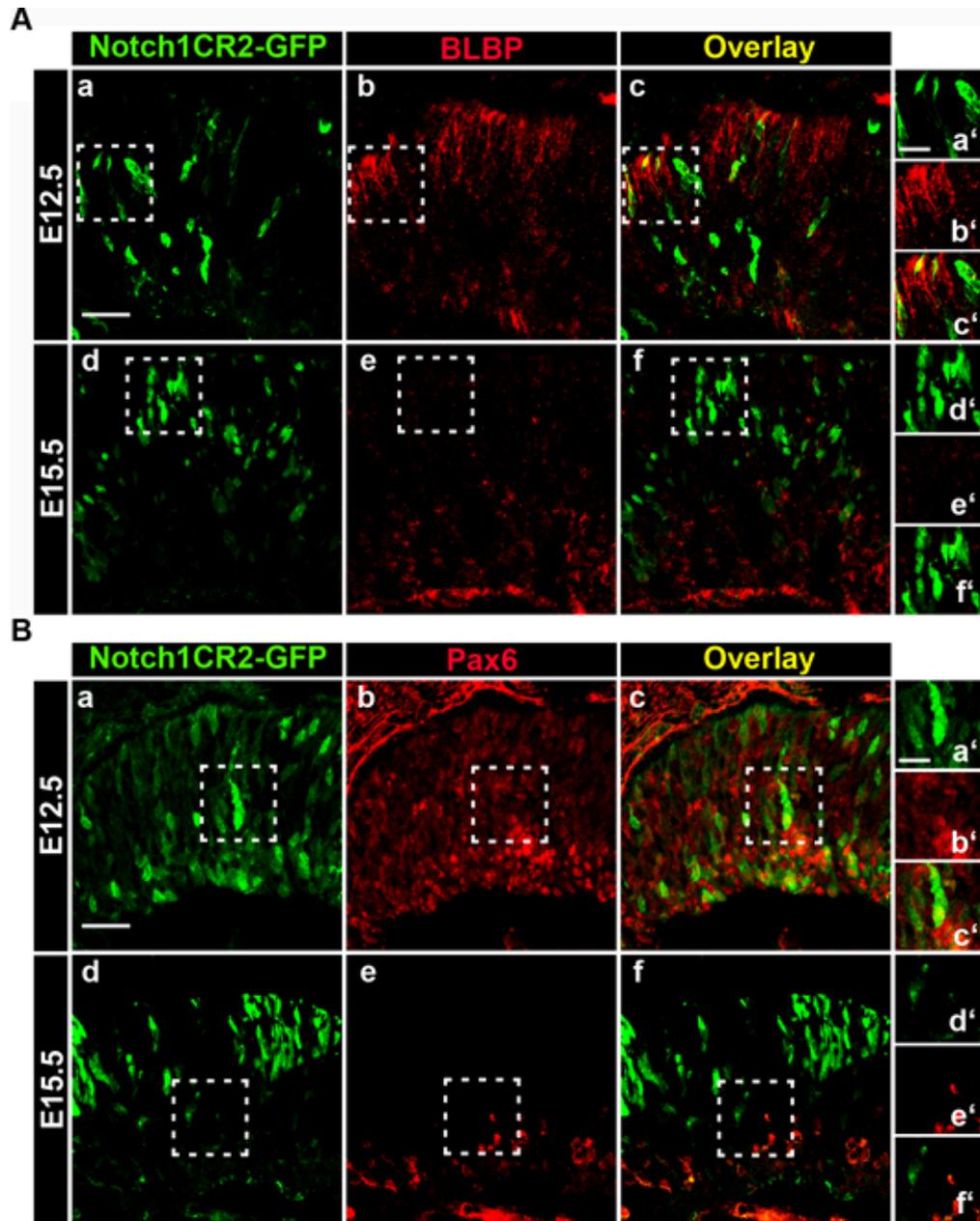
Figure 5.15. Notch1CR2-GFP$^+$ cells are a mixture of radial glia and neural progenitors.
(A) Radial glial marker BLBP co-localizes with Notch1CR2-GFP$^+$ cells at E12.5 but not at E15.5. **(B)** Neural progenitor marker, Pax6, co-localizes with Notch1CR2-GFP$^+$ cells at E12.5 but not E15.5. Transgenic mice were sacrificed at embryonic days 12.5 and 15.5. *Scale bar = 20 µm.*

A

Notch1CR2-GFP | Brn3 | Overlay
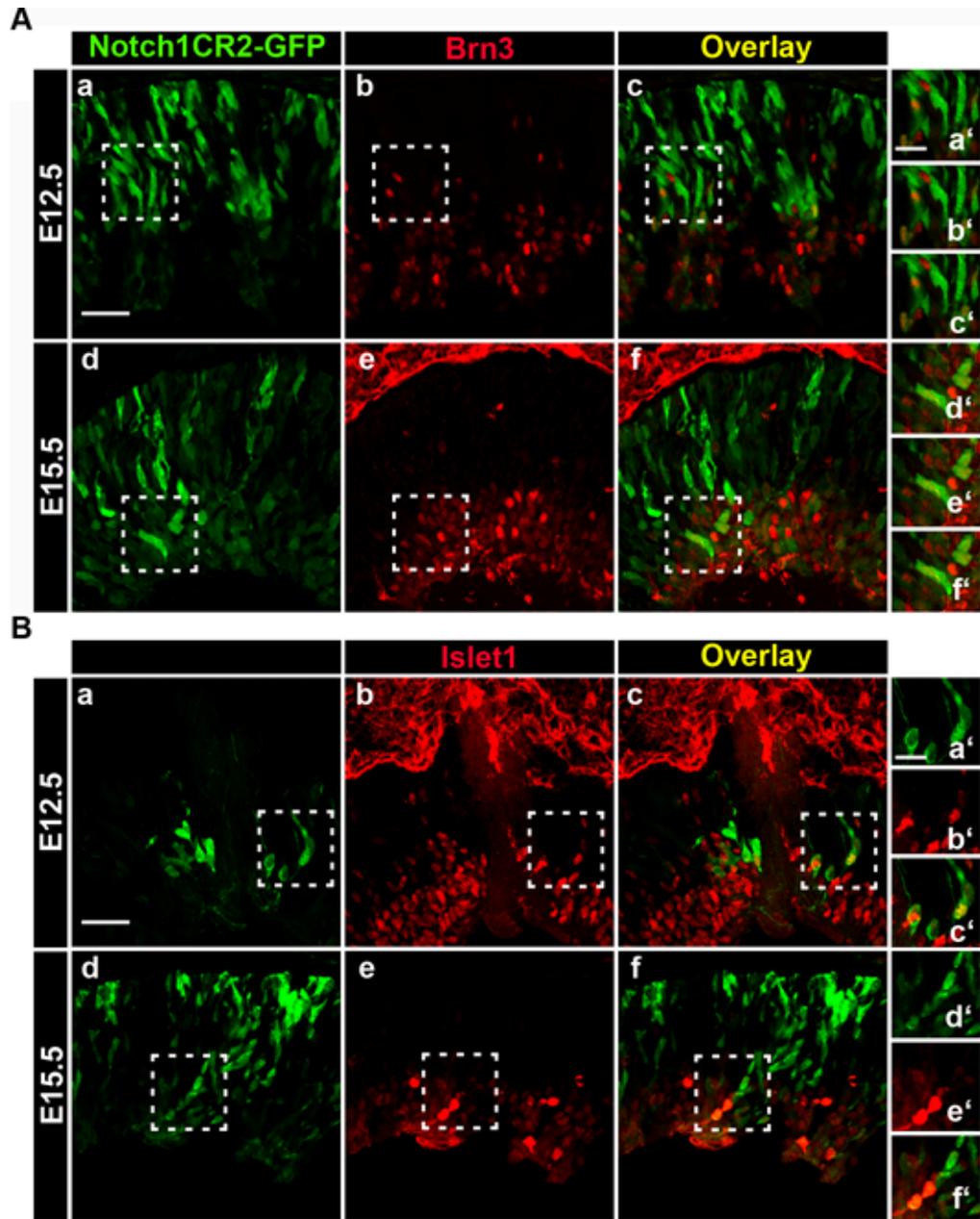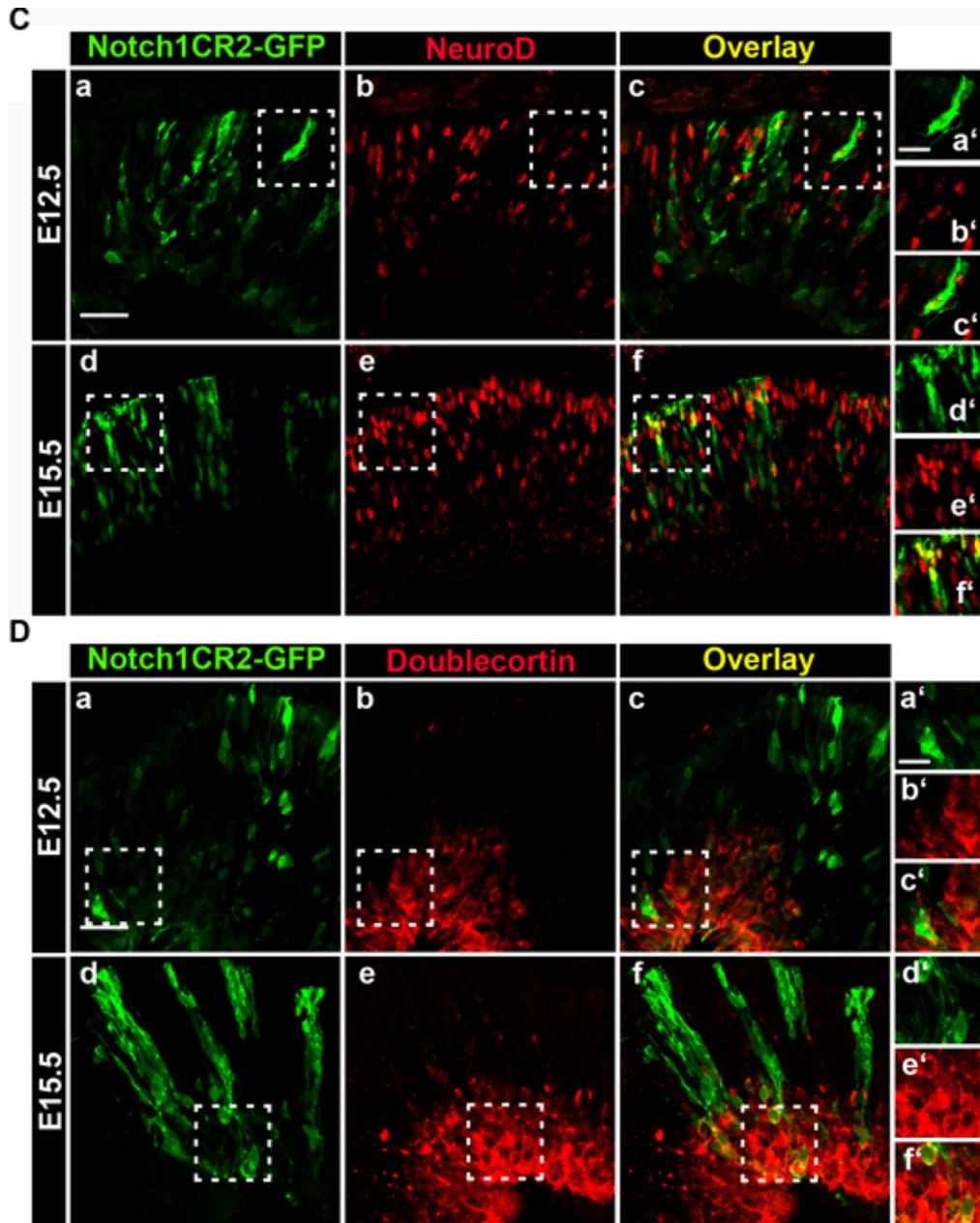
Figure 5.16. Notch1CR2-GFP$^+$ contain newborn neurons, ganglion cells, or amacrine and photoreceptors.
(A) Ganglion cells as marked by Brn3 co-localize with GFP at E12.5 and E15.5. **(B)** Similarly, a few GFP$^+$ cells are ganglion cells (Islet1$^+$) at both stages. **(C)** NeuroD, which marks amacrine cells and photoreceptors, is also prevalent in the Notch1CR2-GFP$^+$ population, especially at E15.5. **(D)** Few Notch1CR2-GFP$^+$ cells are newborn neurons as marked by doublecortin at both E12.5 and E15.5. *Scale bar = 20 μm.*

The spinal cord also supports a neurogenic profile of Notch1CR2 at embryonic stages. Coronal sections of the spinal cord were stained with anti-GFP and either stem/progenitors cell markers or neuronal markers. The results complement the phenotype of Notch1CR2 in the retina and the cortex with GFP recovery. Montages of the stained sections allowed for an overall comparison of patterns of Notch1CR2 expression and antibody staining. Feint GFP$^+$ cells occupy the VZ/SVZ in a radial fashion while bright GFP$^+$ cells seem to orbit the outer layers. Antibodies for progenitor/stem cells stain the VZ/SVZ around the central canal while antibodies for more differentiated cells stain the outer layers.

Radial cells in the spinal cord expressing feint GFP are stem/progenitor cells. Antibodies for radial glia (anti-Notch1 and anti-BLBP) and for mitotis (anti-Ki67 and anti-pH3) show the strongest staining around the central canal and therefore co-localize with the radial cells with feint GFP (Figure 5.17A-B). Staining with early stem cell markers (Nestin and Sox2) is more difficult to discern but shows strongest co-localization in the outermost ventral cord. The most striking observation is that the majority of spinal cord cells at E12.5 are involved in the process of asymmetric division (as marked by NuMa), suggesting that Notch1CR2 is active during neurogenesis. In addition, Notch1CR2-GFP co-localizes with several neuronal markers including Brn3a, Islet1, NeuroD, NeuN, and doublecortin (Figure 5.18). As determined by the GFP recovery experiment in the cortex (Section 5.6), it is expected that anti-GFP retrieves signal that is up to seven days old in the spinal cord as well. Therefore, the immuhistochemical profile of Notch1CR2 activity (both high/low or new/old) consists of asymmetrically dividing cells and a mixture of neuronal subtypes.

A

Images from Zeiss Fluorescent Microscope
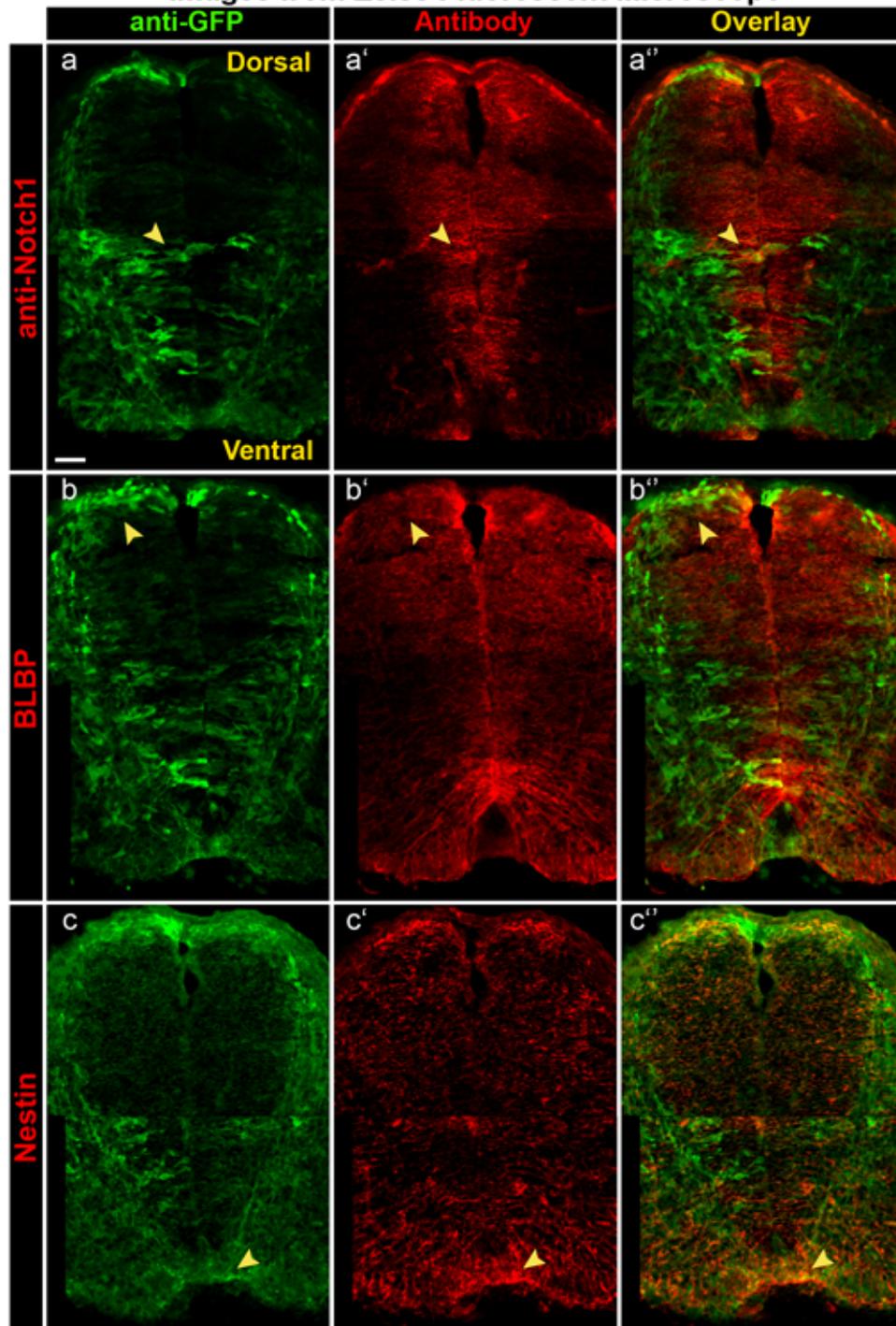
B

Images from Zeiss Fluorescent Microscope
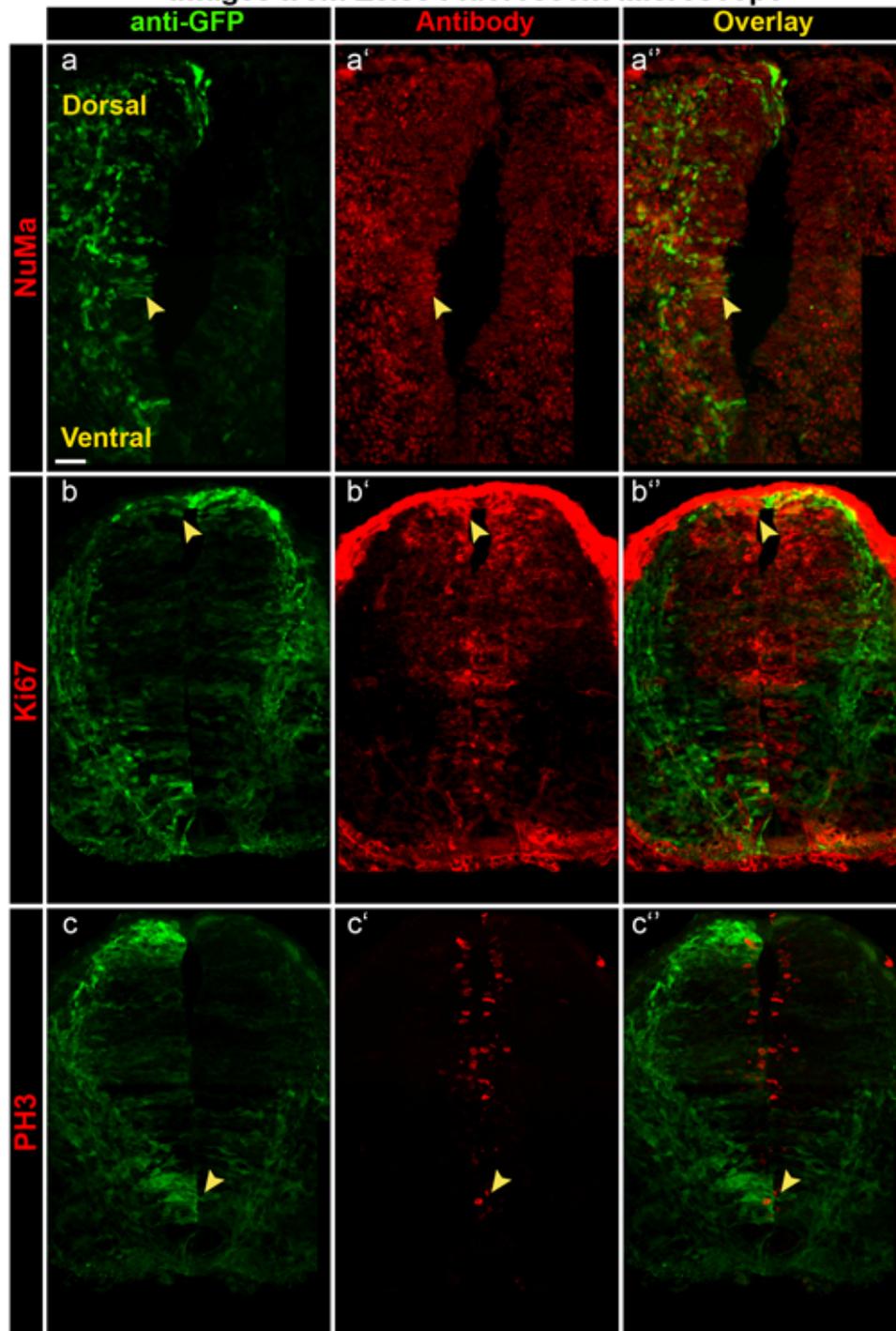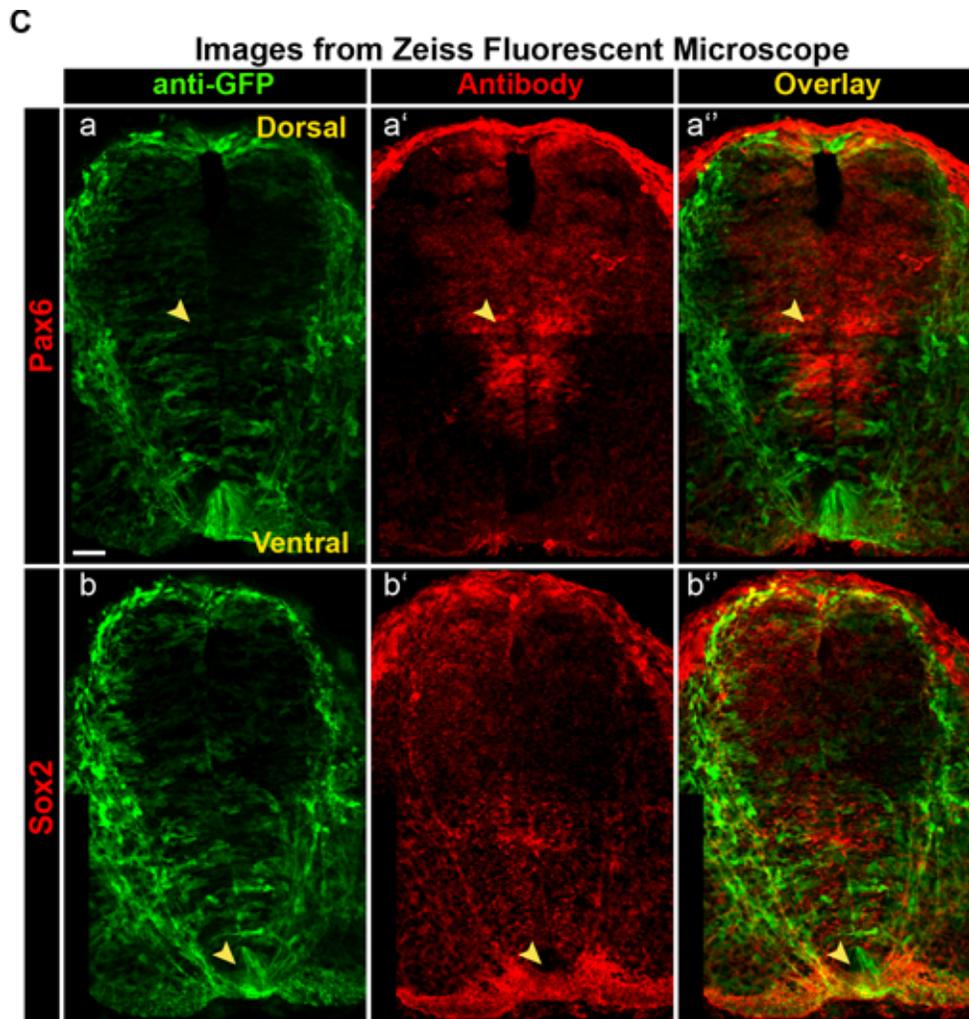
Figure 5.17. Majority of Notch1CR2-GFP^{+} cells in the E12.5 spinal cord are NuMa[+] asymmetrically dividing cells.

All spinal cord sections are stained with anti-GFP.

[A] Anti-Notch1, BLBP, and Nestin proteins are present in radial glia/neural stem cells. Staining with antibodies against these proteins occupy regions that are distinct from Notch1CR2-GFP. **(a)** Anti-Notch1 marks the VZ around the central canal while the strongest Notch1CR2-GFP expression is present in outer layers of the spinal cord. **(b)** BLBP is strongest at the ventral/dorsal nodes, where it co-localizes with strong Notch1CR2-GFP, and in the VZ of the central canal. However, the lateral-outer layers are not strongly co-localizing with BLBP. **(c)** Nestin has a dispersed staining pattern, which shows strongest co-localization at the dorsal/ventral nodes. However, similar to BLBP, co-localization in the lateral outer layers is not prominent.

[B] NuMa, Ki67, and PH3 are nuclear markers of mitosis. **(a)** NuMa stains the majority of the spinal cord at E12.5, and thus co-localizes with the majority of Notch1CR2-GFP^{+} cells. This protein is asymmetrically distributed into the progenitor after division. **(b)** Ki67 marks the VZ/SVZ. Few feint-GFP cells co-localize with Ki67. However, the majority of the brightest GFP expressers does not co-localize with Ki67 and is located in

the outer layers. **(c)** PH3 only marks a few cells of the VZ and does not co-localize with Notch1CR2-GFP.

[C] Pax6 and Sox2 are nuclear transcription factors of neural progenitors and stem cells, respectively. **(a)** Pax6 labels the VZ/SVZ around the canal while the majority of Notch1CR2-GFP expression surrounds Pax6. **(b)** Sox2 expression is strongest the dorsal/ventral nodes, which co-localizes with Notch1CR2.

Arrows denote a cell with co-localization. Coronal sections were obtained from the same E12.5 samples (with the exception of NuMa), and therefore, the region represented is within a 200 μm-thick region. All samples are stained with anti-GFP. Each picture is a montage of two separate images. *Scale bar = 20μm.*

A

Images from Zeiss Fluorescent Microscope

anti-GFP	Antibody	Overlay

Brn3

a   Dorsal   Ventral   a'   a''

Islet1

b   b'   b''

NeuroD

c   c'   c''
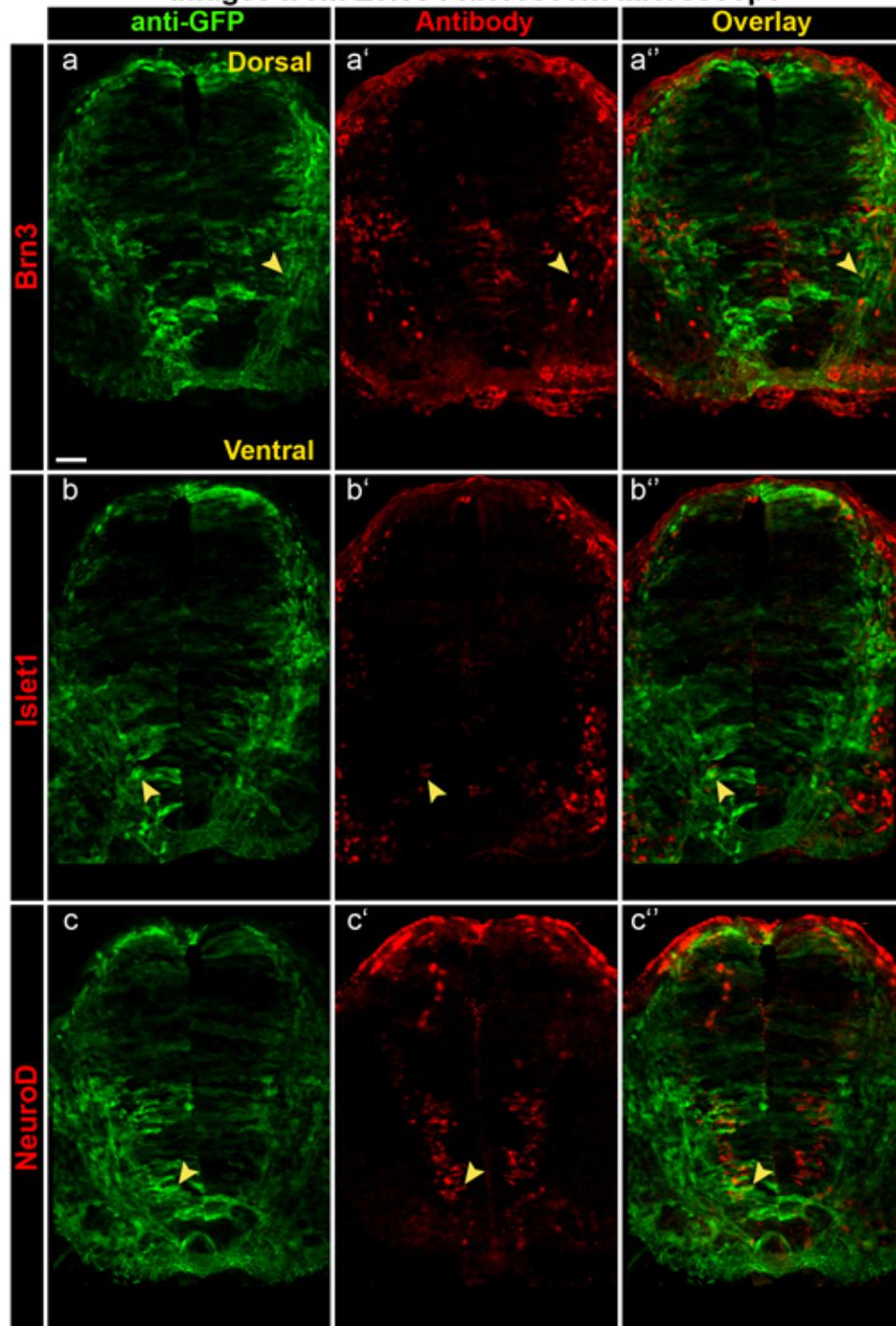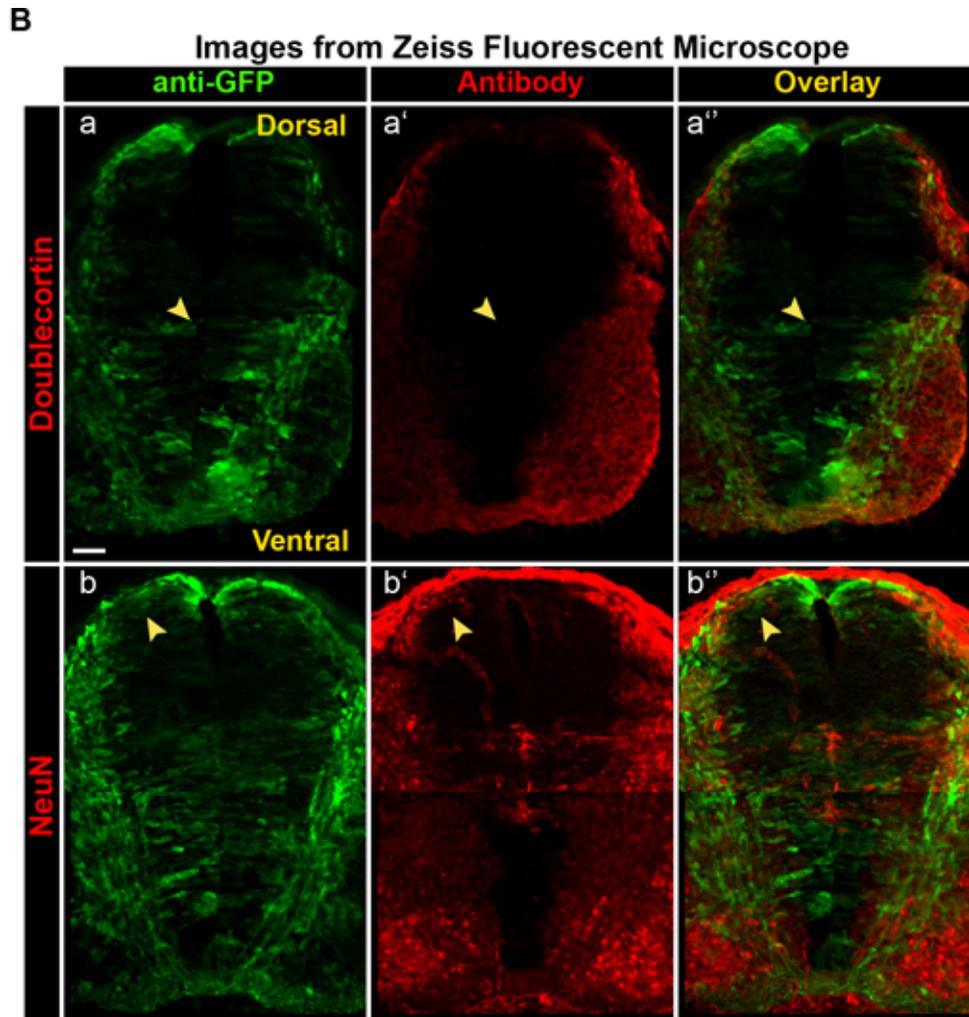
Figure 5.18. Notch1CR2-GFP$^+$ expression in the E12.5 spinal cord co-localizes with various types of neurons when stained with anti-GFP.

All spinal cord sections are stained with anti-GFP.

[A] Brn3, Islet1, and NeuroD are neuronal proteins expressed in the nucleus. These proteins are not present in VZ/SVZ but rather are found in distinct regions of the spinal cord. Antibodies against these proteins occupy regions that are distinct from Notch1CR2-GFP. **(a)** Brn3 is present in the mid-outer layers of the spinal cord and co-localizes with the horizontal and radial GFP$^+$ cells. **(b)** Islet 1, which primarily marks the outer layers of the spinal cord, does not co-localize with GFP. However, there are a few Islet1$^+$ cells located in the mid-regions in the ventral cord, which co-localize with GFP. **(c)** NeuroD, which is expressed in the inner layer of the spinal cord, co-localizes with radial GFP$^+$ cells.

[B] Doublecortin and NeuN are markers of early and mature neurons, respectively. **(a)** Doublecortin covers the mid-outer layers of the spinal cord. It co-localizes with the horizontal but not the radial GFP$^+$ cells. **(b)** NeuN, which is primarily present in the mid-ventral cord as well as the outer layers, co-localizes with GFP. E12.5 samples were sectioned coronally from the same sample (with the exception of NuMa), and therefore, the region represented is within a 200 μm-thick region.

5.8 Discussion

The motivation behind this chapter was to extend the analysis of Notch1CR2 into another species in order to (a) confirm the evolutionary conservation of Notch1CR2 and (b) establish a complete temporal and spatial map of Notch1CR2-GFP expression. The mouse model was selected because it was most suitable for both of these goals. Not only would it address the question of conservation, but it would also serve as a more relevant model to human than chick. Because mouse is extensively studied, available resources for mouse surpass what is available for chick, including antibodies, *in situ* hybridization databases (GENSAT) [99], and embryonic brain atlases (Allen Brain Atlas) [100]. Finally, the most attractive feature of the mouse model was the opportunity to develop a transgenic mouse of Notch1CR2-βGP-GFP at the Transgenic/Knock-Out Mouse Facility at the Cancer Institute of New Jersey.

The first finding from the transgenic mouse came from the comparison of Notch1CR2-GFP expression in chick to mouse. It was determined that Notch1CR2 is evolutionarily significant because its temporal and spatial expression patterns in chick are analogous to mouse. Notch1CR2 expression patterns in chick (E4-E8) and in mouse (E10.5 to P0) correspond to their respective periods of neurogenesis during CNS development. During normal chick development, neurogenesis occurs from E3 to E9 [45-47]. In mouse, the corresponding period of neurogenesis correlates to the peak of BLBP expression at E13 [37] . Radial glial proteins are expressed as early at E9.5 (i.e. nestin) [39, 40] or E13 (i.e., BLBP) [37, 41]. Notch1 continues to express in the postnatal brain in the SVZ, the rostral migratory stream, and the dentate gyrus [49, 101].

Because of the expression of Notch1CR2 in the CNS during neurogenic periods, it was hypothesized that Notch1CR2 is active in radial glia. The results from the transient transfections in chick and mouse embryos support the hypothesized neural stem/progenitor phenotype of Notch1CR2 because the Notch1CR2-GFP^{+} cells possess a phenotype of neural progenitors and not neurons. The results correspond to the known role of Notch1 in inhibiting neuronal differentiation [35, 36]. Notch1 maintains its stem cell state through lateral inhibition, a process by which the expression of Notch1 ligand in one cell prevents its own differentiation through interaction with an inhibitory ligand (i.e. Delta) of another cell [102].

In accordance with the *in ovo* and *in utero* transient experiments, GFP expression in the transgenic mouse is exclusively expressed in the CNS only during a period of neurogenesis (E10.5 to P0). Notch1CR2-GFP^{+} cells are not newborn neurons at E15.5 (negative for doublecortin) and are not neurons or glia at P0 (negative for NeuN, Tbr1, and GFAP). Instead, they undergo asymmetric division (marked by NuMa), which is consistent with another reported property of Notch1^{+} cells. During horizontal cleavage, Notch1 is asymmetrically inherited by the basal (top) cell [103, 104]. Recently, a radial glia-like progenitor cell has been reported to arise from asymmetric divisions of radial glia, to reside in the outer SVZ, and to generate neurons. These cells sound like they have the potential to be Notch1CR2[+]. However, it is not certain whether these cells can undergo asymmetric division themselves [105].

Despite the evidence supporting the radial glial phenotype of Notch1CR2, other observations from the transgenic Notch1CR2-βGP-GFP mice challenged it. There were three striking phenomena in the cortex, retina, and spinal cord that were inconsistent with

the radial glial phenotype. (1) Expression of Notch1CR2-GFP was limited to the ventral CNS as seen in the whole mounts. Long, radial GFP^{+} cells illuminate the VZ/SVZ of only the ganglionic eminences at E15.5 (Figure 5.4A). Based on the initial hypothesis, it was expected that Notch1CR2-GFP^{+} cells span the VZ of the entire neocortex. (2) GFP is not limited to the VZ/SVZ at P0 (Figure 5.7-Figure 5.9). (3) Only some of Notch1CR2-GFP^{+} cells co-localize with radial glial markers. If most Notch1CR2-GFP^{+} cells are not radial glia, neurons, or glia, what are they?

Since Notch1CR2-GFP is strongly expressed in proliferative zones (Figure 5.7), GFP^{+} cells were thought to be mitotic. Perhaps they are not radial glia but rather a more committed precursor? A panel of mitotic markers was tested including pH3 and Ki67. PH3 is associated with chromatin condensation, and it marks late G2 when Histone 3 becomes phosphorylated until the beginning of anaphase when it is dephosphorylated [26]. PH3 staining is in the VZ but it is scarce and does not co-stain with Notch1CR2. Ki67 is expressed in proliferating cells during all phases of the cell cycle [24, 25]. Ki67 was shown to co-localize with Notch1CR2 *in utero* (Figure 5.2). However, it was the antibody NuMa that first showed that Notch1CR2 is active in dividing cells. NuMa is different because it is active in asymmetrically dividing cells [27, 28]. After division, NuMa protein gets asymmetrically allocated to the cell that maintains the progenitor phenotype. The other cell begins its journey towards a committed fate. Since Notch1CR2-GFP co-localizes with NuMa, Notch1CR2 may be involved in regulating asymmetric division. Interestingly, it has been published that Notch1 protein is asymmetrically allocated to the basal side of the dividing cell. This published finding corresponds well with the observation that Notch1CR2 is active in asymmetrically

dividing cells. This data led to the following question: if Notch1CR2 is present in asymmetrically dividing progenitors, what is the fate of the other daughter cell?

Additional information about the fated path of Notch1CR2-GFP cells came from observations of the upper layers of the neocortex, the caudate putamen, and the olfactory bulb. Results show that these cells are fated to become interneurons based on the following observations: (1) GFP co-stains with GAD65/67, a marker for GABAergic interneurons/interneuron precursors [87, 96] and (2) some processes of GFP$^+$ cells co-stain with VGAT, a marker for GABAergic interneurons. It has been reported that some GAD65 interneurons continue to divide even at postnatal time points [96], and therefore marks both interneuron progenitors and interneurons. Further experiments with GFP recovery provided more evidence that Notch1CR2 regulates the genesis of interneurons. <u>Results from the GFP recovery experiment support a revised hypothesis: Notch1CR2 is active in interneuron precursors.</u>

The underlying idea of GFP retrieval is that anti-GFP can track the cell fate of cells with abated Notch1CR2-GFP expression for up to seven days (Section 5.6). Unexpectedly, anti-GFP reveals GFP$^+$ cells in the most basal layer of the neocortex at E12.5 and E15.5. After Notch1CR2 activity subsides, cells may differentiate into interneurons that tangentially migrate into the neocortex [106]. Although there is no Notch1CR2-GFP at P7, anti-GFP reveals GFP$^+$ cells in the eppendyma, hippocampus, and the cortical plate. Interestingly, the hippocampus contains GABAergic inhibitory cells. This data begs the following question: are Notch1CR2$^+$ cells fated to become GABAergic interneurons after Notch1CR2 activity is ablated? <u>Based on this evidence, it</u>

was hypothesized that Notch1CR2-GFP cells are mitotic precursors of interneurons. This hypothesis will be referred to as the interneuron progenitor hypothesis.

The interneuron progenitor (IP) hypothesis was supported by further immunohistochemistry with interneuronal markers. Results show that Notch1CR2-GFP$^+$ cells are asymmetrically dividing and are GABAergic interneurons, as marked by GAD65/67. It is not surprising that GABAergic neurons are regulated by a conserved regulatory element because GABA signaling is conserved in different species during neurogenesis [107]. The IP hypothesis may also explain the cortical GFP expression at P0. Radial, feint GFP$^+$ cells are present in the neocortex at P0 in a dispersed fashion. Cortical interneurons migrate to the cortex from the ventral ganglionic eminences [82-88]. Similarly, cells migrating tangentially through the IVZ/VZ will turn and migrate radially towards the basal surface [86, 108, 109]. Therefore, the cortical expression patterns support this hypothesis.

The following list is a summary of the evidence presented above that supports the IP hypothesis:

(1) Notch1CR2-GFP is expressed exclusively in the CNS during peak neurogenesis. During this time, interneuron precursors give rise to interneurons.

(2) Radial Notch1CR2-GFP$^+$ cells illuminate the embryonic ganglionic eminences, which are regions of interneuron generation.

(3) In newborn pups, Notch1CR2-GFP$^+$ cells undergo asymmetric division in the ventricular zone as well as in the upper layers of the neocortex, the caudate putamen, and the olfactory bulb.

(4) Anti-GFP unveils GFP expression in newborn neurons of the basal neorcortex. Based on this data, it can be speculated that cells with diminished Notch1CR2-GFP expression tangentially migrate from the GE to the neocortex.

(5) Notch1CR2-GFP expresses in the hippocampus and the cortex which are final destinations of interneurons.

(6) Notch1CR2-GFP$^+$ cells co-localize with GAD65/67, which has been shown to be present in dividing GABAergic interneuron precursors.

-PAGE LEFT BLANK INTENTIONALLY-

6   Interneuron Transcription Factors Bind to Notch1CR2

In Chapter 5, Notch1CR2 activity was characterized in interneuron progenitors. In this chapter, a mechanism is proposed for regulation by Notch1CR2. It is hypothesized that one transcription factor or a combination of factors bind to Notch1CR2 and thereby drive the expression of GFP. However, it is inefficient and unresourceful to test these factors one-by-one because Notch1CR2 contains 164 transcription factor binding sites (TFBS) (121 unique sites), as determined by MatInspector (Figure 9.2). A combination of computational analysis and binding assays were used to narrow down the list of potential binding transcription factors. TFBSs with 100% conservation between mouse and chick were selected for further experimental testing. Only five TFs are 100% conserved: Brn3, Barx2, Gsh1, Crx, and Fhxb (Section 6.1) three of which share a common core binding sequence (Brn3, Barx2, and Gsh1). To identify regions of highest *in vitro* binding potential, electrophoretic mobility shift assays (EMSAs) were performed (Section 6.2). In a series of mutagenesis experiments, the TFBS for Brn3/Barx2/Gsh1 was deleted from Notch1CR2-βGP-GFP. Transfection of this mutated construct ablates GFP expression *in ovo* suggesting the importance of Brn3/Barx2/Gsh1 in the activity of Notch1CR2 (Section 6.3). Chromatin immunoprecipitation (ChIP), an in vivo binding assay, supported these results (Section 6.5). Furthermore, a subregion of Notch1CR2, consisting of the Gsh1 binding site, can independently drive GFP expression *in ovo* (Section 6.4).

In order to take a closer look at the potential transcription factors in the stem cell genetic network, the TFBSs of other stem cell genes and known stem cell enhancers were examined. Publically available resources and databases were utilized including (1)

current literature (Appendix: Table 6.1), (2) databases of known neural stem cell enhancers (Section 6.6), and (3) novel predictions of evolutionarily conserved regions of another stem cell gene (Section 6.6). The available literature on the TFBSs of Notch1CR2 was studied in order to determine which transcription factors had known neural function and/or any known interactions with Notch1. This analysis provides information on the common *potential* transcription factors in the stem cell *trans-*regulatory network and will guide future selection of TFBS for experimental testing.

6.1   Conserved TFBSs across *mus musculus* and *gallus gallus*

The list of potential binding transcription factors was narrowed upon examination of the conservation of the TFBSs across mouse and chick. As shown in Figure 4.2 and Figure 5.13, Notch1CR2 is active in both murine and avian species, thus validating its conservation across these species. Thus, it was hypothesized that the TFBS with the highest potential of binding to Notch1CR2 would have 100% conserved core binding sequences between *m. musculus* and *g. gallus*. The 399-base pair sequence Notch1CR2 of *m. musculus* (see Appendix Figure 9.2) was blasted against Notch1 in *g. gallus* (Accession Number: NC 006104.2) using a discontinuous megablast. Out of the 399 base pairs of Notch1CR2, a 155-base pair region of Notch1CR2 (position 48 to 198 on the mouse sequence) had an 83% overlap with *g. gallus* Notch1 (128/155 identical base pair matches) and 3% gaps (4/155 missing base pairs) (See Appendix: Table 9.3 for detailed list of conserved TFBS in *g. gallus*).
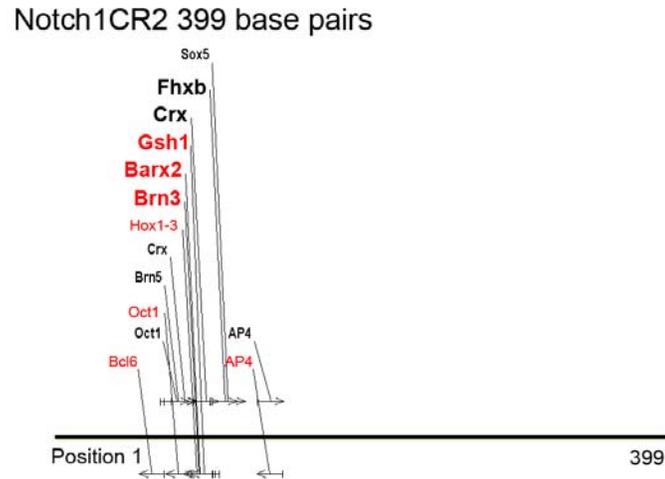
Figure 6.1. Conserved TFBS of Notch1CR2 across *mus musculus* and *gallus gallus*. There are 13 transcription factors conserved across murine and avian species. Brn3, Barx2, Gsh1, Crx, and Fhxb are 100% conserved. *(black = forward DNA strand, red = reverse DNA strand)*

6.2 Highest Potential TFBS of Notch1CR2 as determined by EMSA

Predictions of potential transcription factors based on conservation across chick and mouse are highly selective, and therefore, risk premature elimination. Therefore, in conjunction with computational analysis, regions were also narrowed using EMSA, which is an *in vitro* protein-to-DNA binding assay. The binding assay was performed using a DNA probe and nuclear protein extract from E8 chick brains (from the telencephalon reaching to the cervical spinal cord). DNA probes were designed based on dense regions of neural-related TF binding sites. Probes 1-5 were designed between base pairs 1-100, which had the highest concentration of TFBSs (See Appendix: Table 9.1). Probe 5 contained the TFBS for Gsh1, Brn3, Barx2, and Crx, which are four of the 100% conserved TFBS as determined in Section 6.1.

As shown in Figure 6.2, probes 2 and 3 show the strongest binding. The binding is specific as shown by the successful competition of the band upon addition of the non-

labeled competition probe. Probe 5 also shows specific yet weaker binding. The binding shown with Probe 1 is not specific because there is also binding with its competition control. Binding was not present with Probe 4.

In a second binding assay, Probes 2, 3 and 5 were run as forward or reverse single strands to determine more information about specific binding patterns (Figure 6.2a). The reverse strand of Probe 2 shows specific binding, while the forward strand shows no binding. Therefore, the TFs on the forward strand were de-prioritized as potential *in vivo* binding elements of Notch1CR2. Both the forward and reverse strands of Probes 3 and 5 show binding. The potential transcription factors present on Probes 2 (reverse), 3, and 5 were cross-referenced with the literature (Appendix: Table 9.2).

The reverse strand of Probe 5 shows the strongest, specific, and consistent binding. One of the TFBS on Probe 5, Gsh1, is particularly interesting because it is expressed in interneuron progenitors and is involved in the decision-making process of excitatory and inhibitory neurons [110, 111]. Dlx1/2 is another interesting factor because it is present in interneuron precursors in the VZ/SVZ of the ganglionic eminences [68]. Its pattern is similar to Notch1CR2 at E15.5. Therefore, these two TFBS were chosen to be tested for *in vivo* binding to Notch1CR2 via mutagenesis.
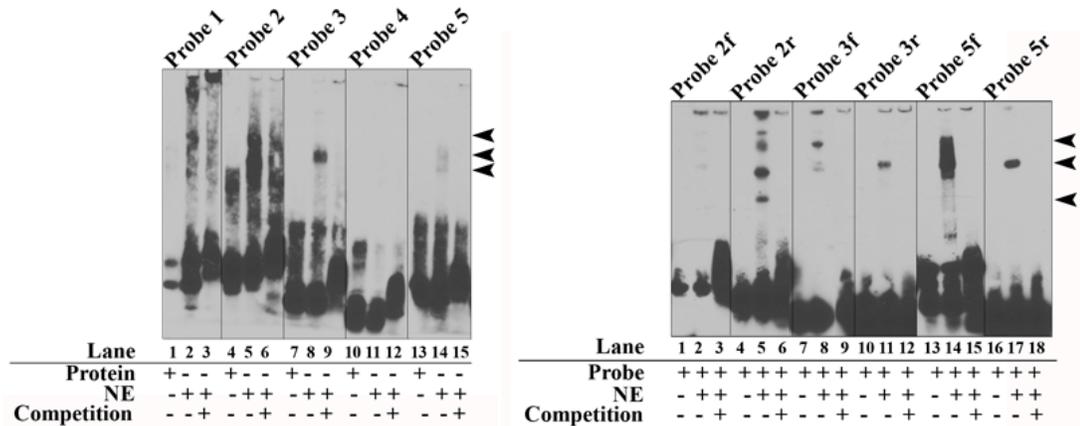
Figure 6.2. EMSA shows binding in particular regions of Notch1CR2.
Probes 1-5 were designed based on the 399-base pair region of Notch1CR2. The binding assay was performed with E8 chick brain nuclear extract. (A) Probes 2, 3, and 5 show bands, which are competed away in the competition controls. Probe 5 shows weakest binding, which is specific as shown in the competition control. Probes 1 and 4 do not show any binding. (B) The forward and reverse strands of Probes 2, 3, and 5 were run separately. The reverse strand of Probe 2 shows specific binding. Their competition controls compete away the signal indicating specific binding. However, the forward-alone strand does not show binding. Probes 3 and 5 show binding with the forward-alone and reverse-alone strands of these probes, respectively.

Based on results from EMSA, certain predictions could be made to prioritize the potential of binding of certain transcription factors. First, any transcription factors on Probes 1 and 4 were de-prioritized because they do not show binding. The TFBSs on the forward strand of 2 also held less priority than the TFBSs on the reverse strand of Probe 2. Probe 3 is a subset of Probe 2. Therefore, the remaining transcription factors with the highest binding potential to Notch1CR2 are based on the TFBSs on the reverse strand of Probe 2 and both strands of Probe 5 (Table 6.1).

Table 6.1. Transcription factors with the highest binding potential (based on EMSA results)

Probe	Position on Notch1CR2	Sequence (forward)	TFBS (based on core binding region)		
Probe 2	60-92	Ctagtgctg ggaagccac gcataattaat cacacagca ggccgg	Staf Stat5 Stat5 Bcl6 Stat Ahrarnt Pax5 S8 Dlx1 Ipf1 Lhx6 Pou3f3 Hoxc8	Brn5 Lhx3 Hmga Brn3 Vax2 Msx nkx12 Oct1 Bright Brn3 Vax2 Barx2 Nkx6-3	Pax6 Oct1 Hoxc8 Nkx2-5 S8 Nkx6-1 Pax4 Dlx2 Ipf1 Lmx1b Atbf1
Probe 5	80-100	ctagtaatca cacagcatta atcgccggc cgg	Hox1-3 Brn3 Barx2	Hoxb8 Gsh1 Hmx1 Hoxc9	Phox2 Nkx61 Crx

* Black = transcription factor is located on forward strand
  Red = transcription factor is located on forward strand
  Grey = transcription factors identified through mutagenesis

It is important to note that the use of single-stranded probes (either forward or reverse) may eliminate important information because some true binding sites need both strands and multiple transcription factor binding sites. *Trans*-acting factors are often inverted repeats or occur multiple times in the same location. However, the binding site with the highest binding potential (refer to Section 6.3) is not an inverted repeat, and therefore, a double-stranded probe was not necessary to obtain information from the EMSA analysis.

6.3 Mutation of the binding site for Brn3/Barx2/Gsh1 ablates GFP expression

Position 91-94 on Notch1CR2 codes for the core binding sequences of 3 transcription factors (Brn3, Gsh1, and Barx2), which are 100% conserved in the mouse and chick. These factors are particularly interesting because Brn3 and Gsh1 are

expressed in neural progenitors, and therefore, have high potential for binding to Notch1CR2, which has been shown to be active in interneuron precursors (Chapter 5). The mutation (through deletion) of various core binding sequences (as described in Figure 6.3A) would result in a loss of Notch1CR2-GFP expression. The mutated construct was co-transfected *in ovo* with CAG-DsRed, which controlled for transfection efficiency.

The results show that GFP expression is ablated after mutating the core binding sequence for Brn3/Barx2/Gsh1 (deletion at position 91-94) while CAG-DsRed continues to express (Figure 6.3B, also summarized in Table 6.2). Two samples out of the two surviving embryos showed this pattern.

Interestingly, a mutation at the Crx core binding motif (deletion at position 95-96) does not ablate but rather diminishes GFP expression. The TFBS for Crx is also 100% conserved between mouse and chick. This mutation neighbors the TFBS for Brn3/Gsh1/Barx2 described above. It is possible that the reduction of GFP from the deletion of 95-96 is due to the perturbation of peripheral binding sequences of Brn3/Gsh1/Barx2. One out of one surviving embryo showed this pattern.

Although Dlx2 is not 100% conserved, it is another transcription factor of interest because it expresses in the ganglionic eminences and regulates neurogenesis of interneurons. This pattern corresponds to the dominant expression of Notch1CR2 in the radial glia of the ganglionic eminences (refer to Chapter 5). The TFBS of Dlx2 also shares the same core binding sequence as 26 other transcription factors. This TFBS might be important if it has been reported for so many known binding sites. However, deletion of the core binding sequence for Dlx2 and the other 26 factors (position 76-79)

A|

Notch1CR2 399 base pairs
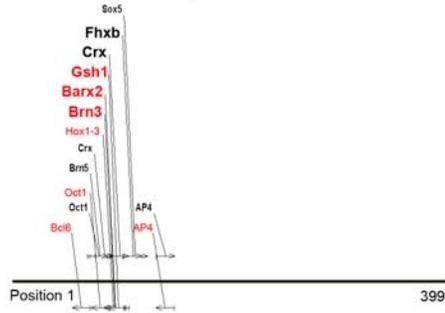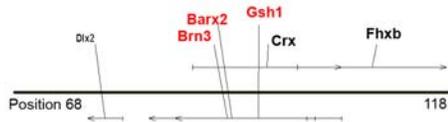
Sox5
Fhxb
Crx
Gsh1
Barx2
Brn3
Hox1-3
Crx
Brn5
Oct1
Oct1
AP4
Bcl6
AP4

Position 1   399

no mutation

Dlx2   Barx2   Gsh1
              Brn3   Crx   Fhxb

Position 68   118   ccacgcatAATTaatcacacagcATTAatcgcctcccaacaatagctgctg

m91-94

Dlx2   Ba X2   G X1
              B X3   C X   Fhxb

Position 68   118   ccacgcatAATTaatcacacagc----atcgcctcccaacaatagctgctg

m95-96

Dlx2   Barx2   Gsh1
              Brn3   C X   Fhxb
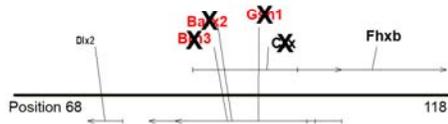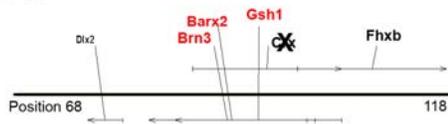
Position 68   118   ccacgcatAATTaatcacacagcAT--atcgcctcccaacaatagctgctg

m76-79

        X   Barx2   Gsh1
              Brn3   Crx   Fhxb
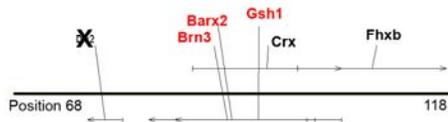
Position 68   118   ccacgcat----aatcacacagcATTAatcgcctcccaacaatagctgctg

m235-239

                        X
Position 215   265   ccccccccaaaaaaagcaaa----aaaaaaaagtagtgtgcattcattagt

B

Activity of Mutated Notch1CR2-bGP-GFP Variants
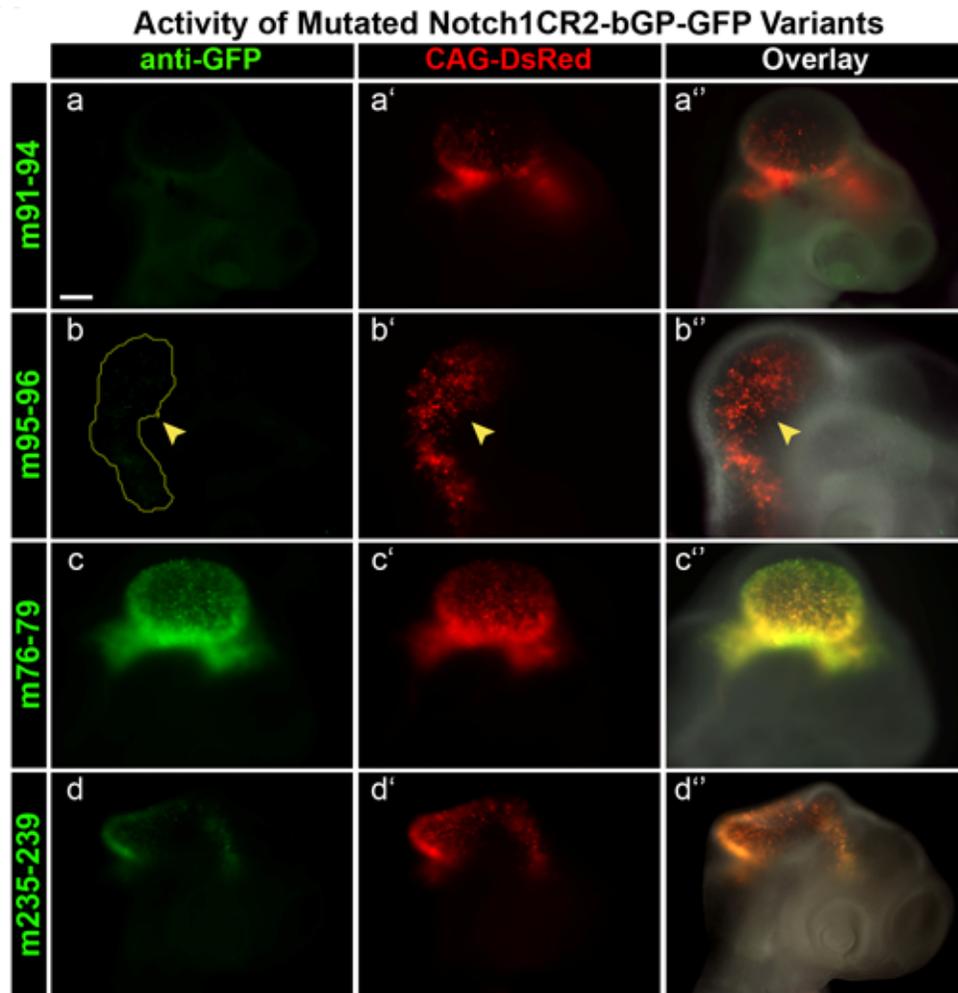
Figure 6.3. Mutations in Gsh1/Brn3/Barx2 (m91-94) in Notch1CR2 ablate GFP expression

[A] Mutations of Notch1CR2 were generated at various binding sites.
The graphical representation displays only the affected core binding sites that are 100% conserved between chick and mouse. Mutation at position 91-94 (m91-94) removes the core binding site for Brn3/Barx2/Gsh1/Crx, and m95-96 removes Crx. As negative controls, m76-79 removes the Dlx2 factor for interneuron progenitor, and m235-239 removes no binding sites. *(black = forward DNA strand, red = complimentary DNA strand).*

[B] Mutations in Gsh1/Brn3/Barx2 (m91-94) in Notch1CR2 ablate GFP expression.
(a) GFP expression was ablated with when position 91-94 was deleted from Notch1CR2-βGP-GFP. **(b)** GFP expression was diminished when position 95-96 was deleted. **(c&d)** GFP expression was not affected after deleting position 76-79 or 235-239.

Table 6.2. Primers for mutated transcription factor binding sites of Notch1CR2

Deletion Region of Notch1CR2 (Position 1 to 399 bp)	Mutated TFBS			Mutated Primer	Abolished GFP?
76-79	S8	Vax2	Nkx6-1	ctgggaagccacgcataatcaca cagcattaatcg	No
	Dlx1	Msx1	Pax4		
	Ipf1	Nkx12	Dlx2		
	Lhx6	Oct1	HoxB8		
	Hoxc8	Bright1	Lmx1b		
	Brn5	Barx2	Pit1		
	Lhx3	Nkx6-3	HoxC9		
	Hmga	Pax6	Atbf1		
	Brn3	Nkx2-5	Crx		
91-94	Brn3*			cgcataattaatcacacagcatcg cctcccaacaatagctgctg	YES
	Barx2 *				
	Gsh1 *				
95-96	Crx *			cataattaatcacacagcattacg cctcccaacaatagctgctg	Diminished
235-239	None			cccaaaaaaagcaaaaaaaaa agtagtgtg	No

* 100 % conserved between mouse and chick

does not abolish GFP expression. Therefore, Notch1CR2 activity is not dependent on Dlx2. Two samples out of two surviving embryos exhibited this pattern.

Although Dlx2 is not 100% conserved, it is another transcription factor of interest because it expresses in the ganglionic eminences and regulates neurogenesis of interneurons. This pattern corresponds to the dominant expression of Notch1CR2 in the radial glia of the ganglionic eminences (refer to Chapter 5). The TFBS of Dlx2 also shares the same core binding sequence as 26 other transcription factors. This TFBS might be important if it has been reported for so many known binding sites. However, deletion of the core binding sequence for Dlx2 and the other 26 factors (position 76-79) does not abolish GFP expression. Therefore, Notch1CR2 activity is not dependent on Dlx2. Two samples out of two surviving embryos exhibited this pattern.

As another negative control, four base pairs at position 235-239, containing no transcription factors, was deleted. As expected, GFP expression was not ablated. No new TFBS appear after any of the above mentioned deletions.

6.4 The GSH1 binding site can direct GFP expression independent of the Brn3a and Barx2 binding site

Sub-regions of Notch1CR2 with the Gsh1 TFBS were cloned into the βGP-GFP backbone to test whether the Gsh1 binding site can drive Notch1CR2-GFP expression independent of Brn3/Barx2. The independence of Brn3 and Barx2 could not be tested in this manner because they share the same core binding motif. The first sub-region, Notch1CR2.1, is a 50 bp sequence of Notch1CR2 from position 68-118 and contains the conserved binding motifs of Brn3, Barx2, Gsh1, Crx, and Fhxb as well as the non-conserved binding motif Dlx2. The second sub-region, Notch1CR2.2, is an 18 bp sequence from position 86-104 and contains the conserved binding motif of Gsh1 and Crx. Since Crx is primarily expressed in the retina and not the brain, Gsh1 is considered as the sole binding site in Notch1CR2.2. Results show that both Notch1CR2.1 and Notch1CR2.2 can independently drive GFP expression. The conserved Gsh1/Crx binding site can independently drive GFP expression.

6.5 Binding of Brn3 to Notch1CR2 by ChIP analysis

Chromatin immunoprecipitation (ChIP), an *in vivo* binding assay, tested whether Brn3a protein can bind to Notch1CR2 chromatin. Chromatin was attained from chick brain at E8. The binding of Brn3a is greater than the negative control and slightly weaker

A

B

C
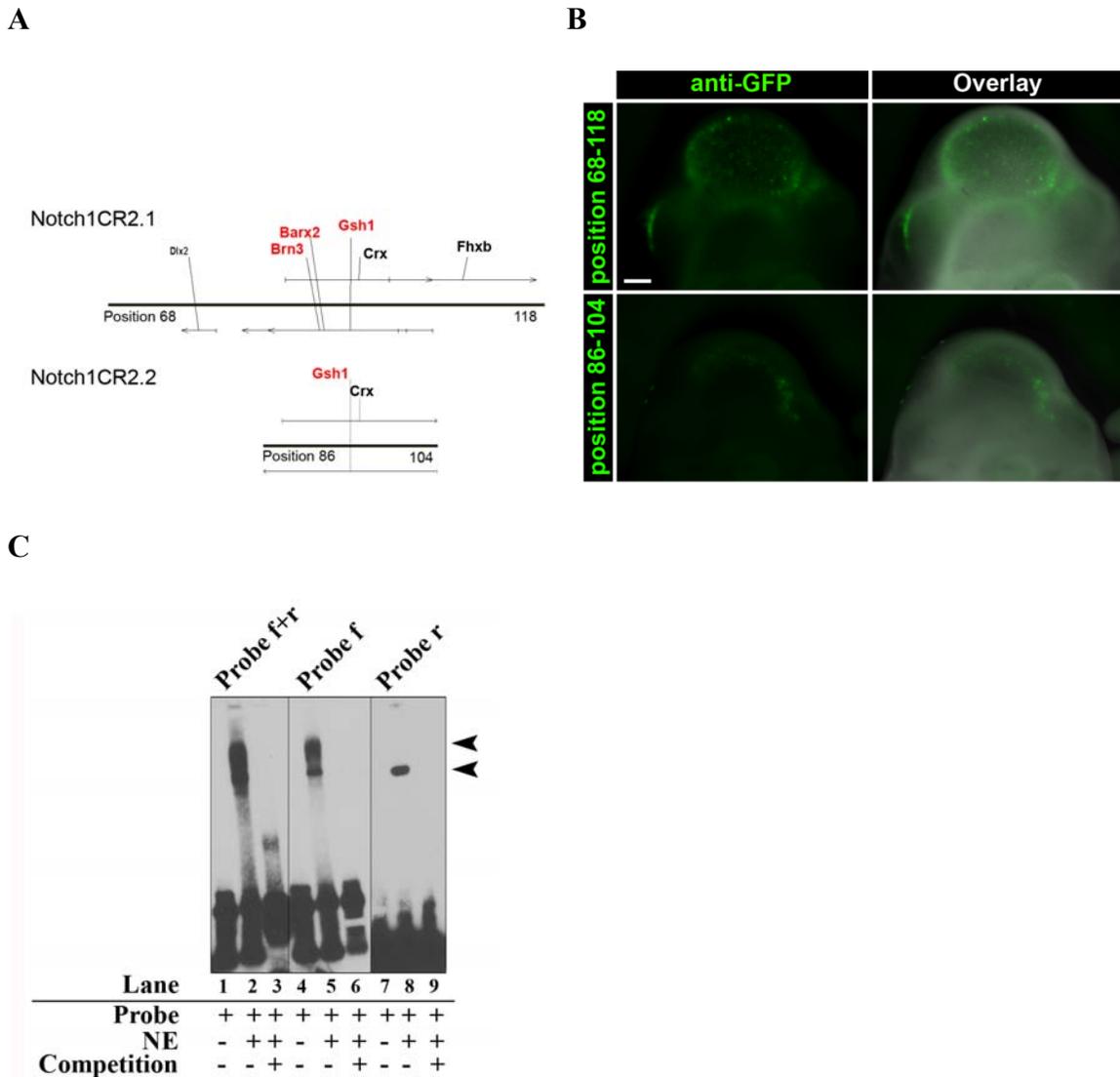
Figure 6.4. The Gsh1/Brn3/Barx2 TFBS of Notch1CR2 is important for driving GFP expression

[A] Notch1CR2.1 and Notch1CR2.2 represent subregions of Notch1CR2 focusing on the conserved binding motifs. Notch1CR2.1 is a 50 bp sequence representing position 68-188 of Notch1CR2 and consists of the conserved binding motifs of Brn3, Barx2, Gsh1, Crx, and Fhxb as well as non-conserved binding motif Dlx2. Notch1CR2.2 is an 18 bp sequence at position 86-104, which consists of the Gsh1 and Crx binding motif.

[B] Notch1CR2.1 and Notch1CR2.2 independently drive GFP expression. The Gsh1 binding motif is present in both subclones.

[C] Notch1CR2 region with the Gsh1 binding motif shows binding with EMSA. The probe represents position 80-100 on Notch1CR2. The binding assay was performed with E8 chick brain nuclear extract. The probe was run as a double strand (lanes 1-3), as a forward strand alone (lanes 4-6), and as reverse strand along (lanes 7-9). All three probes show specific binding that is competed away by the non-labeled competition controls.

than the input. Brn3a is a potential binding candidate since it is expressed in sensory

neural precursors. It also co-localizes with Notch1CR2 in the retina (Figure 5.16A). It is

important to note that this data has not been reproduced. A ChIP assay using mouse

chromatin would be better for confirming these results.
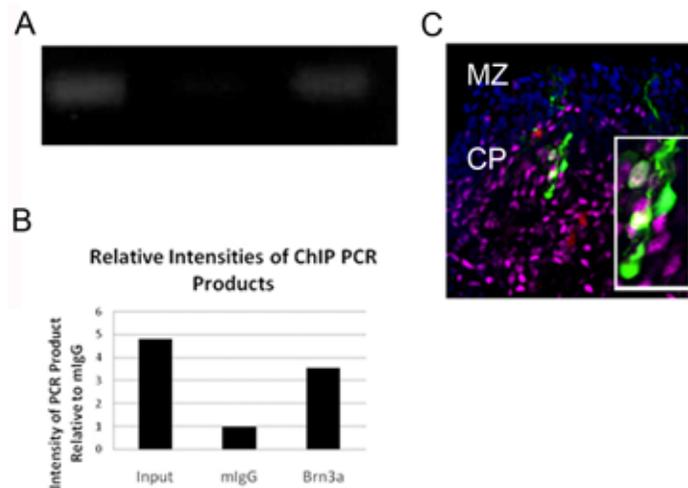
Figure 6.5. Brn3a binds to Notch1CR2 region of chick chromatin
(A) Chromatin immunoprecipitation shows that Brn3a binds to the Notch1CR2 of chick
chromatin. **(B)** Quantification of intensities show that Brn3a binding is stronger than the
negative control (mIgG) and weaker than Input. **(C)** Using the same antibody, Brn3a also
co-localizes with Notch1CR2 in E8 chick brain.

Results from the mutagenesis experiments (Figure 6.3) and from the Notch1CR2.1-

2.2 subclones (Figure 6.4) provide stronger evidence for Gsh1 as a *trans*-acting factor for

Notch1CR2. Another ChIP analysis with Gsh1 protein would confirm these results.

However, since the Gsh1 antibody for ChIP is not available at the moment, the

experiment will need to be pursued in the future.

6.6 Computational exploration of TFBSs: Gsh1, Brn3, and Barx2 are common TFBS sites that exist between Notch1CR2 and other known/predicted neural enhancers

Common TFBSs amongst similar neural stem cell genes may provide insight into the active *trans*-acting factors of Notch1CR2. Therefore, the transcription factor binding sites of known neural enhancers were compared to the TFBS of Notch1CR2. Genes were first selected for comparison if they were (1) related to the neural stem cell phenotype and (2) present in the VISTA Enhancer Browser, which is a public resource containing non-coding human and mouse sequences. This database contained known enhancers for two genes of interest: Sox2 and Nkx6-1. Only enhancers showing specific activity in the CNS were selected for comparison. Sox2, a stem cell marker, has three known enhancers that are specifically active in the nervous system (hs-488, hs-189, hs-1322). Nkx6.1 is a transcription factor found in ventral neural progenitor cells and has one known enhancer (hs-680). Using MatInspector, known TFBS were determined for Notch1CR2 as well as these other four known enhancers.

As shown in Table 6.3, there are 40 TFBSs in common between Notch1CR2 and these three known enhancers of Sox2. There are 50 factors in common between Notch1CR2 and the one known enhancer of Nkx6-1 (hs-680). Many of these common factors are related to neural development. In addition, the five 100%-conserved transcription factors (Gsh1, Barx2, Brn3, Crx, and Fhxb) are present in the enhancers of Sox2 and Nkx6-1 (marked in red in Table 6.3), which provides additional evidence for their importance in the regulation of stem cells.

Table 6.3. Common TFBS between Notch1CR2 and known enhancers for Sox2 & Nkx6-1 or predicted enhancers for Msi1

Notch1CR2 vs. Sox2	Notch1CR2 vs. Nkx6-1	N1CR2 vs. Msi1	Notch1CR2 vs. Sox2 and Nkx6-1	Notch1CR2 vs. Sox2, Nkx6-1, Msi1
ATATA	AP4	ATATA	BRN3	GSH1
TBF1	BRN3	ATBF1	BRN5	GSH2
BARBIE	BRN5	CRX	BRN5	HOXB8
BRIGHT	DLX2	DLX2	FAST1	HOXC9
BRN3	ER	DLX3	GSH1	NFAT
BRN4	FAST1	DLX5	GSH2	NKX12
BRN5	SH1	FAST1	HHEX	NKX25
CRX	GSH	GC	HMGA	NKX61
FAST1	HBP1	GLIS3	HOX1-3	NKX63
FHXB	HHEX	GSH1	HOXB8	OCT1
GSH1	HMGA	GSH2	HOXC9	PAX4
GSH2	HMX1	HOXA3	NFAT	PCE1
HHEX	HOX_PBX	HOXB8	NKX12	PHOX2
HMGA	HOX1-3	HOXC8	NKX25	PIT1
HOX1-3	HOXA3	HOXC9	NKX61	STAT
HOXB3	HOXB8	INSM1	NKX63	
HOXB8	HOXC9	IPF1	OCT1	
HOXC8	HSF1	ISL2	OCT3_4	
HOXC9	HSF2	KLF6	PAX4	
LHX6	IPF1	LHX6	PBX_HOXA9	
LMX1B	ISL2	LHX8	PCE1	
NANOG	KLF6	LMX1B	PHOX2	
NFAT	LHX3	MAZR	PIT1	
NKX12	MAZ	MOK2	RHOX6	
NKX25	MAZR	MYOGENIN	SOX5	
NKX61	MOK2	NEUROG	STAT	
NKX63	MYOGENIN	NFAT	VAX2	
OCT1	NEUROG	NKX12		
OCT3_4	NFAT	NKX25		
PAX4	NKX12	NKX61		
PBX_HOXA9	NKX25	NKX63		
PCE1	NKX61	NOBOX		
PHOX2	NKX63	NUDR		
PIT1	NOBOX	OCT1		
RHOX6	OCT1	PAX4		
SOX5	OCT3_4	PAX6_HD		
STAT	PAX2	PCE1		
TGIF	PAX4	PHOX2		
TST1	PAX5	PIT1		
VAX2	PBX_HOXA9	PLAG1		
	PCE1	RREB1		
	PHOX2	S8		
	PIT1	STAT		
	POU3F3	ZBP89		
	RHOX6			
	RREB1			
	S8			
	SOX5			
	STAT			
	VAX2			

Factors highlighted in red are 100% conserved in mouse and chick sequences of Notch1CR2.
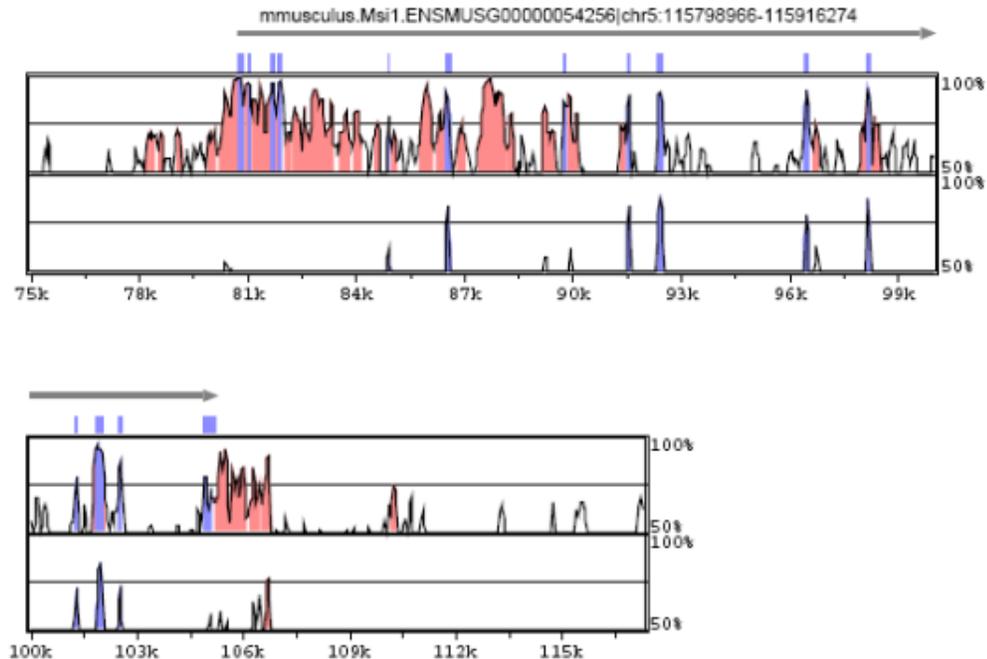
Figure 6.6. Regions of Musashi1 (Msi1) are conserved across mouse, human, and chick.
Msi1 gene sequence for mouse was compared to human and chick. Peaks above 70% represent regions of high conservation. *Pink = noncoding regions, blue = coding regions*

The TFBSs in conserved regions of another important neural stem cell gene – Musashi1 (Msi1) were also compared to Notch1CR2. Using the non-coding sequence retrieval system based on comparative genomics, a global pair-wise alignment was performed, which is the same method used to predict Notch1CR2 [75] (see Figure 6.6). An alignment across mouse, human, and chick genomes revealed four regions possessing 70% or greater conservation. The TFBSs were determined for these four regions, based on MatInspector, and were subsequently compared to the entire list of TFBS of Notch1CR2. Of the 164 TFBS in Notch1CR2, 43 were also present in the Msi1 conserved regions as shown in Table 6.3. It is interesting to see so many common TFBS between the conserved non-coding regions of Notch1CR2 and another stem cell gene.

6.7 Discussion

As shown in previous chapters, the regulatory activity of Notch1CR2 is largely in interneuron progenitors. This chapter explores the potential mechanism by which Notch1CR2 acts as a regulatory element. Activation of Notch1CR2 is through the binding of one or more *trans*-acting factors. There are 164 predicted TFBS on Notch1CR2 as predicted by MatInspector. However, only five of them (Gsh1, Brn3, Barx2, Crx, and Fhxb) are 100% conserved between mouse and chick. Since regulatory elements involved in development have been shown to be highly conserved, it was hypothesized that these five transcription factors had the highest potential of binding to Notch1CR2.

There are several pieces of evidence that support Gsh1/Barx2/Brn3 as the highest potential binding site for Notch1CR2. Mutagenesis of this site ablated GFP expression (Figure 6.3). In fact, mutating a region adjacent to its core binding site (but still part of its entire binding sequence) diminishes GFP expression. In addition, previous results show that Brn3 already co-localizes with Notch1CR2 in the retina (Figure 5.16) and Brn3a binds to Notch1CR2 chromatin of the chick (Figure 6.5). However, evidence for the *trans*-acting factor of Notch1CR2 is stronger for Gsh1 than Brn3a because the Notch1CR2.2 subclone can drive GFP expression with only the Gsh1 binding site (Figure 6.4). These results point to Gsh1 as a *trans*-acting factor of Notch1CR2 and thus provide a mechanism for regulation by Notch1CR2.

It can be speculated that Notch1CR2-GFP$^+$ interneuron progenitors would also express one or a combination of Gsh1, Barx2, and Brn3 progenitor markers. Interestingly, Gsh1 has been reported in interneuron precursors of the brain and spinal

cord [110, 111], Brn3 is primarily studied in retinal auditory sensory progenitors [112], and Barx2 is expressed in the brain and the floor plate of the spinal cord [113, 114]. It might be possible that these three factors play a similar role in different parts of the CNS.

Of particular interest is the repetition of these TFBS in other known enhancers and even predicted regulatory elements of other neural stem cell genes such as Musashi1. This observation lines up with a consistent theme in developmental research. Coding and non-protein coding regions of significance in development play similar roles in a wide range of species. This is the reason why scientists can apply discoveries of Notch1 in Drosophila to vertebrates. In the larger spectrum, these basic developmental processes connect the species on this Earth.

7   Notch1CR2: A Tool to Study Interneuron Progenitors in *reeler*

Thus far, a non-protein coding region of Notch1 has been identified as a regulator of interneuron progenitor (IP) cells. In Chapters 4 & 5, Notch1CR2 was presented as an active regulatory element in both chick and mouse during neurogenesis, specifically in IP cells. Thus, it is expected that this GFP-tagged regulatory element can be used to trace interneuron progenitor cells in disease models. In this chapter, the IP population is examined in *reeler* mutant mouse, a mouse deficient in Reelin protein. Although proliferating cells are normal in *reeler*, neural development of *reeler* is abnormal due to inverted neuronal migration and lamination [115]. A decrease of Notch1CR2 activity in *reeler* shows that this regulatory element is silenced in the absence of Reelin. However, wildtype expression patterns of Notch1CR2 in IP cells can be recovered at P0 with anti-GFP, validating the activity of Notch1CR2 in interneuron progenitors in *reeler*.

7.1   Notch1CR2-GFP is diminished in embryonic/neonatal *reeler* mice

It was initially hypothesized that Notch1CR2 activity would identify a normal IP population in *reeler* because proliferating cells function correctly in *reeler*. Although tangential neuronal migratory patterns are defective in *reeler*, stem cells and progenitors remain normal. To test this hypothesis, Notch1CR2 transgenic mice and *reeler* mice were crossed to obtain Notch1CR2^{+}/*reeler* $^{-/-}$ mice. The number of cells expressing GFP is diminished in Notch1CR2^{+}/*reeler*$^{-/-}$ at E15.5 compared to the wildtype Notch1CR2^{+}/*reeler*$^{+/+}$ (Figure 7.1B). By P0, GFP expression was feint and limited to the rostral region of the lateral ventricle (Figure 7.1C). Samples were stained with anti-GFP to amplify low levels or residual GFP. Although the distribution of GFP was reduced, the phenotype of GFP^{+} cells in *reeler* remained radial glial and non-neuronal.
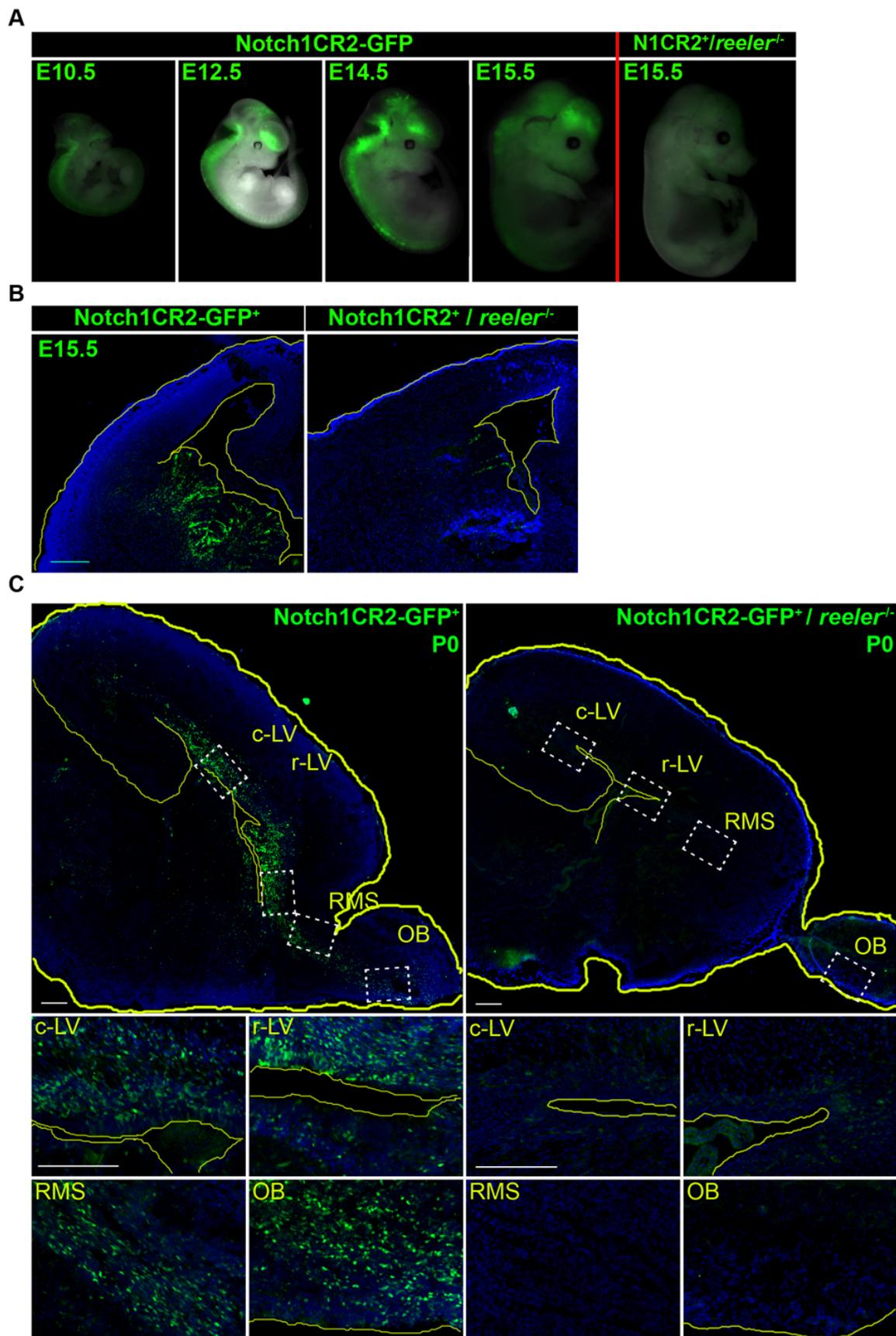
Figure 7.1. GFP expression in Notch1CR2$^+$/*reeler* $^{-/-}$ mice is reduced compared to Notch1CR2$^+$ transgenic wildtypes.
(A) Notch1CR2-GFP is expressed exclusively in the CNS from the telencephalon to the sacral spinal cord at E10.5, E11.5, E12.5, E14.5, E15.5. In comparison, a Notch1CR2$^+$/*reeler* $^{-/-}$ embryo at E15.5 has diminished GFP. (B) Coronal sections at E15.5 show GFP expression in the GE of Notch1CR2$^+$. However, GFP is dramatically reduced in the GE of Notch1CR2$^+$/*reeler* $^{-/-}$. (C) Saggittal sections of P0 wildtype have GFP$^+$ cells in the olfactory bulb, the rostral migratory stream, and regions surrounding the lateral ventricle. In comparison, Notch1CR2$^+$/*reeler* $^{-/-}$ P0 pups have a drastic reduction in GFP expression. Feint GFP expression is detected only at the rostral lateral ventricle. Saggittal sections were stained with nuclear marker Dapi and were imaged using a fluorescent microscope. The images were subsequently organized into a montage. (*Scale bar = 20 μm, GE = ganglionic eminences, c-LV= caudal lateral ventricle, r-LV – rostral lateral ventricle, RMS = rostral migratory stream, VZ = ventricular zone*) (Note: Wildtype images from Figure 5.4 are included in order to provide a side-by-side comparison of wildtype to *reeler*.)

7.2 Radial glia, but not neuronal positioning, are normal in

Notch1CR2$^+$/*reeler*$^{-/-}$ at E15.5

The radial morphology of GFP$^+$ cells is maintained in Notch1CR2$^+$/*reeler* $^{-/-}$ mice. Although there are fewer GFP$^+$ cells in *reeler*, these GFP$^+$ cells remain radial and stretch across the LGE. Immunostaining with radial glial markers, Notch1 and BLBP, at E15.5 remains unchanged in early *reeler* embryos compared to the wildtype (Figure 7.2a-d).

In contrast, neuronal antibody staining patterns are different between *reeler* and the wildtype. Early neurons are more dispersed in *reeler* compared to the wildtype as indicated by the thicker stained regions of doublecortin early neurons at E15.5 (Figure 7.2e-f) and Tbr1$^+$ Layer VI neurons at P0 (Figure 7.3) in *reeler*. This result corresponds with the known *reeler* phenotype of dispersed neuronal distribution and disrupted organization of Layer VI, as marked by Tbr1 [116, 117]. The lack of co-staining with doublecortin is evident at E15.5 in both the control and *reeler* indicating that premature neuronal differentiation is not occurring in Notch1CR2-GFP$^+$ IP cells of *reeler*. The co-

staining patterns of neuronal markers Tbr1 and NeuN at P0 are also different in Notch1CR2-GFP^{+}/*reeler*$^{-/-}$ cells compared to the wildtype (Figure 7.3). While Tbr1 and NeuN do not co-stain with Notch1CR2-GFP^{+} in the wildtype, there are a few GFP^{+} cells in *reeler* that co-localize with Tbr1 and NeuN. However, this GFP^{+} signal is very faint.
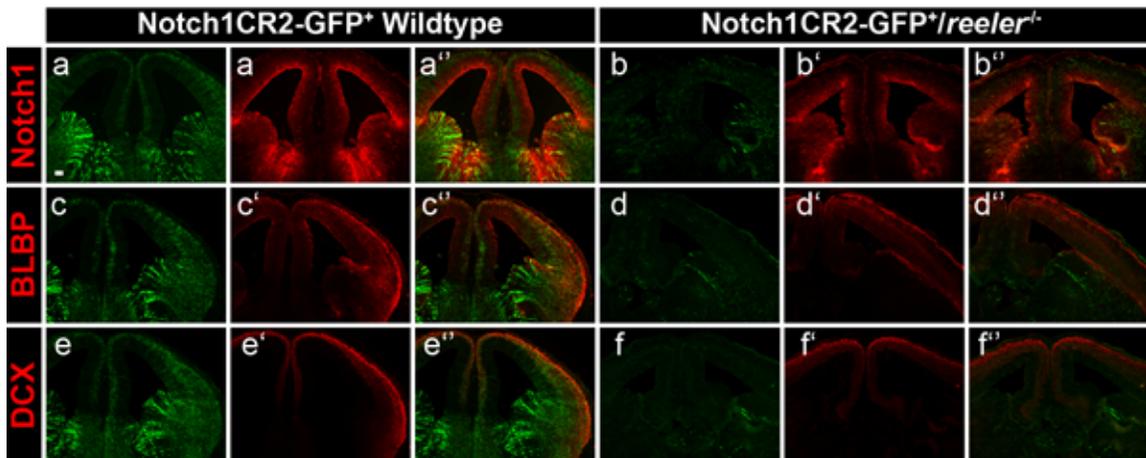
Figure 7.2. Radial glia remain unchanged in Notch1CR2-GFP^{+}/*reeler*$^{-/-}$ mice while early neurons are more dispersed.
(a,b) Notch1 staining is similar between Notch1CR2-GFP^{+}/*reeler*$^{-/-}$ and the wildtype.
(c,d) BLBP staining is also similar between the experimental the wildtype. **(e,f)** However, early neurons, as marked by doublecortin, are more dispersed in the *reeler*$^{-/-}$ compared to the wildtype.
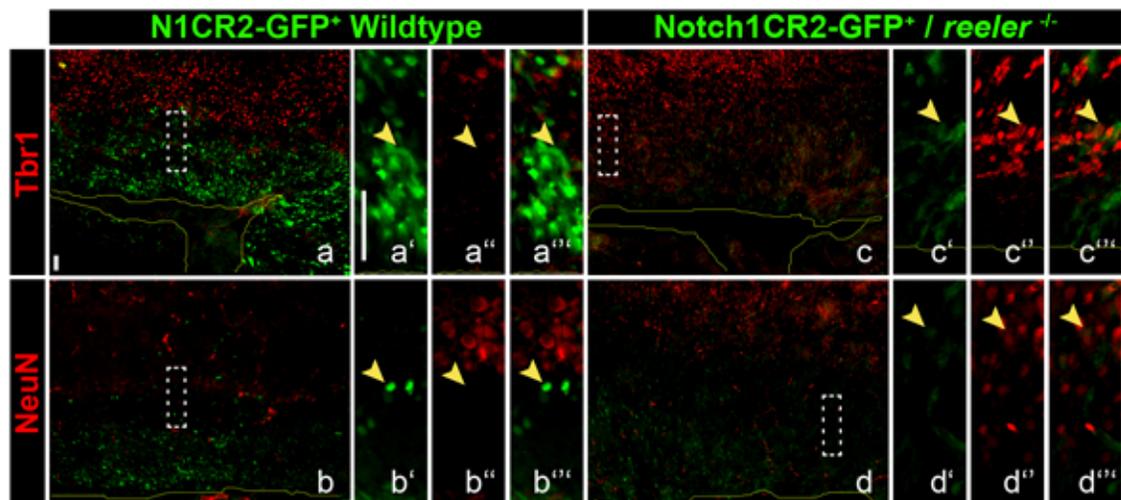
Figure 7.3. Neuronal patterning is dispersed in *reeler* at P0
(a,c) Some GFP^{+} cells in *reeler* co-localize with Tbr1^{+} neurons while the wildtype shows no co-localization. In *reeler*, Tbr1^{+} neurons are not properly located in Layer VI. **(b,d)** Similarly, some GFP^{+} cells in *reeler* but none in the wildtype co-localize with NeuN.

7.3   Asymmetric division is reduced in *reeler* at E15.5

In addition to abnormal neuronal distribution in *reeler*, the IP population is also affected as seen by the decrease of GFP$^+$ cells after retrieval with anti-GFP (Figure 7.2). There is no neocortical GFP expression in *reeler* except for scarce horizontal interneuronal-like cells. The lack of anti-GFP$^+$ retrieval in the embryonic neocortex may indicate a developmental deficiency of *reeler* not only in the existence of the IP population but more specifically in the ability of interneurons to migrate tangentially.

At E15.5, only few of the GFP$^+$ cells in Notch1CR2$^+$/*reeler*$^{-/-}$ are dividing. The few remaining cells do not co-localize with anti-Notch1$^+$, BLBP$^+$, or NuMa (Figure 7.4). In fact, the entire NuMa staining pattern in *reeler* is diminished compared to the wildtype (Figure 7.4c,g). The lack of co-localization is most evident in the low magnification image of BLBP in Figure 7.4f. A group of GFP$^+$ radial cells stretch across the lateral ganglionic eminence in an area distinct from the region of BLBP staining.
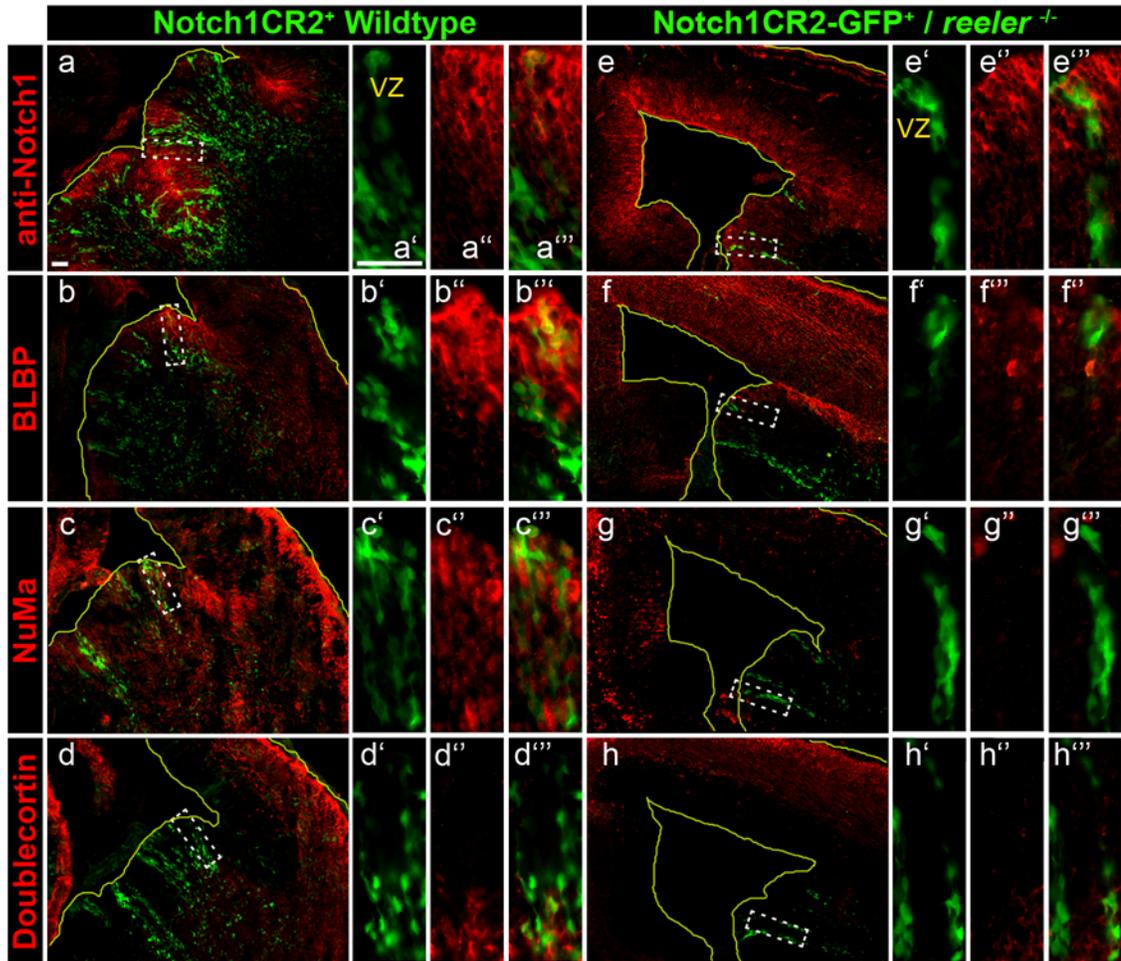
Figure 7.4. GFP$^+$ cells of Notch1CR2-GFP$^+$/*reeler$^{-/-}$* have diminished co-localization with markers of radial glia and asymmetric mitotic division.
(a,e & b,f) In Notch1CR2-GFP$^+$/*reeler$^{-/-}$*, anti-Notch1 and BLBP co-localize with few GFP$^+$ cells, similar to the wildtype. (c,g) *reeler* shows a decrease in asymmetric division as denoted by the decrease of NuMa staining as well as the lack of co-localization with NuMa. (d,h) Finally, co-localization with doublecortin remains low in both the control and the experimental.

7.4 Postnatal Notch1CR2-GFP$^+$ cells are interneuron progenitors

Although there are few, faint GFP$^+$ cells at P0, anti-GFP amplifies GFP$^+$ signal in cells that are neurons. Anti-GFP$^+$ cells in Notch1CR2-GFP$^+$/*reeler$^{-/-}$* samples co-localize with NuMa and GAD65/67 in serial sections indicating that they are asymmetrically dividing cells and interneuron progenitors (Figure 7.5). NeuN and VGAT are not present in GFP$^+$ areas around the lateral ventricle. At P7, there is no detectable GFP in

Notch1CR2-GFP$^+$/*reeler*$^{-/-}$ mice or the wildtype until anti-GFP is applied. Anti-GFP amplifies GFP in the rostral lateral ventricle. Note that the lateral ventricles of *reeler* are naturally larger at this stage of development.
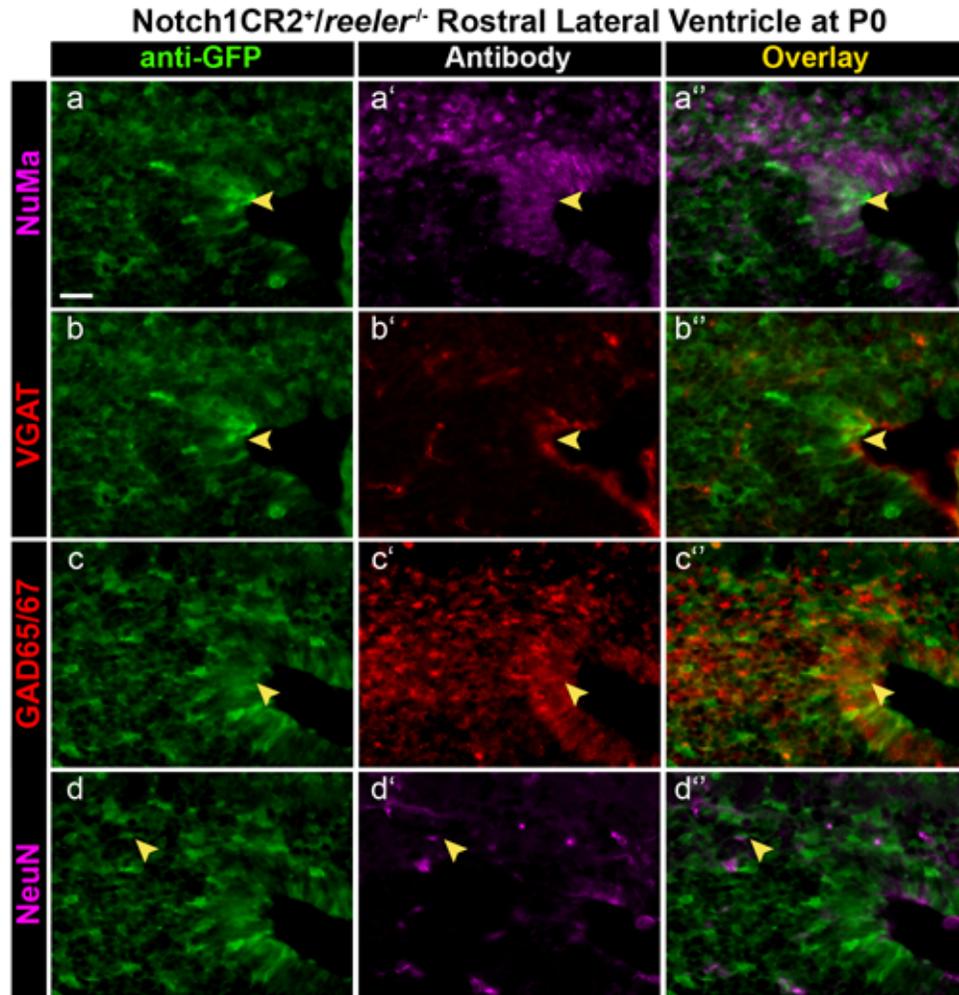
Figure 7.5. Anti-GFP$^+$ cells in the P0 lateral ventricle are interneuron precursors. NuMa/VGAT and GAD65/67/NeuN combinations were used to co-stain serial sections. **(a,c)** NuMa and GAD65/67 co-localize with anti-GFP. **(b)** VGAT is present in the VZ but does not clearly co-localize with anti-GFP. **(d)** NeuN is not present in the region of anti-GFP staining. Saggittal sections were stained with anti-GFP. Images are taken at the rostral lateral ventricle.
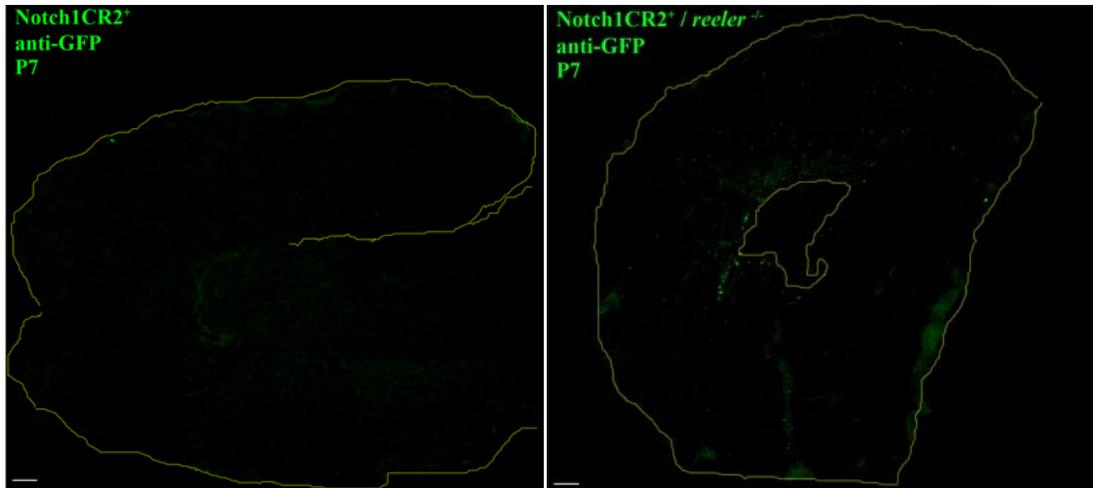
Figure 7.6. Anti-GFP is present in rostral lateral ventricle of both Notch1CR2⁺ wildtype and Notch1CR2⁺/*reeler* ⁻/⁻ mice.
Although Notch1CR2-GFP is not detectable in *reeler* or wildtype at P7, staining with anti-GFP reveals GFP ⁺ cells around the lateral ventricle and dispersed throughout the cortex. The above sections are from the saggittal view. Scale bar = 40 μm.

7.5   Discussion

In this chapter, the interneuron progenitor population is examined in *reeler* mutant mice, which are deficient in Reelin protein. Abnormal traits of *reeler* include abnormal interneuron positioning following migration into the cortex amongst other reported deficiencies [118]. Reelin does not guide migration but rather acts as a detachment signal in tangential chain-migration during postnatal neurogenesis [90, 119]. It is well established that neurons migrate along the radial glial shaft to their final laminar position. Molecular evidence of this interaction is found in the interaction of Notch1 and Reelin, which is necessary for neuronal migration. Expression levels of BLBP and Notch1 are even decreased in *reeler* [120]. However, there are no reported deficiencies in radial glial proliferation or phenotype in *reeler*. Based on current knowledge, radial glial proliferation remains independent of Reelin.

Initially, it was hypothesized that the interneuron progenitor population would remain unaltered in *reeler* since Reelin deficiencies do not affect proliferating cells. However, the results were surprising: the interneuron progenitor population decreases in *reeler*. This trend is reported both in the embryo (two days after the *reeler* phenotype first appears [115] and at birth. At P0, amplified GFP is found in interneuron progenitors, similar to the wildtype. Although stem/progenitor cells are normal in *reeler*, this chapter reports a change in the activity of a regulatory element of IP cells as a result of Reelin deficiencies. It can be speculated that Reelin might play a role in maintaining the population of interneuron progenitors via Notch1CR2.

Reelin might also influence the tangential migration of interneurons. GFP signal is recovered in interneuron progenitors but not in neurons as shown at P0 (Figure 7.5). GFP is also not recovered in early neurons at E15.5 *reeler* in contrast to the wildtype, which showed GFP-retrieval in the basal neuronal layers of the neocortex at E15.5 (Figure 5.10). Since Reelin acts as a detachment signal in tangential migration [90], the lack of GFP in the *reeler* embryonic neocortex indicates a breech in migration from the ganglionic eminence.

The decrease of Notch1CR2-GFP$^+$ cells in *reeler* might also be explained by a mis-communication between migrating neurons and their progenitors. Migrating neurons in *reeler* do not form proper layers leading to improper signaling back to the progenitors and an eventual decrease of activity of regulatory elements. Constant feedback between neurons and stem cells determines the balance between cell division and cell maturation. There is also an overall reduction of NuMa in *reeler*, indicating that the asymmetric division process is abnormal under Reelin deficiencies. Perhaps asymmetrically dividing

cells require positive feedback from neurons that have reached their final destination in order to continue producing more interneuron daughter cells. A better understanding of the asymmetric division process in *reeler* is needed to draw any further conclusions about the role of Reelin in the interneuron progenitor population.

Notch1CR2 may have a role in *reeler* relevant to certain diseases of psychosis, which have been shown to possess abnormal GABAergic interneurons. Reelin heterozygote mice have already been proposed as a genetic model for studying schizophrenia [121]. There is a known relationship between Reelin and GAD67, which is found in GABAergic neurons, in schizophrenia. First, it has been shown that both Reelin and GAD67 are downregulated in the prefrontal cortex and other brain regions of patients with schizophrenia and other bipolar disorders [122]. Also, the promoters of both Reelin and GAD67 are activated through similar mechanisms [123]. It has been shown that Reelin is expressed in GABAergic neurons of Layer I and II of the neocortex; Layer I contains the Reelin-producing Cajal-Retzius cells. An insufficiency of Reelin leads to a decrease of GABAergic neurons, but the mechanism by which this occurs is unknown. Based on the above data showing a down-regulation of the activity of an IP regulatory element (Notch1CR2), it is possible that Notch1CR2 is involved in regulating the effect of Reelin on GABAergic interneurons in schizophrenia. The role of Notch1CR2 and Reelin in schizophrenia is a future direction worth exploring.

8   Concluding Remarks and Future Direction

For the first time, a regulatory element of Notch1 has been identified in the interneuron progenitor (IP) population. Is the IP population solely dependent on the activity of this region? Is it enhancing or repressing Notch1 or is it acting on another gene? Notch1CR2 might not be enhancing Notch1 because Notch1CR2 is not active in all Notch1-expressing cells. Similarly, Notch1 is not expressed in all Notch1CR2-GFP$^+$ cells. This observation suggests that Notch1CR2 does not solely regulate the radial glial state but is rather regulating neurogenesis. It is clear that Notch1CR2 is active in asymmetrically dividing cells and in GABAergic IP cells. Therefore, Notch1CR2 can be used as a model for studying IP cells in other disease models, in addition to *reeler*.

What do Notch1CR2$^+$ IP cells become and where do they go once Notch1CR2 is no longer active? Since the temporal activity pattern of Notch1CR2 is specific to the neurogenic period, it is expected that Notch1CR2$^+$ cells differentiate into interneurons and subsequently lose Notch1CR2 activity. The appearance of anti-GFP$^+$ cells in the basal (top) layers of the embryonic neocortex is reminiscent of the tangential migration of interneurons from the ganglionic eminences through the marginal zone into the neocortex. However, this evidence alone does not prove the fate of cells once Notch1CR2 activity subsides.

Several experiments can be designed to test the cell fate at the end of Notch1CR2-GFP$^+$ activity. First, dividing cells can be tracked with DNA-intercolating molecules such as BrDU at various embryonic time points. The intensity of BrDU can be correlated with the IP profile and Notch1CR2 activity. Second, explants could also be cultured, and the location of GFP$^+$ cells can be tracked *in vitro*. An advantage of *in vitro* experiments

is the ability to track the same set of cells over shorter periods of time. Third, GFP⁺ cells can be isolated from the brains of transgenic mice via fluorescence activated cell sorting (FACS). *In vitro* differentiation assays might reveal the differentiation capacity of these cells. Fourth, an alternative to isolating GFP⁺ cells from the Notch1CR2 transgenic mouse is to transiently transfect a cell line with Notch1CR2-βGP-GFP and then determine cell fate from *in vitro* differentiation assays. An interesting candidate cell line for this experiment is a neural progenitor clone with the potential to give rise to GABAergic interneurons [124]. It would be expected that Notch1CR2 can drive GFP in this interneuron progenitor cell line.

As other regulatory elements are discovered and characterized for cells in the ganglionic eminences, a better understanding of interneuron specification and migration will be achieved. For example, it has been shown that another interneuron marker, Lhx6, directly regulates an Shh enhancer in MGE neurons [125]. Might a component of the Reelin pathway even be involved in regulating the interneuron precursor population? A correlation between Reelin and GAD67 GABAergic interneurons has already been reported [122, 123], and now, this work presents a mechanism through Notch1CR2 by which Reelin may be influencing GABAergic interneurons.

Additional experiments can be performed to confirm that Gsh1 is a *trans*-acting factor of Notch1CR2. Gsh1 is the most probable binding factor based on the literature because Gsh1 is expressed in interneuron progenitors of the spinal cord and brain [110, 111] which corresponds to the phenotype of Notch1CR2⁺ cells. A ChIP binding assay using an antibody against Gsh1 could be performed to test whether Gsh1 is part of the

Notch1CR2 chromatin. The effect of Gsh1 silencing on Notch1CR2-GFP expression could also be tested.

As research continues on the regulatory elements for stem cells, the methods of identifying and characterizing functional regulatory elements must be assessed. Conservation is a widely appreciated approach for identifying functional regulatory elements. However, it is not known as to what proportion of functional binding sites is conserved in distant species. In one report, an analysis of the known transcription factor bindings sites of the promoters of 51 human genes were compared to homologous sequences in mouse [60]. At least one-third of these sites were not functional in rodents. Therefore, studies should not be limited to conserved regions for the identification of all regulatory elements.

Currently, the best way to validate *cis*-regulatory elements *in vivo* is by cloning the sequences into plasmids and testing them one-by-one with a reporter gene. No experimental technique exists to screen large nucleotide sequences efficiently in vertebrates [66]. Knock-out models are the only way to remove these elements from context to determine if they are truly necessary for regulation. However, this method quickly becomes expensive because a different knock-out is required for each regulatory element. Alternatively, high throughput analysis of DNA-protein interactions can be determined using ChIP-Seq technology on a genome-wide scale [126]. An antibody against the protein of interest is used to immunoprecipitate chromatin with the protein of interest. Then ultrahigh-throughput sequencing determines the sequences that bind to the protein of interest. In the case of Notch1CR2, it would be interesting to determine what

DNA sequences bind to Gsh1. It would be expected that Notch1CR2 amongst other possible regulatory elements are one of the DNA sequences that Gsh1 can bind to *in vivo*.

Notch1CR2 and its regulatory mechanisms contribute to the comprehensive knowledge of the stem cell genetic network. This information can be used to engineer IP cells for transplant in patients with GABAergic interneuron deficiencies such as schizophrenia and psychosis. Gsh1 is a factor to consider when engineering these cells. As the regulatory elements of IP cells are better understood, one could eventually imagine the availability of bioengineered-IP cells for personalized medicine.

9 Appendix
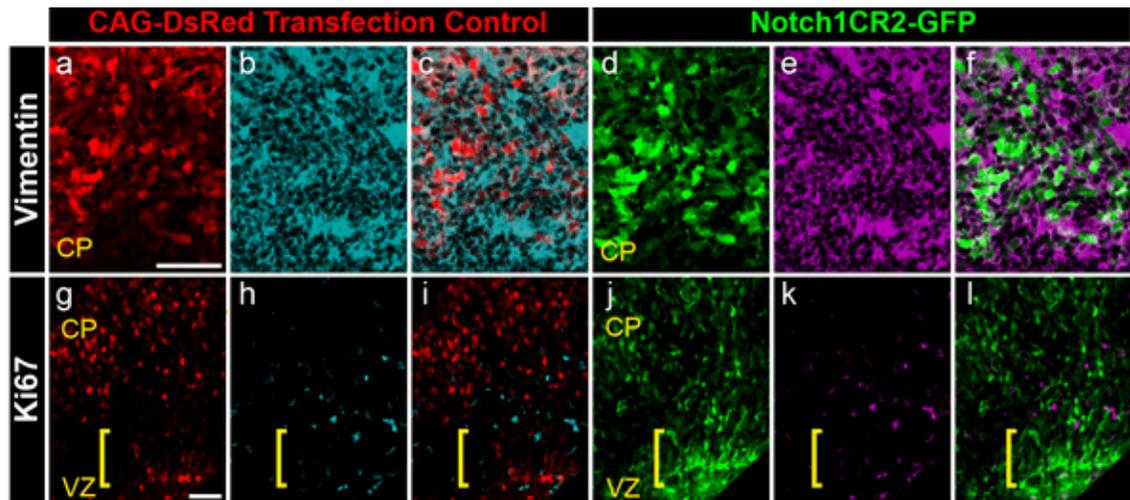
Figure 9.1. Vimentin but not Ki67 is prevalent in E17.5 *in utero* co-transfected embryos.

(a-f) Both CAG-DsRed and **(d-f)** Notch1CR2 are expressed in regions of vimentin expression. Images in (a-c) and (d-f) are identical since these samples were co-transfected. **(g-l)** There is a decrease in Ki67 staining compared to E14.5 (Figure 5.2m-r) as well as a decrease in colocalization with CAG-DsRed and Notch1CR2. The bracket marks a region in the VZ, which has more Notch1CR2-GFP expression than CAG-DsRed, suggesting that Notch1CR2$^+$ cells are slower to leave the VZ. *Scale bar = 20 μm.*
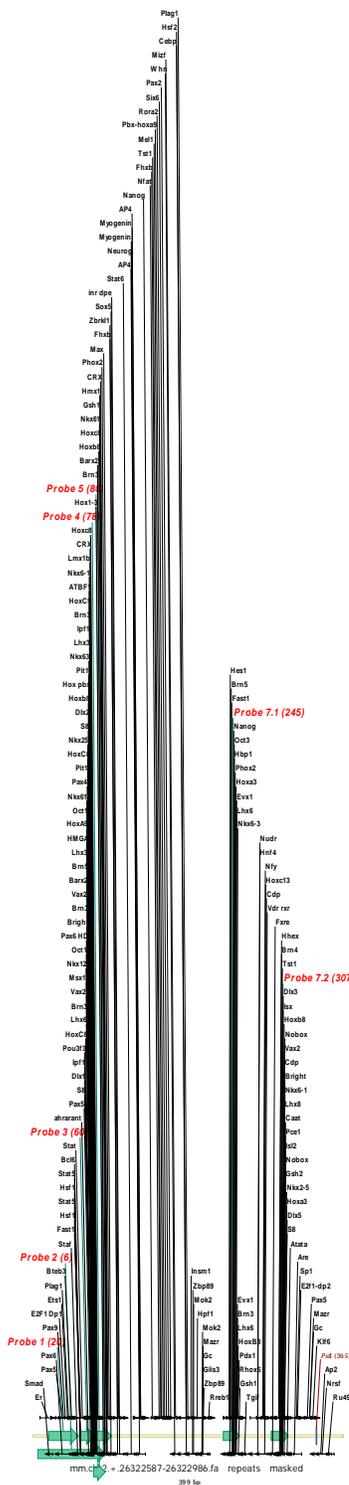
Figure 9.2. Transcription factor binding sites of Notch1CR2 based on MatInspector.

The 399-base pair sequence of Notch1CR2 contains 164 transcription factor binding sites (121 unique sites) as reported by MatInspector.

Table 9.1. DNA Probes for EMSA and their TFBS (based on core binding region)

Probe	Position on Notch1CR2	Sequence (sense)	TFBS (based on core binding region)		
Probe 1	20-57	Ctagtagacc aaggagcaca gaggcgagga aggggggttgta caggccgg	Pax5 Pax6 Pax9 E2f1_Dp Plag1 Bteb		
Probe 2	60-92	Ctagtgctgg gaagccacgc ataattaatcac acagcaggcc gg	Staf Stat5 Stat5 Bcl6 Stat Ahrarnt Pax5 S8 Dlx1 Ipf1 Lhx6 Pou3f3 Hoxc8 Brn5 Lhx3 Hmga	Brn3 Vax2 Msx Nkx12 Oct1 Bright Brn3 Vax2 Barx2 Nkx6-3 Pax6 Hoxa9 Oct1 Hoxc8 Nkx2-5 S8	Lhx3 Nkx6-1 Pax4 Dlx2 Hoxb8 Ipf1 Lmx1b Pit1 Hox_pbx Brn3 Pit1 Hoxc9 Atbf1 Nkx6-1 Crx Hoxc8
Probe 3	60-78	Ctagtctggg aagccacgca taaggccgg	Staf Stat5 Stat5 Bcl6 Stat Ahrarnt	Pax5 Ipf1 Lhx6 Pouf3 HoxC8 Brn5	Brn3 Vax2 Nkx1-2 Oct1 Nkx2-5 S8
Probe 4	78-92	ctagtttaatca cacagcatgg ccgg	Lhx3 Hoxa9 Lhx3 Nkx6-1 Hoxb8	Pit1 Hox_pbx Brn3 Pit1	HoxC9 Nkx6-1 Crx HoxC8
Probe 5	80-100	ctagtaatcac acagcattaat cgccggccgg	HoxC8 Hox1-3 Brn3 Barx2	Hoxb8 Gsh1 Hmx1 Hoxc9	Phox2 Nkx61 Crx

*Yellow marks the TFBS that ablated GFP expression when mutated.

Table 9.2. Literature review on potential TFBS (based on EMSA results)

Transcription Factor	TF Functions During This Process:	Location	Relationship to Notch1	Ref.
Ahrarnt				
Atfb1	Induction of cell cycle arrest Association with neuronal differentiation Suppression of Nestin and activation of NeuroD1 promoter (neurons)	Neurons	None reported	[127]
Barx2	TF regulator during development homeobox genes regulate morphogenesis by controlling expression patterns of CAMs	TE, SC, DRG, floor plate, Rathke's pouch craniofacial	Barx2 binds to NgCAM and L1 (cell adhesion molecules)	[113, 114]
Bcl6	Maintains expression of Pitx2 in the left lateral plate mesoderm during the patterning of left-right asymmetry	Left-right asymmetry	- forms a complex with BCL6 corepressor (BCoR) on promoters of selected Notch target genes such as enhancer of split related 1 - BCL6 inhibits transcription of these genes by competing for the Notch1 intracellular domain, preventing the coactivator Mastermind-like1 (MAM1) from binding	
Bright			None	
Brn3	Sensory specification	Postmitotic retinal ganglion cells, differentiated hair cells	- Notch influences whether cells of common lineage in a sensory patch differentiate as either hair cells or supporting cells - Brn3 may prevent NGN-2 expression through Notch1 activation. NGN-2 regulates the differentiatiation of sensory neurons and glia	[112, 128]
Brn5	Consensus sequence strongly resembles POU-IV (Brn3)	Nervous, endocrine, and immune systems	None	[129]
Crx	Cone-rod formation, photoreceptor precursors	Retinal cones/rods	Inhibition of Notch1 leads to Crx$^+$ cells	[130]
Dlx1			None reported	[131, 132]
Dlx2	Neurogenesis and proliferation	Subcortical TE neurogenesis Progenitors in	Mash1(bHLH) and DLX1/2 regulate Notch Dlx1/2 are required to	[133]

		GE Cortical interneurons	downregulates Notch signaling during specification and differentiation of 'late' progenitors	
Gsh1	Decision-making between excitatory and inhibitory state of neurons	Sensory interneuron progenitors	Ascl1 upregulates Notch1 to ensure proper generation of excitatory neurons	[110, 111]
HMGA	Restricted astrocyte differentiation	Neural progenitor cells	None reported	
Hmx1	Sensory organ development Homeobox genes	Neurons, retina, sympathetic nerve ganglia, cranial neural ganglia, dorsal root	None reported	[134, 135]
Hox13	Morphogenesis of caudal neural tube	Hindbrain	None reported	[136]
Hoxb8	Motor neurons, sensory spinal development	Neural stem cells, dorsal horn of spinal cord	None reported	[137]
HoxC8	End of gastrulation in embryo	Neural tube	None reported	[138, 139]
Hoxc9	Anteroposterior patterning of mouse skeleton	Neural stem cells of spinal cord	None reported	[140, 141]
Hox_Pbx	Pbx binds as heterodimer or complex with Hox Posterior neural, hindbrain and neural crest development	Facial/hindbrain motor neurons	Transmits signals to the Notch1 cascade to regulate vulval cell fates	[142-144]
Ipf1	Neural stem cells of the fore/hindbrain, GE, hypothalamus and inferior colliculus	Neural stem cells near VZ	None reported	[145]
Lhx3	Transcriptional regulator during morphogenesis and/or maintenance/ differentiation of the pituitary, motor neurons, and pineal gland	Glutamatergic V2a-interneurons in spinal cord	Stem cells from anterior bovine pituitary gland were Notch1^{+}/Lhx3^{+}	[146]
Lhx6	Promotes tangential migration of interneurons Directly regulates the expression of SHH enhancer in MGE neurons	Interneurons	None reported	[125, 147]

Lmx1b	Maintenance of Wnt1 expression Control of the constriction of the neural tube which eventually defines the ME/MT boundary Control of differentiation of multiple neuronal subtypes in the ventral midbrain	Otic placode specification of dopamine neurons ventral midbrain	Notch blockade induced the expansion of non-neural genes, Lmx1	[148]
Msx	Epithelial-mesenchymal interactions Embryonic neural crest development		mRNA of Notch1, Shh, BMP4 and Msx2 increased in grey/white matter around injury Msx1/2 decreased BMP2/4 and Notch1 signaling Msx1 regulates the Notch1/Delta pathway	[149-151]
Nkx1.2	Posterior neurogenesis	Adult cerebral cortex, hippocampus, diencephalon, pons/medulla, and cerebellum Embryonic ME/MY	Pnx (Nkx1 family) does not inhibit Notch1	[152]
Nkx2.5	Heart specification	Heart	Notch1 regulates cardiomyocyte commitment through Nkx2-5	[153, 154]
Nkx6.1		Pancreas, ventral spinal cord, brain	Reduction of Nkx2.2, Nkx6.1, Olig2, Pax6, and Dbx1 in the ventral spinal cord of Notch1 cKO mice	[155]
Nkx6.3	V2 interneuron differentiation Early non-neural ectoderm	Caudal hindbrain, non-neural ectoderm	None reported	[156]
Oct1		Neural stem cell	Oct1 binds to the nestin enhancer in E8.5 mouse and Oct1, Brn1, and Brn2 bind to this enhancer at E10.5 and E12.5	[157, 158]
Pax4	Islet cell fate in pancrease	Endocrine progenitors	Activation of Notch in Pax4^{+} progenitors inhibits their differentiation into α and β endocrine cells Downstream factors of Notch1 affect Pax4	[159, 160]

			expression	
Pax5	In neural tube right after closure	Mid/hind brain boundary	None reported	[161]
Pax6	Neural stem cell specification	Neural stem cells	Notch1 knockout shows a decrease in pax6, olig2, nkx6.1, nkx2.2, and dbx1	[155]
Pax9	Pax5 and Msx1 in tooth morphogenesis	Teeth, foregut endoderm, somites, limb mesenchyme, midbrain, and neural crest	Pax9 and Notch1 are regulated by Gli3 for anterior limb mesenchyme	[162]
Phox2	Branchio-visceromotor neuron development Determination of peripheral axonal phenotype and thus the decision to stay within the neural tube or to project out of it	Neural tube CNS/PNS Ventral neural progenitors of the hindbrain for the production of branchio-visceral motoneuronal precursors	None reported	[163]
Pou3F3	Brn1 Found in regions of progenitors and immature neurons	Neural stem cells	Mash1 and the POU proteins interact on the promoter of the Notch ligand Delta and synergistically activate Delta1 transcription, a key step in neurogenesis	[157, 164]
S8	Cartilege homeoprotein		None reported	[165]
Vax2	Vax2 controls the proliferation of ventral eye and brain progenitors	Ventral neural progenitors of eye and brain Eye D/V axis	None reported	[166]

Central nervous system (CNS), Dorsal root ganglion (DRG), Telencephalon (TE), Ganglionic eminences (GE), Peripheral nervous system (PNS), Transcription factor (TF)

Table 9.3. Regions of Notch1 *g. gallus* conserved with Notch1CR2 *m. musculus* (399 base pair regions) based on MatInspector analysis

TFBS of *g. gallus* Notch1 conserved region	TFBS of Notch1CR2 (*m.s.* ∩ *g.g.*)	100% conserved core sequence (*m.s.* ∩ *g.g.*)	Start position (referenced to Notch1CR2)	End position (referenced to Notch1CR2)
HIC1.02				
BCL6.04	BCL6.04		53	69
STAT5.01	STAT5.01		52	70
STAT.01	STAT.01		54	72
BRN5.01	BRN5.01		67	89
HOX1-3.01				
OCT1.03	OCT1.03		70	86
CRX.01	CRX.01		74	90
TCF11MAFG.01				
JUNDM2.02				
PAX3.02				
HOX1-3.01	HOX1-3.01		81	99
BRN3.03	BRN3.03	Brn3.03	83	101
BARX2.01	BARX2.01	Barx2.01	83	101
HMGA.01				
TST1.01				
GSH1.01	GSH1.01	Gsh1.01	86	104
CRX.01	CRX.01	Crx.01	88	104
TCF2.01				
FHXB.01	FHXB.01	Fhxb.01	100	116
SL1.01				
SOX5.01	SOX5.01		100	116
AP4.02	AP4.02		130	146
MYOGENIN.02	MYOGENIN.02		129	145
ATOH1.01				
MYOGENIN.02	MYOGENIN.02		177	187
LEF1.02				
CHR.01				
PBX1_MEIS1.01				
HBP1.02				
IRF4.01				
ILF1.01				
EVI1.06				
MTATA.01				
HOXC9.02				
PAX6.01				
WHN.01				
CREB.02				
RFX4.01				

References

1.   Jenq, R.R. and M.R. van den Brink, *Allogeneic haematopoietic stem cell transplantation: individualized stem cell and immune therapy of cancer.* Nat Rev Cancer. **10**(3): p. 213-21.

2.   Griffith, L.G. and G. Naughton, *Tissue engineering--current challenges and expanding opportunities.* Science, 2002. **295**(5557): p. 1009-14.

3.   Thai, H.M., et al., *Implantation of a three-dimensional fibroblast matrix improves left ventricular function and blood flow after acute myocardial infarction.* Cell Transplant, 2009. **18**(3): p. 283-95.

4.   Geron, *www.geron.com.* Accessed on November 2011.

5.   Takahashi, K., et al., *Induction of pluripotent stem cells from fibroblast cultures.* Nat Protoc, 2007. **2**(12): p. 3081-9.

6.   Gaiano, N., J.S. Nye, and G. Fishell, *Radial glial identity is promoted by Notch1 signaling in the murine forebrain.* Neuron, 2000. **26**(2): p. 395-404.

7.   Fu, C., et al., *GABAergic Interneuron Development and Function Is Modulated by the Tsc1 Gene.* Cereb Cortex.

8.   Ramon y Cajal, S., *Nobel Prize in Physiology Lecture.* 1906.

9.   Golgi, C., *Nobel Prize in Physiology Lecture.* 1906.

10.   Graziadei, P.P. and G.A. Graziadei, *Neurogenesis and neuron regeneration in the olfactory system of mammals. I. Morphological aspects of differentiation and structural organization of the olfactory sensory neurons.* J Neurocytol, 1979. **8**(1): p. 1-18.

11.   Graziadei, P.P. and R.S. DeHan, *Neuronal regeneration in frog olfactory system.* J Cell Biol, 1973. **59**(2 Pt 1): p. 525-30.

12.   Angevine, J.B., Jr. and R.L. Sidman, *Autoradiographic study of cell migration during histogenesis of cerebral cortex in the mouse.* Nature, 1961. **192**: p. 766-8.

13.   Altman, J., *Are new neurons formed in the brains of adult mammals?* Science, 1962. **135**: p. 1127-8.

14.   Das, G.D. and J. Altman, *Postnatal neurogenesis in the caudate nucleus and nucleus accumbens septi in the rat.* Brain Res, 1970. **21**(1): p. 122-7.

15.   Kaplan, M.S. and J.W. Hinds, *Neurogenesis in the adult rat: electron microscopic analysis of light radioautographs.* Science, 1977. **197**(4308): p. 1092-4.

16.   Kaplan, M.S., *Neurogenesis in the 3-month-old rat visual cortex.* J Comp Neurol, 1981. **195**(2): p. 323-38.

17.   Rakic, P., *Neuron-glia relationship during granule cell migration in developing cerebellar cortex. A Golgi and electronmicroscopic study in Macacus Rhesus.* J Comp Neurol, 1971. **141**(3): p. 283-312.

18.   Goldman, S.A. and F. Nottebohm, *Neuronal production, migration, and differentiation in a vocal control nucleus of the adult female canary brain.* Proc Natl Acad Sci U S A, 1983. **80**(8): p. 2390-4.

19.   Harrison, R., *Observations on the living developing nerve fiber.* The Anatomical Record, 1907. **1**: p. 116-128.

20.   Hatten, M.E., *Embryonic cerebellar astroglia in vitro.* Brain Res, 1984. **315**(2): p. 309-13.

21. Reynolds, B.A. and S. Weiss, *Generation of neurons and astrocytes from isolated cells of the adult mammalian central nervous system.* Science, 1992. **255**(5052): p. 1707-10.

22. Reynolds, B.A., W. Tetzlaff, and S. Weiss, *A multipotent EGF-responsive striatal embryonic progenitor cell produces neurons and astrocytes.* J Neurosci, 1992. **12**(11): p. 4565-74.

23. Artavanis-Tsakonas, S., M.D. Rand, and R.J. Lake, *Notch signaling: cell fate control and signal integration in development.* Science, 1999. **284**(5415): p. 770-6.

24. Ohsie, S.J., et al., *Immunohistochemical characteristics of melanoma.* J Cutan Pathol, 2008. **35**(5): p. 433-44.

25. Ladstein, R.G., et al., *Ki-67 expression is superior to mitotic count and novel proliferation markers PHH3, MCM4 and mitosin as a prognostic factor in thick cutaneous melanoma.* BMC Cancer. **10**: p. 140.

26. Hendzel, M.J., et al., *Mitosis-specific phosphorylation of histone H3 initiates primarily within pericentromeric heterochromatin during G2 and spreads in an ordered fashion coincident with mitotic chromosome condensation.* Chromosoma, 1997. **106**(6): p. 348-60.

27. Knoblich, J.A., *Mechanisms of asymmetric stem cell division.* Cell, 2008. **132**(4): p. 583-97.

28. Siller, K.H. and C.Q. Doe, *Spindle orientation during asymmetric cell division.* Nat Cell Biol, 2009. **11**(4): p. 365-74.

29. Vescovi, A.L., et al., *bFGF regulates the proliferative fate of unipotent (neuronal) and bipotent (neuronal/astroglial) EGF-generated CNS progenitor cells.* Neuron, 1993. **11**(5): p. 951-66.

30. (GWAS), G.-W.A.S., *http://gwas.nih.gov/.* Accessed on November 2011.

31. Sakabe, N.J. and M.A. Nobrega, *Genome-wide maps of transcription regulatory elements.* Wiley Interdiscip Rev Syst Biol Med. **2**(4): p. 422-37.

32. Browser, V.E., *http://enhancer.lbl.gov/.* Accessed November 2011.

33. Louvi, A. and S. Artavanis-Tsakonas, *Notch signalling in vertebrate neural development.* Nat Rev Neurosci, 2006. **7**(2): p. 93-102.

34. Lowell, S., et al., *Notch promotes neural lineage entry by pluripotent embryonic stem cells.* PLoS Biol, 2006. **4**(5): p. e121.

35. Nye, J.S., R. Kopan, and R. Axel, *An activated Notch suppresses neurogenesis and myogenesis but not gliogenesis in mammalian cells.* Development, 1994. **120**(9): p. 2421-30.

36. Ishibashi, M., et al., *Persistent expression of helix-loop-helix factor HES-1 prevents mammalian neural differentiation in the central nervous system.* EMBO J, 1994. **13**(8): p. 1799-805.

37. Noctor, S.C., et al., *Neurons derived from radial glial cells establish radial units in neocortex.* Nature, 2001. **409**(6821): p. 714-20.

38. Malatesta, P., E. Hartfuss, and M. Gotz, *Isolation of radial glial cells by fluorescent-activated cell sorting reveals a neuronal lineage.* Development, 2000. **127**(24): p. 5253-63.

39. Misson, J.P., et al., *Identification of radial glial cells within the developing murine central nervous system: studies based upon a new immunohistochemical marker.* Brain Res Dev Brain Res, 1988. **44**(1): p. 95-108.

40. Chanas-Sacre, G., et al., *Radial glia phenotype: origin, regulation, and transdifferentiation.* J Neurosci Res, 2000. **61**(4): p. 357-63.

41. Hartfuss, E., et al., *Characterization of CNS precursor subtypes and radial glia.* Dev Biol, 2001. **229**(1): p. 15-30.

42. Schmid, R.S., Y. Yokota, and E.S. Anton, *Generation and characterization of brain lipid-binding protein promoter-based transgenic mouse models for the study of radial glia.* Glia, 2006. **53**(4): p. 345-51.

43. Feng, L., M.E. Hatten, and N. Heintz, *Brain lipid-binding protein (BLBP): a novel signaling system in the developing mammalian CNS.* Neuron, 1994. **12**(4): p. 895-908.

44. Takahashi, T., R.S. Nowakowski, and V.S. Caviness, Jr., *The leaving or Q fraction of the murine cerebral proliferative epithelium: a general model of neocortical neuronogenesis.* J Neurosci, 1996. **16**(19): p. 6183-96.

45. Ono, T. and R.S. Tuan, *Vitamin D and chick embryonic yolk calcium mobilization: identification and regulation of expression of vitamin D-dependent Ca2(+)-binding protein, calbindin-D28K, in the yolk sac.* Dev Biol, 1991. **144**(1): p. 167-76.

46. Fujita, S., *Analysis of Neuron Differentiation in the Central Nervous System by Tritiated Thymidine Autoradiography.* J Comp Neurol, 1964. **122**: p. 311-27.

47. Ferretti, P. and K. Whalley, *Successful neural regeneration in amniotes: the developing chick spinal cord.* Cell Mol Life Sci, 2008. **65**(1): p. 45-53.

48. Alvarez-Buylla, A., M. Theelen, and F. Nottebohm, *Proliferation "hot spots" in adult avian ventricular zone reveal radial cell division.* Neuron, 1990. **5**(1): p. 101-9.

49. Stump, G., et al., *Notch1 and its ligands Delta-like and Jagged are expressed and active in distinct cell populations in the postnatal mouse brain.* Mech Dev, 2002. **114**(1-2): p. 153-9.

50. Yoon, K. and N. Gaiano, *Notch signaling in the mammalian central nervous system: insights from mouse mutants.* Nat Neurosci, 2005. **8**(6): p. 709-15.

51. Ge, W., et al., *Notch signaling promotes astrogliogenesis via direct CSL-mediated glial gene activation.* J Neurosci Res, 2002. **69**(6): p. 848-60.

52. de Jong, H., *Modeling and simulation of genetic regulatory systems: a literature review.* J Comput Biol, 2002. **9**(1): p. 67-103.

53. Long, X. and J.M. Miano, *Remote control of gene expression.* J Biol Chem, 2007. **282**(22): p. 15941-5.

54. Gomez-Skarmeta, J.L., B. Lenhard, and T.S. Becker, *New technologies, new findings, and new concepts in the study of vertebrate cis-regulatory sequences.* Dev Dyn, 2006. **235**(4): p. 870-85.

55. Finlay, B.L. and R.B. Darlington, *Linked regularities in the development and evolution of mammalian brains.* Science, 1995. **268**(5217): p. 1578-84.

56. Ip, Y.T., et al., *The dorsal morphogen is a sequence-specific DNA-binding protein that interacts with a long-range repression element in Drosophila.* Cell, 1991. **64**(2): p. 439-46.

57.   Papatsenko, D. and M. Levine, *Quantitative analysis of binding motifs mediating diverse spatial readouts of the Dorsal gradient in the Drosophila embryo.* Proc Natl Acad Sci U S A, 2005. **102**(14): p. 4966-71.

58.   Bonn, S. and E.E. Furlong, *cis-Regulatory networks during development: a view of Drosophila.* Curr Opin Genet Dev, 2008. **18**(6): p. 513-20.

59.   Liberman, L.M. and A. Stathopoulos, *Design flexibility in cis-regulatory control of gene expression: synthetic and comparative evidence.* Dev Biol, 2009. **327**(2): p. 578-89.

60.   Dermitzakis, E.T. and A.G. Clark, *Evolution of transcription factor binding sites in Mammalian gene regulatory regions: conservation and turnover.* Mol Biol Evol, 2002. **19**(7): p. 1114-21.

61.   Emerson, J.J., et al., *Natural selection on cis and trans regulation in yeasts.* Genome Res. **20**(6): p. 826-36.

62.   Jeziorska, D.M., K.W. Jordan, and K.W. Vance, *A systems biology approach to understanding cis-regulatory module function.* Semin Cell Dev Biol, 2009. **20**(7): p. 856-62.

63.   Blackwood, E.M. and J.T. Kadonaga, *Going the distance: a current view of enhancer action.* Science, 1998. **281**(5373): p. 60-3.

64.   Khoury, G. and P. Gruss, *Enhancer elements.* Cell, 1983. **33**(2): p. 313-4.

65.   Bulger, M. and M. Groudine, *Enhancers: the abundance and function of regulatory sequences beyond promoters.* Dev Biol. **339**(2): p. 250-7.

66.   Haeussler, M. and J.S. Joly, *When needles look like hay: how to find tissue-specific enhancers in model organism genomes.* Dev Biol. **350**(2): p. 239-54.

67.   Echols, H., *Multiple DNA-protein interactions governing high-precision DNA transactions.* Science, 1986. **233**(4768): p. 1050-6.

68.   Su, W., et al., *DNA-looping and enhancer activity: association between DNA-bound NtrC activator and RNA polymerase at the bacterial glnA promoter.* Proc Natl Acad Sci U S A, 1990. **87**(14): p. 5504-8.

69.   Chen, J.L., et al., *Enhancer action in trans is permitted throughout the Drosophila genome.* Proc Natl Acad Sci U S A, 2002. **99**(6): p. 3723-8.

70.   Griffith, J., A. Hochschild, and M. Ptashne, *DNA loops induced by cooperative binding of lambda repressor.* Nature, 1986. **322**(6081): p. 750-2.

71.   Kramer, H., et al., *lac repressor forms loops with linear DNA carrying two suitably spaced lac operators.* EMBO J, 1987. **6**(5): p. 1481-91.

72.   Kanehisa, M. and S. Goto, *KEGG: kyoto encyclopedia of genes and genomes.* Nucleic Acids Research, 2000. **28**(1): p. 27-30.

73.   Wahlbuhl, M., et al., *Transcription factor Sox10 orchestrates activity of a neural crest-specific enhancer in the vicinity of its gene.* Nucleic Acids Research.

74.   Ensembl, *www.ensembl.org.* Accessed December 2011.

75.   Doh, S.T., et al., *Non-coding sequence retrieval system for comparative genomic analysis of gene regulatory elements.* BMC Bioinformatics, 2007. **8**: p. 94.

76.   Genomatix, *http://www.genomatix.de/.* Accessed December 2011.

77.   Doh, S.T., *Computational prediction and experimental verification of gene regulatory elements in neuronal development.* Thesis (Ph.D.), Rutgers University, 2010.

78. Brittis, P.A., et al., *Unique changes of ganglion cell growth cone behavior following cell adhesion molecule perturbations: a time-lapse study of the living retina.* Mol Cell Neurosci, 1995. **6**(5): p. 433-49.

79. Norris, C.R. and K. Kalil, *Guidance of callosal axons by radial glia in the developing cerebral cortex.* J Neurosci, 1991. **11**(11): p. 3481-92.

80. Rakic, P., *Guidance of neurons migrating to the fetal monkey neocortex.* Brain Res, 1971. **33**(2): p. 471-6.

81. Rakic, P., *Mode of cell migration to the superficial layers of fetal monkey neocortex.* J Comp Neurol, 1972. **145**(1): p. 61-83.

82. Anderson, S.A., et al., *Interneuron migration from basal forebrain to neocortex: dependence on Dlx genes.* Science, 1997. **278**(5337): p. 474-6.

83. Lavdas, A.A., et al., *The medial ganglionic eminence gives rise to a population of early neurons in the developing cerebral cortex.* J Neurosci, 1999. **19**(18): p. 7881-8.

84. Wichterle, H., et al., *Young neurons from medial ganglionic eminence disperse in adult and embryonic brain.* Nat Neurosci, 1999. **2**(5): p. 461-6.

85. Nery, S., G. Fishell, and J.G. Corbin, *The caudal ganglionic eminence is a source of distinct cortical and subcortical cell populations.* Nat Neurosci, 2002. **5**(12): p. 1279-87.

86. Ang, E.S., Jr., et al., *Four-dimensional migratory coordinates of GABAergic interneurons in the developing mouse cortex.* J Neurosci, 2003. **23**(13): p. 5805-15.

87. Lopez-Bendito, G., et al., *Preferential origin and layer destination of GAD65-GFP cortical interneurons.* Cereb Cortex, 2004. **14**(10): p. 1122-33.

88. Morozov, Y.M., M. Torii, and P. Rakic, *Origin, early commitment, migratory routes, and destination of cannabinoid type 1 receptor-containing interneurons.* Cereb Cortex, 2009. **19 Suppl 1**: p. i78-89.

89. Smart, I.H., *A pilot study of cell production by the ganglionic eminences of the developing mouse brain.* J Anat, 1976. **121**(Pt 1): p. 71-84.

90. Hack, I., et al., *Reelin is a detachment signal in tangential chain-migration during postnatal neurogenesis.* Nat Neurosci, 2002. **5**(10): p. 939-45.

91. Keilani, S. and K. Sugaya, *Reelin induces a radial glial phenotype in human neural progenitor cells by activation of Notch-1.* BMC Dev Biol, 2008. **8**: p. 69.

92. Sibbe, M., et al., *Reelin and Notch1 cooperate in the development of the dentate gyrus.* J Neurosci, 2009. **29**(26): p. 8578-85.

93. Hamilton, V.a.H., HL, *A series of normal stages in the development of the chick embryo.* Journal of Morphology, 1951. **88**(1): p. 49-92.

94. Caprioli, A., et al., *Expression of Notch genes and their ligands during gastrulation in the chicken embryo.* Mechanisms of Development, 2002. **116**(1-2): p. 161-164.

95. Corish, P. and C. Tyler-Smith, *Attenuation of green fluorescent protein half-life in mammalian cells.* Protein Eng, 1999. **12**(12): p. 1035-40.

96. Riccio, O., et al., *New Pool of Cortical Interneuron Precursors in the Early Postnatal Dorsal White Matter.* Cereb Cortex.

97. Meller, K. and W. Tetzlaff, *Scanning electron microscopic studies on the development of the chick retina.* Cell Tissue Res, 1976. **170**(2): p. 145-59.

98.   Cook, T., *Cell diversity in the retina: more than meets the eye.* Bioessays, 2003. **25**(10): p. 921-5.

99.   University, R., *The GENSAT Project: Gene Expression Nervous System Atlas.* www.genesat.org, Accessed November 2011.

100.   Science, A.B.I.f.B., *Allen Brain Atlas.* www.brain-map.org, Accessed November 2011.

101.   Breunig, J.J., et al., *Notch regulates cell fate and dendrite morphology of newborn neurons in the postnatal dentate gyrus.* Proc Natl Acad Sci U S A, 2007. **104**(51): p. 20558-63.

102.   Chitnis, A.B., *The role of Notch in lateral inhibition and cell fate specification.* Mol Cell Neurosci, 1995. **6**(6): p. 311-21.

103.   Chenn, A. and S.K. McConnell, *Cleavage orientation and the asymmetric inheritance of Notch1 immunoreactivity in mammalian neurogenesis.* Cell, 1995. **82**(4): p. 631-41.

104.   Williams, S.E., et al., *Asymmetric cell divisions promote Notch-dependent epidermal differentiation.* Nature. **470**(7334): p. 353-8.

105.   Wang, X., et al., *A new subtype of progenitor cell in the mouse embryonic neocortex.* Nat Neurosci. **14**(5): p. 555-61.

106.   Kriegstein, A.R. and S.C. Noctor, *Patterns of neuronal migration in the embryonic cortex.* Trends Neurosci, 2004. **27**(7): p. 392-9.

107.   Wang, D.D. and A.R. Kriegstein, *Defining the role of GABA in cortical development.* J Physiol, 2009. **587**(Pt 9): p. 1873-9.

108.   Tanaka, D., et al., *Multimodal tangential migration of neocortical GABAergic neurons independent of GPI-anchored proteins.* Development, 2003. **130**(23): p. 5803-13.

109.   Polleux, F., et al., *Control of cortical interneuron migration by neurotrophins and PI3-kinase signaling.* Development, 2002. **129**(13): p. 3147-60.

110.   Mastick, G.S., et al., *Pax-6 functions in boundary formation and axon guidance in the embryonic mouse forebrain.* Development, 1997. **124**(10): p. 1985-97.

111.   Mizuguchi, R., et al., *Ascl1 and Gsh1/2 control inhibitory and excitatory cell fate in spinal sensory interneurons.* Nat Neurosci, 2006. **9**(6): p. 770-8.

112.   Bryant, J., R.J. Goodyear, and G.P. Richardson, *Sensory organ development in the inner ear: molecular and cellular mechanisms.* Br Med Bull, 2002. **63**: p. 39-57.

113.   Jones, F.S., et al., *Barx2, a new homeobox gene of the Bar class, is expressed in neural and craniofacial structures during development.* Proc Natl Acad Sci U S A, 1997. **94**(6): p. 2632-7.

114.   Meech, R., et al., *A binding site for homeodomain and Pax proteins is necessary for L1 cell adhesion molecule gene expression by Pax-6 and bone morphogenetic proteins.* Proc Natl Acad Sci U S A, 1999. **96**(5): p. 2420-5.

115.   D'Arcangelo, G., et al., *A protein related to extracellular matrix proteins deleted in the mouse mutant reeler.* Nature, 1995. **374**(6524): p. 719-23.

116.   Hevner, R.F., et al., *Tbr1 regulates differentiation of the preplate and layer 6.* Neuron, 2001. **29**(2): p. 353-66.

117.   Chen, Y., et al., *On the epigenetic regulation of the human reelin promoter.* Nucleic Acids Research, 2002. **30**(13): p. 2930-9.

118. Yabut, O., et al., *Abnormal laminar position and dendrite development of interneurons in the reeler forebrain.* Brain Res, 2007. **1140**: p. 75-83.

119. Magdaleno, S., L. Keshvara, and T. Curran, *Rescue of ataxia and preplate splitting by ectopic expression of Reelin in reeler mice.* Neuron, 2002. **33**(4): p. 573-86.

120. Hashimoto-Torii, K., et al., *Interaction between Reelin and Notch signaling regulates neuronal migration in the cerebral cortex.* Neuron, 2008. **60**(2): p. 273-84.

121. Nullmeier, S., et al., *Region-specific alteration of GABAergic markers in the brain of heterozygous reeler mice.* Eur J Neurosci. **33**(4): p. 689-98.

122. Guidotti, A., C. Pesold, and E. Costa, *New neurochemical markers for psychosis: a working hypothesis of their operation.* Neurochem Res, 2000. **25**(9-10): p. 1207-18.

123. Kundakovic, M., et al., *The reelin and GAD67 promoters are activated by epigenetic drugs that facilitate the disruption of local repressor complexes.* Mol Pharmacol, 2009. **75**(2): p. 342-54.

124. Li, H., et al., *Isolation of a novel rat neural progenitor clone that expresses Dlx family transcription factors and gives rise to functional GABAergic neurons in culture.* Dev Neurobiol.

125. Flandin, P., et al., *Lhx6 and Lhx8 coordinately induce neuronal expression of Shh that controls the generation of interneuron progenitors.* Neuron. **70**(5): p. 939-50.

126. Johnson, D.S., et al., *Genome-wide mapping of in vivo protein-DNA interactions.* Science, 2007. **316**(5830): p. 1497-502.

127. Jung, C.G., et al., *Homeotic factor ATBF1 induces the cell cycle arrest associated with neuronal differentiation.* Development, 2005. **132**(23): p. 5137-45.

128. Ota, M. and K. Ito, *BMP and FGF-2 regulate neurogenin-2 expression and the differentiation of sensory neurons and glia.* Dev Dyn, 2006. **235**(3): p. 646-55.

129. Rhee, J.M., et al., *Highly cooperative homodimerization is a conserved property of neural POU proteins.* J Biol Chem, 1998. **273**(51): p. 34196-205.

130. Tzekov, R.T., et al., *Autosomal dominant retinal degeneration and bone loss in patients with a 12-bp deletion in the CRX gene.* Invest Ophthalmol Vis Sci, 2001. **42**(6): p. 1319-27.

131. Lo, L., et al., *Comparison of the generic neuronal differentiation and neuron subtype specification functions of mammalian achaete-scute and atonal homologs in cultured neural progenitor cells.* Development, 2002. **129**(7): p. 1553-67.

132. Ghanem, N., et al., *Distinct cis-regulatory elements from the Dlx1/Dlx2 locus mark different progenitor cell populations in the ganglionic eminences and different subtypes of adult cortical interneurons.* J Neurosci, 2007. **27**(19): p. 5012-22.

133. Suh, Y., et al., *Interaction between DLX2 and EGFR regulates proliferation and neurogenesis of SVZ precursors.* Mol Cell Neurosci, 2009. **42**(4): p. 308-14.

134. Yoshiura, K., et al., *Cloning, characterization, and mapping of the mouse homeobox gene Hmx1.* Genomics, 1998. **50**(1): p. 61-8.

135. Wang, W., et al., *Hmx: an evolutionary conserved homeobox gene family expressed in the developing nervous system in mice and Drosophila.* Mech Dev, 2000. **99**(1-2): p. 123-37.

136. van de Ven, C., et al., *Concerted involvement of Cdx/Hox genes and Wnt signaling in morphogenesis of the caudal neural tube and cloacal derivatives from the posterior growth zone.* Development. **138**(16): p. 3451-62.

137. Holstege, J.C., et al., *Loss of Hoxb8 alters spinal dorsal laminae and sensory responses in mice.* Proc Natl Acad Sci U S A, 2008. **105**(17): p. 6338-43.

138. Belting, H.G., C.S. Shashikant, and F.H. Ruddle, *Multiple phases of expression and regulation of mouse Hoxc8 during early embryogenesis.* J Exp Zool, 1998. **282**(1-2): p. 196-222.

139. Juan, A.H. and F.H. Ruddle, *Enhancer timing of Hox gene expression: deletion of the endogenous Hoxc8 early enhancer.* Development, 2003. **130**(20): p. 4823-34.

140. Mao, L., et al., *HOXC9 links cell-cycle exit and neuronal differentiation and is a prognostic marker in neuroblastoma.* Cancer Res. **71**(12): p. 4314-24.

141. Jung, H., et al., *Global control of motor neuron topography mediated by the repressive actions of a single hox gene.* Neuron. **67**(5): p. 781-96.

142. Cooper, K.L., W.M. Leisenring, and C.B. Moens, *Autonomous and nonautonomous functions for Hox/Pbx in branchiomotor neuron development.* Dev Biol, 2003. **253**(2): p. 200-13.

143. Takacs-Vellai, K., et al., *Transcriptional control of Notch signaling by a HOX and a PBX/EXD protein during vulval development in C. elegans.* Dev Biol, 2007. **302**(2): p. 661-9.

144. Maeda, R., et al., *Xpbx1b and Xmeis1b play a collaborative role in hindbrain and neural crest gene expression in Xenopus embryos.* Proc Natl Acad Sci U S A, 2002. **99**(8): p. 5448-53.

145. Schwartz, P.T., et al., *Pancreatic homeodomain transcription factor IDX1/IPF1 expressed in developing brain regulates somatostatin gene transcription in embryonic neural cells.* J Biol Chem, 2000. **275**(25): p. 19106-14.

146. Joshi, K., et al., *LMO4 controls the balance between excitatory and inhibitory spinal V2 interneurons.* Neuron, 2009. **61**(6): p. 839-51.

147. Marin, O., S.A. Anderson, and J.L. Rubenstein, *Origin and molecular specification of striatal interneurons.* J Neurosci, 2000. **20**(16): p. 6063-76.

148. Deng, Q., et al., *Specific and integrated roles of Lmx1a, Lmx1b and Phox2a in ventral midbrain development.* Development. **138**(16): p. 3399-408.

149. Revet, I., et al., *The MSX1 homeobox transcription factor is a downstream target of PHOX2B and activates the Delta-Notch pathway in neuroblastoma.* Exp Cell Res, 2008. **314**(4): p. 707-19.

150. Chen, J., S.Y. Leong, and M. Schachner, *Differential expression of cell fate determinants in neurons and glial cells of adult mouse spinal cord after compression injury.* Eur J Neurosci, 2005. **22**(8): p. 1895-906.

151. Chen, Y.H., et al., *Msx1 and Msx2 are required for endothelial-mesenchymal transformation of the atrioventricular cushions and patterning of the atrioventricular myocardium.* BMC Dev Biol, 2008. **8**: p. 75.

152. Bae, Y.K., et al., *A homeobox gene, pnx, is involved in the formation of posterior neurons in zebrafish.* Development, 2003. **130**(9): p. 1853-65.

153. Boni, A., et al., *Notch1 regulates the fate of cardiac progenitor cells.* Proc Natl Acad Sci U S A, 2008. **105**(40): p. 15529-34.

154. Rones, M.S., et al., *Serrate and Notch specify cell fates in the heart field by suppressing cardiomyogenesis.* Development, 2000. **127**(17): p. 3865-76.

155. Yang, X., et al., *Notch1 signaling influences v2 interneuron and motor neuron development in the spinal cord.* Dev Neurosci, 2006. **28**(1-2): p. 102-17.

156. Hafler, B.P., et al., *Expression and function of Nkx6.3 in vertebrate hindbrain.* Brain Res, 2008. **1222**: p. 42-50.

157. Jin, Z., et al., *Different transcription factors regulate nestin gene expression during P19 cell neural differentiation and central nervous system development.* J Biol Chem, 2009. **284**(12): p. 8160-73.

158. Williams, D.C., Jr., M. Cai, and G.M. Clore, *Molecular basis for synergistic transcriptional activation by Oct1 and Sox2 revealed from the solution structure of the 42-kDa Oct1.Sox2.Hoxb1-DNA ternary transcription factor complex.* J Biol Chem, 2004. **279**(2): p. 1449-57.

159. Greenwood, A.L., et al., *Notch signaling reveals developmental plasticity of Pax4(+) pancreatic endocrine progenitors and shunts them to a duct fate.* Mech Dev, 2007. **124**(2): p. 97-107.

160. Habener, J.F., D.M. Kemp, and M.K. Thomas, *Minireview: transcriptional regulation in pancreatic development.* Endocrinology, 2005. **146**(3): p. 1025-34.

161. Asano, M. and P. Gruss, *Pax-5 is expressed at the midbrain-hindbrain boundary during mouse development.* Mech Dev, 1992. **39**(1-2): p. 29-39.

162. McGlinn, E., et al., *Pax9 and Jagged1 act downstream of Gli3 in vertebrate limb development.* Mech Dev, 2005. **122**(11): p. 1218-33.

163. Hirsch, M.R., et al., *Forced expression of Phox2 homeodomain transcription factors induces a branchio-visceromotor axonal phenotype.* Dev Biol, 2007. **303**(2): p. 687-702.

164. Castro, D.S., et al., *Proneural bHLH and Brn proteins coregulate a neurogenic program through cooperative binding to a conserved DNA motif.* Dev Cell, 2006. **11**(6): p. 831-44.

165. Karg, H., et al., *Spatiotemporal expression of the homeobox gene S8 during mouse tooth development.* Arch Oral Biol, 1997. **42**(9): p. 625-31.

166. Barbieri, A.M., et al., *A homeobox gene, vax2, controls the patterning of the eye dorsoventral axis.* Proc Natl Acad Sci U S A, 1999. **96**(19): p. 10729-34.

Curriculum Vitae

Evangeline Tzatzalos

Education

September 2005 – 2012   Ph.D. in Biomedical Engineering
Rutgers, The State University of New Jersey, Piscataway, NJ

September 2001 – May 2005   S.B. in Chemical Engineering
Massachusetts Institute of Technology, Cambridge, MA

Publications

Chang YW, Goff LA, Li H, Kane-Goldsmith N, **Tzatzalos E**, Hart R, Young W, Grumet M. "Rapid Induction of Genes Associated with Tissue Protection and Neural Development in Contused Adult Spinal Cord After Radial Glial Cell Transplantation." *Journal of Neurotrauma* (2009) **26**(7):979-973.

Stachowiak A., Bershteyn A, **Tzatzalos E**, Irvine D. "Bioactive Hydrogels with an ordered Cellular Structure Combine Interconnected Macroporosity and Robust Mechanical Properties." *Advanced Materials* (2005) **17**:399-403.